

THE ELECTRON MICROSCOPY OF TISSUE SECTIONS

WITH SPECIAL REFERENCE TO THE STRUCTURE

OF SPINAL GANGLIA

Thesis submitted to the University of Glasgow

for the Degree of Ph.D.

by

James Hossack, B.Sc.

May, 1955.

ProQuest Number: 13838882

All rights reserved

INFORMATION TO ALL USERS

The quality of this reproduction is dependent upon the quality of the copy submitted.

In the unlikely event that the author did not send a complete manuscript and there are missing pages, these will be noted. Also, if material had to be removed, a note will indicate the deletion.



ProQuest 13838882

Published by ProQuest LLC (2019). Copyright of the Dissertation is held by the Author.

All rights reserved.

This work is protected against unauthorized copying under Title 17, United States Code  
Microform Edition © ProQuest LLC.

ProQuest LLC.  
789 East Eisenhower Parkway  
P.O. Box 1346  
Ann Arbor, MI 48106 – 1346

## ACKNOWLEDGMENTS

The work reported in this thesis was carried out in the Chemistry Department of the University of Glasgow.

The author desires to express his gratitude to Professor G. M. Wyburn and to Dr. I. M. Dawson of this University for their constant guidance, help and encouragement, without which this work would not have been possible. The author wishes also to record his indebtedness to Dr. A. Young for his patience and skill in performing the necessary dissections.

Thanks are due to Messrs. Barr and Stroud of Glasgow for their assistance in carrying out some of the modifications to the Spencer Microtome.

During the entire period of this research, the author was in receipt of the Barbour-Scott Scholarship in Anatomy of the University of Glasgow.

# T A B L E O F C O N T E N T S

## Chapter 1. METHODS AVAILABLE FOR PRODUCING THIN SECTIONS

1. Introduction	page 1
a) The Light Microscope	1
b) Specimen Considerations in Electron Microscopy	2
2. The Development of Thin Sectioning	11
a) Early Experimental Work	11
b) Methods in Current Use	13
c) Fixation Problems	19

## Chapter 2. EXPERIMENTAL

1. Apparatus	27
a) Microtome	27
b) Knife Holders	29
c) Cutting Edges	30
2. Methods	34
a) Removal of Tissues	34
b) Fixation	35
c) Embedding	36
d) Sectioning	37
e) Mounting	40
f) Examination	40
g) Other Techniques	41

**3. Discussion of Techniques** page 48

- a) Estimation of Section Thickness by Interference Colours 48
- b) Advance Mechanisms 50
- c) Section Defects 52

**Chapter 3. THE STRUCTURE OF THE SPINAL GANGLION CELL**

- 1. Description 55
  - a) Cellular Capsule 56
  - b) Cytoplasm 58
  - c) Nucleus 63
  - d) Nerve Fibre 70
  - e) The Effect of Delayed Fixation 71
- 2. Discussion 74
  - a) Nissl's Substance 74
  - b) Neurofibrillae 77
  - c) Nuclear Membrane 79
  - d) Golgi Apparatus 87

**Chapter 4. FREEZE-DRYING FOR THE ELECTRON MICROSCOPE**

- 1. Introduction 88
- 2. Description 90
  - a) Kidney fixed in Osmic Acid 90
  - b) Frozen-Dried Tissues 91
- 3. Conclusion 92

# INTRODUCTION

## 1.1

The field investigation was carried out in the form of a series of tests. The first test was carried out by the limit of the distance of the observation distance and the distance of the observation point. The second test was carried out by the distance of the observation point and the distance of the observation point. The third test was carried out by the distance of the observation point and the distance of the observation point.

## CHAPTER 1.

### METHODS AVAILABLE FOR PRODUCING THIN SECTIONS.

## 1. INTRODUCTION

### a) The Light Microscope

The maximum useful magnification which can be obtained in light microscopy is determined by the limit of resolution, which is reached when the separation distance between two points in the specimen becomes equal to just less than half the wavelength of the light with which the specimen is being examined. This means that, when two objects are separated by less than this distance, they are viewed in the light microscope as a single object, and fine structure of less than this order of magnitude is consequently invisible.

Structure which is below the limit of resolution of the light microscope can, however, be resolved by the electron microscope, which employs a beam of electrons with an associated wavelength many times shorter than that of light rays. In recent years, the electron microscope has been employed with increasing frequency for investigations of biological problems which involve the determination of sub-microscopic structure, and biologists have been concerned with developing new techniques which will take advantage of the much higher resolving power available to them.

Normal sections of biological tissue are too thick to be used as specimens for the electron microscope. This is due to the characteristics of a beam of electrons, which is completely stopped by a thickness of material which would have little effect on a light beam. Special methods must therefore be used to provide sections of suitable thinness.

b) Specimen Considerations in Electron Microscopy

(1) Resolution Limit

The limit of resolution in microscopy is determined by the numerical aperture of the objective lens, as well as by the wavelength of the incident radiation. The relationship is given by:

$$d_{\min} = \frac{0.61 \lambda}{n \sin \alpha} \dots\dots\dots (1)$$

where  $d_{\min}$  is the limit of resolution,  $\lambda$  is the wavelength of the incident radiation, and  $n \sin \alpha$  is the numerical aperture of the objective lens. While the value of  $n \sin \alpha$  may be of the order of unity in the case of the light microscope, its value for an electron microscope objective is necessarily a very small fraction of this, because of the necessity of minimising errors, due to aberrations in the uncorrected lenses employed. It is possible to calculate a value for the ultimate resolving power,  $d$ , of an electron microscope, when the electron wavelength,  $\lambda_e$ , is known.

A simplified form of the De Broglie wave equation gives, for the wavelength associated with an electron beam:

$$\lambda_e = \frac{12.3}{\sqrt{V}} \text{ \AA} \dots\dots\dots (2)$$

where  $V$  is the accelerating potential. Substituting this in equation (1) gives, with a beam potential of 50 Kv. and a normal value for the numerical aperture of 0.005 radian,

a resolution limit of about 5 Å.

In practice, other factors tend to increase this limit considerably. Spherical aberration and astigmatism in the objective field set a limit, even with a correctly compensated lens, of more than double this value, while the effect of other factors, such as supply voltage fluctuations and disturbing stray fields, will increase this limit still further. With a machine in good adjustment, a value of 20 to 30 Å. can be expected.

A further factor relevant to resolution is the influence of specimen thickness. It is found experimentally that, with increasing thickness, the sharpness of the image decreases. There are two reasons for this phenomenon. In the first place, electrons lose energy during inelastic collisions with atoms of the object, and, with increasing object thickness, the spread of energy of the electrons entering the objective is increased. It can be shown (Zwerykin et al. 1945) that, owing to the chromatic aberration characteristics of the objective lens, electrons from one point of the object are spread over a disc of diameter  $d_c$ , which is given by:

$$d_c = M.k.f.\frac{\Delta\phi}{\phi} \alpha_n$$

where  $M$  is the magnification,  $\alpha_n$  the objective aperture,  $k$  a constant which is characteristic of the lens, and  $f.\frac{\Delta\phi}{\phi}$

is the kinetic energy spread of the electrons. As the value of  $d_c$  increases, the sharpness of the image will be correspondingly less.

In the second place, electrons coming from the interior of a thick specimen are repeatedly deflected in their subsequent transit through the remainder of the specimen, so that they appear to come from points in the object plane differing from the object point. This effect, which is known as "volume scattering", is, however, important only for extremely thick specimens of the order of 0.6 micron or greater; the limit of resolution for thinner specimens is determined mainly by errors due to chromatic aberration alone. The relationship between chromatic aberration and specimen thickness is given approximately by:

$$\frac{\Delta V}{V} = \frac{10^4 \rho x}{v^2}$$

where  $\frac{\Delta V}{V}$  is the energy spread,  $\rho$  is the specimen density,  $x$  is specimen thickness, and  $V$  is the beam potential.

Figure 1 shows the relationship between resolution and specimen thickness for different values of beam potential, and it can be seen that, with increasing beam potential, the resolution limit set by chromatic aberration shows an improvement. For a beam potential of 50 Kv., and a specimen thickness of 0.05 micron, the limit set by chromatic aberration reaches the value, for a specimen consisting of

light atoms (carbon, hydrogen, nitrogen and oxygen), of about 20 Å. which is set by microscope performance alone. This limit would be increased by the presence of heavy atoms as in osmic-acid-fixed material; so that it is obvious, from the theoretical approach, that specimen thickness is a critical factor in determining the resolution obtainable.

(ii) Image Contrast

An image is rendered visible by the brightness differences between its component parts, differences which are interpreted in terms of the original object. In electron microscopy, the image is formed by interaction of the electron beam with the atoms composing the specimen. From the point of view of image formation, the most important aspect of this interaction is the scattering which occurs, and which results in a certain proportion of the incident electrons being diverted from their path sufficiently far to fall outside the area of the objective aperture. The intensity of the image at any point will be a function of this scattering, and, in general, will be less than the brightness of the undeviated beam by an amount which will depend on factors influencing the nature and extent of the scattering which occurs.

Since a rigorously exact treatment of electron scattering encounters mathematical difficulties, a number of simplifications have been introduced, enabling

equations to be derived which, while defective in some respects, nevertheless provide a very useful qualitative insight into the effect of the various parameters. Such a simplified treatment has been described by Hall (1953). This starts with a consideration of the energy changes which occur when an electron collides with an atom of the specimen, on the assumption that both particles will behave like elastic spheres, in accordance with the laws of classical mechanics. Collisions between incident electrons and nuclei of the atoms composing the specimen, and between incident electrons and orbital electrons of the specimen, are considered. From the results, as shown by Hall, it can be deduced that, for forward scattering through an angle of a small fraction of a radian, representing the aperture angle of an electron microscope objective, the energy losses from both types of collisions are insufficient to have any appreciable effect on the final energy of those electrons which reach the imaging screen. Image brightness will depend directly, therefore, only on the proportion of electrons which reach the screen. The validity of this treatment depends on the assumption of elastic collisions. While there is no doubt that inelastic scattering also occurs, as pointed out on page 4, this becomes significant only in the case of specimens thick enough to give rise to the chromatic aberration

or volume scattering effects already dealt with, and therefore, in general, too thick to be regarded as suitable objects for electron microscopy.

In order to estimate what fraction of the incident beam will, in fact, pass through the objective aperture and effectively participate in image formation, it is necessary to take into account the magnitude of the forces acting between the charged particles involved in the collision. When these charge effects are taken into account, an expression can be derived for the fraction of electrons scattered through an angle greater than a given angle,  $\theta$ , (which may be taken to represent the angular aperture) in terms of those parameters which are characteristic only of the specimen:

$$\frac{dN(>\theta)}{N} = \frac{f N_A \cdot z^2 e^2}{A \cdot r^2 \theta^2} \left(1 + \frac{1}{Z}\right) dx$$

The principal defect in this over-simplified treatment, as pointed out by Hall, is the fact that the screening effect of the orbital electrons in the specimen has been ignored in the computation of the charge effects. This effect becomes more pronounced for small angles, and, since the intensity distribution at small values of  $\theta$  is most important in electron microscopy, the screening effect has to be taken into account. Several methods have been developed for computing the magnitude of this effect.

The most accurate is due to Hartree, while a simpler but fairly accurate approximation has been made by Thomas and Fermi. These and other methods are discussed in some detail by Hall (previous reference). They show that the force exerted on a passing electron will be a complicated function of the distance from the nucleus and the atomic number of the atom, and will, as expected, be considerably less than if the atomic electrons were absent or were independent of each other and of the nucleus.

From the practical aspect, an important result can be deduced from these theoretical considerations. This is the dependence of the degree of scattering on the atomic weight (or the atomic number) of the atoms of which the specimen is composed. If a specimen contains for the most part atoms which are of equivalent, or nearly equivalent mass, as is frequently the case with biological specimens consisting of light atoms only, the image contrast is likely to be reduced to an impracticably low value, and, for this reason, methods such as shadowcasting with heavy metal atoms are employed to enhance it. The principles and applications of metallic shadowcasting have been presented in a paper by Williams and Wyckoff (1946).

A second method of increasing contrast which takes advantage of the presence of atoms of high atomic weight, and which is applicable to biological specimens, and, in particular, to tissue blocks for sectioning, utilises the

staining properties of some heavy metal compounds, such as osmic acid. When tissues are treated with this material, differential absorption occurs, and those components which have absorbed most of the heavy metal stain (such as lipids in the case of osmic acid), appear darker on the screen by reason of their greater scattering effect on the electron beam.

(iii) Image Quality in Relation to Beam Potential

The choice of beam potential has considerable influence on the character of the image. In commercial electron microscopy, this choice has been governed to a large extent by practical considerations of power supply design and construction, and by empirical assessment of image appearance. From Equation (2), page 2, it can be seen that an increase in beam potential, by reducing the electron wavelength, should result in a greater resolving power; but this theoretical increase in relation to the other considerations which determine the resolution limit is not of great importance. There are, however, a number of other factors concerning microscope performance which are also dependent, to a considerable degree, on the value of accelerating voltage used.

It has already been shown that a proportion of the incident beam is scattered by the specimen outside the objective aperture. Some of these scattered electrons

reach the screen, where they appear as a diffuse background and decrease the contrast of the image. By increasing the beam potential, the intensity of this background illumination can be reduced. This explains why structures in thick specimens sometimes become visible with an increase in beam potential when they are not discernible at a lower voltage. The same result could be obtained by reducing the size of the objective aperture, which is also effective in reducing the intensity of the diffuse background illumination and thereby increasing the contrast of the image.

The effect of varying the beam potential on the relationship between specimen thickness and resolution can be seen from Figure 1. It can be calculated that, where a specimen is just thicker than the optimum value required to obtain maximum resolution, this may, in fact, be attained by slightly increasing the potential.

## 2. THE DEVELOPMENT OF THIN SECTIONING

### a) Early Experimental Work

The conventional methods of preparation of tissues for light microscopy have had to be modified to suit the requirements of electron microscopy, in particular with regard to fixation methods, thickness of the section, and embedding material.

The importance of ultra-thin sectioning was recognised as early as 1939 by Von Ardenne, who, at the time, devised techniques for cutting thin wedge-shaped sections. He suggested mounting the block so that its forward face was at a slight angle to the knife edge, and, by this means, using a normal microtome, produced sections, the thickness of which tapered off to a low value. The same method was subsequently employed by Richards, Anderson and Hance (1942) using an adapted microtome, and a block consisting of striated rat muscle embedded in hard wax. The normal advance of their microtome was 0.25 micron, but, by adopting the suggestion of Von Ardenne, they were able to obtain wedge sections, the narrow end of which was less than the nominal value, and in places approached 0.1 micron in thickness. It is clear that this technique can have limited application only, since, besides placing considerable restriction on the extent of field available for examination,

it does not provide sufficiently uniform or reliable sections for routine investigations.

A more promising line of approach was taken, in 1943, with the development of high-speed microtomy (O'Brien and McKinley) which took advantage of the fact that relatively uncompressed thin sections should be obtained if the cutting edge was advanced at a rate greater than that of the compression wave travelling through the block. The cutting edge (a portion of razor blade) was mounted at the periphery of a wheel rotating at high speed, and the block to be cut was fed slowly towards the machine. The sections which flew off were caught on a glass slide and sorted for electron microscope examination. The chief disadvantages of this method were the large number of sections produced, of which only a very small percentage were suitable, and the initial expense of the apparatus.

However, in the hands of Fullam and Gessler and co-workers (Fullam and Gessler, 1946; Gessler and Fullam, 1946; Grey and Kelsch, 1948; Grey, Kelsch and Schuster, 1948) the method was sufficiently reliable to give information on fixation, embedding, and the general handling of thin sections. The use of such unconventional methods has, however, proved unnecessary with the adaptation of standard microtomes to produce thin sections.

b) Methods in Current Use

There are four main considerations in the cutting of sections less than one micron in thickness. These are:-

- (1) The properties of the embedding medium
- (2) The quality of the knife edge
- (3) The size of the block
- (4) The advance mechanism of the microtome

In 1948, Pease and Baker outlined a method for producing ultra-thin sections which made use of a standard microtome, modified so as to reduce the advance mechanism to provide a minimum advance of 0.1 micron - the method which has been used in this investigation. In the Spencer Rotary Microtome, the specimen block is moved vertically on its holder past a stationary knife, towards which it advances step by step as pressure is applied to it from a pin sliding against an inclined plane (Figure 2). Pease and Baker modified the angle of the inclined plane by inserting an additional wedge, as shown in Figure 3, which reduced the feed by a factor of ten and permitted an advance, at the minimum thickness setting, of 0.1 micron. The size of the block was reduced to 1 mm. square, while the cutting edge was an ordinary microtome knife, sharpened by conventional methods. With these modifications, Pease

and Baker were able, with normal cutting practice, to produce sections with a fair degree of reliability down to 0.2 micron in thickness.

In 1949, two important new contributions were made to the technical equipment for thin sectioning by Newman, Borysko and Swerdlow (1949a,b). As mentioned, the embedding medium represents one of the most important factors in producing blocks which will yield thin sections, and there was little doubt that ordinary paraffin-wax-embedded blocks were far from satisfactory in this respect. The use of hard waxes such as ester wax (Stedman, 1945) or collodion (Pease and Baker, 1948) represented some improvement. However, it was clear that a material was required whose physical properties differed fundamentally from those of most of the embedding media used up till that time, and suitable mixtures of the methacrylate plastic resins provided such a material. Newman, Borysko and Swerdlow used the monomer of polybutylmethacrylate to infiltrate the specimen, which was then polymerised in fresh monomer to which a free-radical catalyst had been added. This method has been fairly widely used by subsequent investigators. Besides providing a block possessing optimum cutting properties, it has been found possible, by suitable addition of other methacrylate monomers such as methyl (McCulloch, 1951)

or ethyl methacrylate (Massey, 1953), or by adjustment of polymerisation time, to secure blocks of different degrees of hardness.

The second development was the introduction by these authors of a thermal expansion feed for advancing the specimen, to replace the mechanical advance mechanism. This is essentially a device, clamped to the nosepiece of a standard microtome (the Spencer was used in this case) which could be cooled by the admittance of compressed carbon dioxide through a needle valve. On reducing or stopping the flow of gas, the device could be allowed to warm slowly to room temperature, and the resultant forward movement of the block, by the expansion of the nosepiece, allowed a series of thin sections to be cut during this period. This method is inherently less accurate than mechanical methods of advance. However, it has proved adequate to meet the requirements of thin section cutting, and has been fairly widely adopted as an alternative to mechanical advance systems. A rather simpler device employing the same principle was used by Eden, Pratt and Kahler (1950), but, in this case, the holder was warmed above room temperature by a controllable heating coil.

In the same year, Hillier and Gettner (1950a,b) made an extensive investigation of the technical problems involved in thin sectioning. They reduced the number

of variables involved in the selection, fixation and embedding of the tissue by studying a single set of blocks originating from one piece of tissue. In a further modification of the Spencer Microtome embodying the incorporation of a wedge with a very small angle, a vibration-free motor drive, and a strong spring between the frame of the machine and the carriage to increase the rigidity of movement, they were able to reduce the unit advance to 0.02 micron. With the advance gauge set to cut at 0.1 to 0.2 micron, which is large by comparison with the unit advance, they were able to cut sections with a thickness accuracy of 10%. One of the most useful modifications due to Hillier and Gettner was the introduction of a liquid reservoir in front of the cutting edge, on the surface of which the sections were permitted to float as they were cut, and from which they could be picked up directly on the specimen grid.

In 1951, Hillier described a rapid, simplified method of sharpening standard microtome knives to the precision required for ultra-microtomy. By attaching a permanent back to the knife, the cutting facet was automatically brought into the correct angle for sharpening, and, since the knife edge did not suffer the comparatively severe damage which it underwent during normal sectioning, the

restoration of a sufficiently fine edge could be accomplished with a fair degree of speed and accuracy. With this and the other technical advances just described, the cutting of thin sections of about 0.1 or 0.2 micron became a routine procedure.

It must be remembered that, while standard microtomes can, in theory, be modified to reduce the rate of advance to any desired degree, they were not originally designed to operate with this amount of precision. Recent developments have, therefore, tended to concentrate on the construction of new microtomes specially designed for ultra-microtomy. Examples of this sort are the Cantilever Microtome of Cocks and Schwarz (1952), and a number of other machines incorporating completely new design features. (Porter and Blum, 1953; Sjostrand, 1953c; Watson, 1953a).

On the other hand, the standard of quality attained in recent investigations, where standard modified microtomes have been used, is technically satisfactory. Excellent thin sections have been cut by Eaves and Flewett (1954) and Bradfield (1954) with a modified Cambridge Rocking Microtome, and by Leyon (1954) using a modified Spencer Rotary Microtome. Modifications to another standard microtome, the Minot Rotary, had been described in detail by Geren and McCulloch (1951).

These modifications permitted the advance to be reduced to 0.05 micron. Estimations of the thickness of a ribbon of sections, both by shadowcasting and subsequent electron microscopic examination, and by multiple beam interferometry, showed that the thickness variation from section to section was as small as 25%. A Minot Rotary Microtome, adapted in this way, was used by Hartmann (1953) in an investigation of central nervous tissues. It is noteworthy that the design of the Spencer Rotary Microtome manufactured especially for thin sectioning employs the same advance mechanism as did the older model.

A feature of some of the newer designs is that the block, on its upward or return stroke, does not pass the knife edge, and it is claimed that this feature is essential to prevent the occurrence of block wetting when the liquid meniscus is high. In the present investigation, which has used a standard machine with the usual return stroke, wetting of the block has proved troublesome only when the knife is not perfectly sharp; and, indeed, this can be used as a check on edge quality. It is probable that, in the operation of a thin sectioning apparatus, the critical factor is knife edge sharpness, and this will later be discussed in more detail.

c) Fixation Problems

It was clear that fixation, to take advantage of the much higher resolving power of the electron microscope, was likely to be more exacting than fixation for light microscopy, and, as the technical problems associated with thin sectioning were gradually eliminated and sections of increasingly better quality were produced, this problem of fixation became more and more acute. In fixation for the light microscope, the faithful preservation of unresolved fine detail is not a matter of primary importance. Considerations such as the demonstration of a particular cellular or other tissue component, or the ability of the fixative to influence subsequent staining, are generally of greater significance.

A few investigations have been made, using the light microscope, with the primary aim of characterising the action of fixatives in preserving the very fine detail visible under certain conditions in the living cell. The most illuminating of these was that of Strangeways and Canti (1927). In the course of examining the effect of a number of different fixatives, these authors found osmium tetroxide vapour to be the only fixative that did not lead to obvious morphological changes in the appearance of fresh tissue culture cells. Observed under the dark

field microscope, the only alteration shown, when this fixative was used, was a slight increase in light-scattering power in the ground substance of nucleus and cytoplasm. It can be assumed that this could be due to a form of physical or chemical change, such as a change in dispersivity at the molecular level, which could occur without necessarily interfering with the ultra-structure of the cell components. Indeed, the dark field microscope is known to be able to detect changes in particles as small as 60 Å.

Formalin, while not as satisfactory as osmium tetroxide, produced considerably less alteration than the other fixatives tested. The impression obtained from this and other similar work was that, of the common fixatives, both single and mixed, only two, namely formalin and osmium tetroxide, possessed the ability to preserve fine cellular structure, comparatively unchanged, to the limit of resolution of the light microscope; and that, of these two, osmium tetroxide was the more satisfactory.

In the case of the electron microscope, it is, of course, impossible to carry out such experiments with living material. Image quality, lack of "coarseness", and the absence of coagulation or precipitation effects have to be employed as general criteria. It was very early apparent, however, that osmium tetroxide was likely

to prove the fixative of choice for biological work with the new instrument. As early as 1934, before the resolution provided by the light microscope had been exceeded, Marton (1934a,b) described a method for stabilising biological objects for examination with the electron microscope, by impregnating them with osmium tetroxide. Upon exposure to the electron beam, the organic matter was destroyed, and that portion of the specimen which had absorbed osmium (virtually, an osmium replica of the original specimen) could be photographed.

with the development of supporting films, which enabled biological material to be imaged without destruction, this method of osmium impregnation was no longer necessary, and for some time, investigations were carried out on specimens such as bacteria without further treatment. In 1942, however, staining by heavy metal impregnation was employed by Mudd and Anderson, who studied the effect of treatment with solutions of silver nitrate and lead acetate on bacterial suspensions. During an investigation of muscle fibre, some other heavy metal stains, including osmic acid, were tried by Hall, Jakus and Schmidt (1945). These authors found that, from the point of view of increasing the contrast of the electron microscope image, phosphotungstic acid was the most satisfactory of the staining compounds investigated.

However, during the course of an investigation of the action of different fixatives on tissue culture cells, Porter, Claude and Fullam (1945) examined the effect on the preservation of cell morphology of treatment of cultures with osmium tetroxide. From their micrographs, they concluded that fixation with osmium tetroxide was the most satisfactory method of preparing this type of material for electron microscopic examination.

The advent of thin sectioning confirmed the value of osmium tetroxide as a suitable fixative, and, in early attempts to produce thin sections, an aqueous solution of the tetroxide, either alone or in conjunction with other components, was generally employed. Perfusion of the tissue block with the fixation fluid was sometimes adopted. Claude and Fullam (1946) perfused their sample, consisting of guinea-pig liver, with a 2% solution of osmium tetroxide for 24 hours, while Hillier and Gettner (1950) reduced the strength to 1% and perfused in a physiological saline solution. However, with the greater resolution which was by then becoming available, it was clear that the results of osmic acid fixation, as applied to blocks of tissues for thin sectioning, were not altogether satisfactory.

One of the disadvantages of osmic acid, which is also

evident in its use as a fixative for light microscopy, is its slow penetrating power, resulting in the occurrence of post-mortem changes in that part of the interior of the block which is not subjected to the influence of the fixative for some time. Perfusion does not contribute greatly to a solution of the problem. Baker and Moderne (1952) attempted to overcome this disadvantage of osmic acid by obtaining slices of tissue, about 0.1 mm. thick, from their main block, and immersing these in the fixative. Since the penetrating power of osmic acid is about 0.02 mm. per minute, it can be seen that the post-mortem degeneration should be considerably reduced. However, no great improvement in fixation quality was observed.

In the same year, an extensive investigation was reported by Palade (1952) into some of the factors influencing fixation with osmium tetroxide solution. By using slice preparations impregnated with neutral red as acid-base indicator, he found that fixation with solutions of osmium tetroxide was preceded by acidification of the tissue; and that the pH of an originally neutral tissue homogenate was reduced appreciably after fixation. This effect was not mitigated by adding enzyme inhibitors to the system, and so was not a result of the enzymatic breakdown of the organic components. Taking into account

the known appearance of ordinary acid-fixed tissues, both at the light and electron microscope level, Palade concluded that the unsatisfactory fixation of tissue blocks was bound up with this reduction of pH during the diffusion of osmic acid into the cells.

In a further series of experiments, Palade used buffered osmic acid in the range of pH 3.0 to 9.0; and he confirmed that the optimum results, as judged by the quality of the electron micrographs of different tissues at fairly high resolution, were obtained with a sodium acetate-sodium veronal buffer containing 1% osmium tetroxide at a pH of about 7.4. Accordingly, he recommended such a fluid as an appropriate fixative for tissue blocks for thin sectioning.

Subsequent work by other investigators has strengthened the view that such an osmic acid buffer is capable of preserving ultra-structure faithfully to the limit of resolution of the electron microscope. Some of the other factors affecting fixation with buffered osmium tetroxide solutions have recently been studied by Rhodin (1954). He repeated Palade's experiments on the pH of the buffer, and also examined the effects of fixation temperature, osmolar concentration, and size of tissue blocks with regard to the occurrence of post-mortem changes.

The results, with particular reference to the structure of the mouse kidney examined at very high resolution, were, on the whole, in the directions to be expected. By varying the temperature between 0°C. and 45°C., Rhodin found that, at the higher temperature, random precipitation of metallic osmium showed a tendency to take place; while reduction of the temperature slowed up the rate of penetration of the osmic acid to a very slight degree, but appeared to result in rather better fixation. He concluded that, for most purposes, fixation at room temperature was satisfactory. With regard to penetrating power, Rhodin did not detect any appreciable changes in kidney ultra-structure with a delay of five minutes in the commencement of fixation, while a thirty minute delay resulted in a certain amount of deterioration in the internal structure of mitochondria, this distortion increasing with increasing delay time. This question is examined in more detail in connection with present results on the fixation of nervous tissue.

It has already been pointed out on page 8 that osmium tetroxide, in addition to its action as a fixative, possesses the ability to act as an electron stain with a certain degree of specificity, and thereby increase the contrast of the final electron microscope image. It shares this property with such similar compounds as phospho-

tungstic acid, phospho-molybdic acid, and silico-tungstic acid. However, while these electron staining compounds are known also to possess the properties of fixatives, they do not appear to have been used as such in investigations on tissue sections.

**CHAPTER 2.**

**EXPERIMENTAL.**

## 1. APPARATUS

### a) Microtome

The Spencer Rotary Microtome, Model No. 820, has been employed in the present investigation for cutting thin sections. The advance mechanism of this machine is shown diagrammatically in Figure 2. The Specimen, A, which is clamped in the holder, B, moves at each stroke past the knife edge, C, the direction of movement being perpendicular to the plane of the paper. A ratchet, D, engages in the toothed wheel, E, and moves this wheel one notch in a clockwise direction at each cutting stroke when the advance gauge is set to cut at 1 micron. The axle of this wheel is coupled directly to a steel cylinder, F, containing a screw thread with a very low pitch. This screw engages with a steel block, G, threaded to fit it. As the cylinder rotates, this block consequently moves along the thread in the direction shown by the arrow, and the heavy pin, H, which it carries, presses on the wedge, J, and moves it and the specimen holder towards the knife edge.

The extent of this movement will determine the section thickness. Its minimum value depends on the size of teeth in the wheel, E, the pitch of the thread on F, and the angle of the wedge, J. In order to reduce this from

the minimum value of 1 micron with the standard microtome to the value of 0.1 micron necessary to cut sections for the electron microscope, the angle of the wedge was altered, while the other factors remained constant. (Pease and Baker, 1948). The method of carrying out this alteration is shown in Figure 3. An additional wedge was constructed, and was clamped to the original wedge by means of two strong screws, so that the forward movement of the specimen was reduced by a factor depending on the angle of the new wedge. This was designed to permit a minimum advance of 0.1 micron.

Two further modifications were required in order to adapt this machine for the procedure of thin sectioning. Firstly, a strong spring was fitted between the underside of the moveable carriage of the machine and the clamp holding the specimen mount. This removed any tendency for random vertical movement of the specimen during the cutting stroke, with consequent unevenness in the quality of the final section. (Hillier and Gettner, 1950b). Secondly, the knife holder, which, in the original model slides under hand control in a greased runway, was modified so that the movement could be controlled by a screw with a micrometer thread, and the cutting edge thereby set in the correct position with respect to the block just before cutting. (Sjostrand, 1952). These modifications are

clearly visible in Figure 4. The microtome was motor driven at a speed of 35 strokes per minute, and, to reduce vibration from the motor, a fibre driving belt coupled it to the microtome, which was mounted on a block of sponge rubber.

#### b) Knife Holders

Both razor blades and glass knives were employed for sectioning, and suitable holders were constructed to hold these in position. The razor blade holder is shown diagrammatically in Figure 5 and the glass knife holder in Figure 6. They can be clamped in the jaws of the microtome, in place of an ordinary knife.

The razor blade holder was constructed of machined brass, with a brass bath, B, welded in front of the blade holder, H. This holder was designed to maintain the blade in a curved position, giving slight tension without undue strain, and permitting any area of the cutting edge to be moved into the central part of the holder where cutting was being carried out. (Sjostrand, 1952).

The sections, as they were cut, could be floated clear of the blade on to the surface of the liquid in the bath, through a recess, R. This recess was high enough to prevent the liquid leaking round the side of the blade when the meniscus was almost level with the top of the bath.

A clearance angle of from  $5^{\circ}$  to  $10^{\circ}$  was maintained between the back facet of the blade and the direction of movement of the block.

The glass knife holder was also constructed of brass, but had a central steel portion, S, into which the knife was inserted. When the clearance angle, which was as small as possible, was estimated to be correct, the screw, T, was tightened against the knife, K, sufficiently to hold the latter rigid in the holder without fracturing the glass.

### c) Cutting Edges

#### (i) Preparation of Razor Blades

The outline of the method of razor-blade sharpening was suggested by Sjostrand (1952), but the details were developed independently. Blades of the American "Schick" type are convenient for thin sectioning, as they are of suitable size, and sufficiently thick to be free from any tendency to vibrate in the holder. The experimental work necessary to develop a sharpening technique consisted of the construction of chrome-steel hones of various angles, of the selection of a series of abrasive powders, and of the preparation of electron micrographs of dispersions of each powder in different liquids. Examination of the micrographs enabled the powder with smallest and most uniform particle size to be selected; and this powder

was employed, throughout a further series of tests, to determine the correct honing angle, pressure, and direction of stroke which were required to produce a blade edge of the maximum sharpness.

An outline is given of the conditions which were ultimately established for sharpening razor blades:

A 20% suspension of "Linde" abrasive powder was prepared in distilled water, to which had been added a crystal of sodium benzoate to prevent corrosion, and the suspension was allowed to settle for not more than two minutes. About 15 ml. of this was spread over a piece of new sheet glass, 4" by 8" in size, and honing was started immediately. A diagram of the hone used is shown in Figure 7. After inserting the blade, the hone was moved obliquely in a forward direction over the glass surface, at such a speed and with such a pressure that a very faint hiss was audible. The pitch of this sound should be almost above the limit of hearing, and no trace of grating should at any time be heard.

If the hiss cannot be heard, or if it is too "heavy" or too low-pitched, varying the honing stroke may be sufficient to correct it. If not, it can be assumed that the glass has a film of grease on its surface, and the effect of cleaning it with cotton wool and distilled water containing a few drops of detergent may be tried.

However, it has always been found preferable to use new sheet glass, capable of giving correct results without any treatment, since the use of detergent appears to detract from the quality of the glass surface. Each sheet was discarded after sharpening a maximum of six blades on it.

The blade, after sharpening, was examined in a dark-ground "Ultrapack" Microscope at a magnification of 600, and the presence of imperfections such as nicks, facet scores, or rounding of the edge, was noted. A perfectly sharp part of the edge appeared as a very thin, unbroken bright line against a dark background.

Ultimately, when the correct set of conditions had been established, it was possible to produce a sharp edge in about ten minutes; if examination of a blade after this period failed to reveal a suitable edge, further honing was invariably useless, and the blade was discarded.

#### (ii) Glass knives

The preparation of glass knives has been described by Latta and Hartmann (1950), and the present procedure followed this closely. Strips of glass 12" by 1", obtained from a glazier, were scored with a cutting diamond at an angle of  $45^{\circ}$  to the edge. The scores were spaced at intervals of about 1". The glass strip was then gripped with glass pliers, on each side of a score, and

increasing pressure applied until the glass snapped. For cutting the very small tissue blocks necessary in thin sectioning, glass of  $\frac{3^{\text{rd}}}{16}$  was sufficiently thick, and was easier to handle than the thicker sheets used by Latta and Hartmann.

It has not been found possible to check glass knives in the high-power microscope because of the lack of uniformity in the shape of glass edges. However, a certain degree of selection was given by the use of a low-power binocular microscope. Because of this irregularity in the shape of the glass edge, it was found necessary to construct a separate water trough for each knife from hard paraffin wax. This was mounted behind the edge, as shown in the photograph, Figure 9.

## 2. METHODS

### a) Removal of Tissues

The tissues consisted of sympathetic and spinal ganglia and kidney from normal adult rabbits. Where possible, the tissues were removed under anaesthesia, trimmed with a sharp razor blade to a cube of about  $\frac{1}{2}$  mm. side, and immersed at once in the fixative. In other cases, the animals were killed by a blow at the base of the skull, and the tissues dissected out, trimmed, and fixed as rapidly as possible. In the case of nervous tissues, it was found particularly important to carry out the removal as rapidly as possible, since a delay of as little as three minutes was sufficient to cause serious distortion of ultra-structure, due to post-mortem changes. With practice, it was found possible to remove spinal ganglia in just over one minute.

Because of the very slow diffusion rate of osmic acid it was considered that there would be no advantage in perfusion, and, in fact, that the time interval between death and contact of the fixative with the spinal ganglia would thereby be increased.

b) Fixation

The fixative was a 1% solution of osmic acid, buffered at pH 7.4, and the procedure employed followed closely that recommended by Palade (1952). To prepare the fixative, the following solutions were mixed in the order and proportions shown:-

0.14 M. Sodium Acetate (11.5 g/litre)	5 ml.
0.14 M. Sodium Veronal (32 g/litre)	5 ml.
0.2 N. Hydrochloric Acid	2.5 ml.
2% Aqueous Osmium Tetroxide	12.5 ml.

The pH of this buffer is 7.4 to within 0.2 pH unit, and its osmolar concentration is just less than that of 0.65% sodium chloride, or mammalian Ringer's solution. The pH was checked for each supply of fixative prepared, using a B.D.H. Comparator, and phenol red as acid/base indicator.

Fixation was carried out for four hours at room temperature, and the tissues were subsequently washed in a number of changes of water, then dehydrated through a graded series of alcohols. They were allowed to remain for one hour in each series, and finally transferred to dry alcohol (re-distilled over calcium hydride) where they were left for two hours before embedding.

c) Embedding

Embedding was carried out in the monomer of polybutylmethacrylate to which 8% to 10% of methyl methacrylate had been added. The inhibitor was previously removed from the mixture of monomers by treatment with a strong solution of caustic soda, followed by distillation and drying over phosphorus pentoxide. After final dehydration, the tissues were transferred through an alcohol/monomer mixture into the pure monomer, where they were allowed to remain for 30 minutes. Thereafter, they were taken through three further changes of monomer, in each of which they were left for 30 minutes, then embedded in gelatin capsules according to the method of Newman, Borysko and Swerdlow (1949).

One piece of tissue was placed at the bottom of a No. 00 gelatin capsule and about 0.5 ml. of monomer, containing 1% by weight of benzoyl peroxide as a catalyst, was added from a micro-pipette. A small steel supporting bar was placed above the tissue, and the capsule lid replaced.

The polymerisation was effected by mounting the capsules in a steel rack in an oven at 47°C., care being taken to ensure that free circulation of air round the capsules was provided in order to maintain an even

temperature. A period of from 24 to 48 hours was sufficient to secure a fully polymerised block. An alternative method of polymerisation by means of ultra-violet light was also employed. In this method, the rack containing the capsules was mounted about eight or nine inches from an ultra-violet lamp, in front of and slightly above it. In this case, polymerisation was complete after about four hours. The method gave irregular results, since it was frequently found that the plastic round the block was fully polymerised while the interior was soft and spongy. This has been assumed to be a result of absorption of ultra-violet radiation by the osmium-impregnated block. For this reason, the method was abandoned in favour of heat polymerisation. After embedding, the tissue blocks were placed in warm water and the gelatin dissolved out. Each block was then mounted by means of its supporting bar in the microtome jaws, the excess plastic removed, and the block finally trimmed to size with a razor blade.

#### d) Sectioning

##### (i) Sectioning with Razor Blades

When the block had been trimmed to present a face of approximately 0.2 mm. square, the blade holder was set up with an unsharpened blade in position, and the micrometer

screw adjustment used to bring the blade edge close to the surface of the block. These and all subsequent cutting operations were observed through a binocular microscope, which, for the purpose of initial trimming, was fitted with eyepieces giving a magnification of ten times. With the advance gauge set at two microns, sections were now cut by hand, picked up directly from the blade edge, and examined, after flattening with a drop of water on a glass slide, in the light microscope. In this way it was possible to check that all the superficial plastic layer had been removed, and that full sections of tissue were being cut. This initial examination was also useful as a check on the light microscopic appearance of the tissues, and served to indicate the presence of such defects as large-scale trimming distortion, or shrinkage of the block.

The blade was now replaced by a sharpened one, set so that a suitable portion of its edge was in position to cut. Eyepieces giving a magnification of fifteen times were now inserted into the binocular microscope, the driving belt from the motor was coupled up, and the bath filled with 20% aqueous alcohol at room temperature, so that the meniscus was just level with the top of the blade. The advance gauge was set to give a section thickness of 0.1 micron. The motor was now switched on

and a ribbon consisting of about ten sections was cut. With the aid of a dissecting needle, this ribbon was floated clear of the blade edge on to the open surface of liquid in the bath. If wrinkling was observed while the ribbon lay on the liquid surface, gentle heat was applied to the bottom of the bath from a micro-burner; thereafter, the sections were allowed to remain for a further period before being mounted.

#### (ii) Sectioning with Glass Knives

Because of the variation in size and shape of different glass knives, it was found necessary to make an individual water bath for each knife used. After selecting a suitable knife, as judged by examination of the edge with the aid of the binocular microscope, a small paraffin wax bath was constructed and sealed to the rear facet of the glass with a heated needle. The techniques for setting up and cutting were identical with those used when sectioning with razor blades. Should wrinkling be observed in this case, careful insertion of the heated needle point into the liquid near the ribbon was generally sufficient to flatten the sections.

Figure 8 is a photograph showing the razor blade holder in position, and Figure 9 shows the glass knife holder, with a knife in position for sectioning.

### e) Mounting

Copper grids of the mesh type (150 squares to the inch) were found to be convenient for section mounting, and a supply of these was prepared beforehand by coating them with a thin film of Formvar. This was accomplished by placing the grids, shiny side upwards, on a microscope slide at the bottom of a large Petri dish containing about two inches of water. A separate cleaned slide was now flooded with a solution of 0.5% Formvar in ethylene dichloride, allowed to dry, and dipped obliquely below the water surface, when the Formvar film floated off and was deposited on the mounts by removal of the water with a vacuum pump. After drying, the grids were ready to be used for section mounting.

This was done by a spooning motion, in which the grid, held with fine forceps, was placed under the floating ribbon and lifted out of the bath. The grid and sections were drained on filter paper, and, when dry, were ready for examination.

### f) Examination

In addition to the range of interference colours shown by a ribbon of thin sections and discussed later, a further criterion of thickness is provided by the light microscope. Using a standard 16 mm. objective,

it is found that the edge of a suitably thin section ceases to have any apparent depth, and is in sharp focus at only one critical position. The edges of thicker sections display depth of focus to a greater or less degree. Examination with the light microscope also reveals the existence of defects such as knife marks, wrinkling, and cross-banding due to knife vibration.

Examination in the electron microscope was carried out with a Philips "Metalix" microscope, using a 50 micron objective aperture (Le Poole, 1947), and a stabilised beam potential of 60 Kilovolts (Van Dorsten, 1948). Suitable fields were photographed at film magnifications between 3,000 and 20,000, and thereafter enlarged photographically.

#### g) Other Techniques

##### (i) Preparation of Material by Freeze-Drying

The tissues, trimmed as small as possible, were placed on a piece of fine wire mesh and at once immersed in a bath of iso-pentane, maintained at a temperature of about  $-150^{\circ}\text{C}$ . in a liquid-air-filled Dewar flask. After approximately 30 seconds, they were lifted from the mesh, placed on the tray of an "Edwards" Tissue Drier, and dehydrated at  $-40^{\circ}\text{C}$ . and 0.01 mm. of mercury for 48 hours.

The tube carrying the tissue-bearing tray was of the standard type for use with the "Edwards" machine, but a number of modifications were carried out to enable direct vacuum embedding of the tissues in plastic monomer to be effected. These modifications are shown in figure 10.

Between the exhaust tube, A, and the manifold inlet, B, an additional metal stopcock, C, was fitted, allowing the vacuum to be maintained when the freeze-drying tube was removed from the machine. At the side of the tube, just below the metal retaining ring, D, there was added a further glass side-arm, E, carrying a large stopcock, F, and terminating in a "Quickfit" cone, G. The glass apparatus, H, shown on the right of the figure, was designed to fit into this cone, providing a vacuum seal at this point.

After tissue dehydration had been completed, the flask containing the freezing mixture was lowered, and, with the aid of the heater built in to the machine, the tissues were brought slowly to room temperature. Thereafter, the stopcock, C, was closed, and, after removing the seal on the manifold inlet and the heater connections, the freeze-drying tube was lifted clear of the machine.

Careful manipulation of the freeze-drying tube enabled the tissues to be shaken out of the tray and on to the side of the tube, and, by lightly tapping this with the finger, it was possible to direct one tissue into the opening above the stopcock, F. The tube was now supported on a clamp, with the side-arm pointing downwards at an angle of about  $45^{\circ}$ . 5 ml. of plastic monomer was introduced into the bottom of the glass apparatus, H.

This apparatus was placed in position on the "Quickfit" cone, evacuated through the side-arm, J, and the stopcock, K, closed. In order not to contaminate the pump oil with methacrylate vapour during this evacuation, it was found advisable to chill the end of the tube containing the methacrylate monomer in an alcohol/carbon-dioxide freezing mixture. By opening the stopcock, F, and tilting the apparatus further, the tissue resting on F dropped through the stopcock opening into the methacrylate monomer, when, if the freeze-drying had been satisfactory, it absorbed monomer and sank at once. Tap F was closed, side-arm K opened, and the infiltrated tissue removed and inserted into a gelatin capsule, where it was polymerised by the method previously described. This embedding procedure

was repeated for the other tissues in the freeze-drying tube.

In preparing thin sections of frozen-dried tissues, it was found essential to avoid contact of the sections with water, otherwise immediate fragmentation took place. While thin sections of frozen-dried tissues could be cut with a razor blade without a water bath, it was observed that, due to strong attraction to the steel edge, the sections could not be removed without breaking them. This difficulty was not present in the case of glass knives, and, accordingly, these were used for dry sectioning. When cutting a frozen-dried block, the motor was disconnected and the sectioning done by hand, since, in this way, the sharp individual strokes necessary to produce uncompressed sections were more easily achieved. Sections were picked up one at a time from the glass edge with the point of a fine dissecting scalpel, placed on a Formvar-coated grid, and flattened with a drop of 100% alcohol or dioxan. In this case, prior hardening of the Formvar film, by strong heating and subsequent slow cooling, was essential to prevent its dissolution by these solvents.

In the case of spinal ganglion tissues, frozen-dried

controls were required for histological examination with the light microscope. These were prepared by placing them in iso-pentane at  $-150^{\circ}\text{C}$ ., dehydrating them in a standard unmodified tissue drier, and embedding them directly in paraffin. Sections were cut at 10 microns and stained with toluidine blue before examination.

(ii) Shadowcasting

In the case of sections to be shadowcast, previously hardened Formvar mounts were used, since it is necessary to dissolve the embedding medium from the sections before shadowcasting them. In this extraction, distortion may arise due to a number of causes, the most important being the surface forces existing at the time of evaporation of the solvent used to dissolve out the matrix. In an attempt to overcome this problem, some workers used an embedding medium, such as a eutectic mixture of camphor and naphthalene, which sublimed at room temperature (Fullam and Gessler, 1946 ), but this method did not meet with a great deal of success. Rosza and Wyckoff (1950) treated their plastic-embedded specimens with amyl acetate for a short time, while benzene (Dempsey, 1953), toluene (McCulloch, 1951), and xylene (Massey, 1953) have been variously used for periods of up to thirty minutes. Hillier and Canaan (1951)

proposed sublimation of the plastic by the electron beam, and Watson (1953<sup>a</sup>) used this method as a means of increasing the contrast of his material with apparently satisfactory results.

A number of investigators (Palade, 1952; Sjostrand, 1953a) maintain that any attempt to remove the embedding matrix is bound to introduce distortion and artifacts of the type discussed in detail by Porter and Blum (1953). Unfortunately, it is difficult to assess the exact effect of removing the matrix from a particular section, because, unless it is subjected to the full beam intensity during the first few seconds of exposure in the microscope, with consequent sublimation of the plastic, the effect of the beam is to render plastic and Formvar impervious both to further electron bombardment, and to the action of solvents.

In the present investigation, none of the methods mentioned above was found to give consistently satisfactory results, as judged by the preservation of the fine detail which would be expected to be present in a particular tissue. In addition, while some areas of a section appeared quite normal, adjacent ones were found to be badly distorted.

After some trials with other solvents, the following

method was adopted as giving satisfactory results. As soon as the ribbon of sections had been lifted clear of the liquid reservoir, and while it was still wet, a few drops of acetone were allowed to drop on to the mount from a micro-pipette. The acetone, being miscible with water, diffused at a constant rate and reached the plastic in gradually increasing concentration, thus avoiding one of the sources of distortion present when other solvents were used. The mount was allowed to remain in contact with the acetone for 15 seconds, and was then transferred rapidly to a Petri dish containing fresh acetone, where it was left for a further 10 seconds. Thereafter it was removed, dried by contact with a piece of filter paper, and shadowcast in an "Edwards" Coating Unit, using palladium deposited at an angle of  $\tan^{-1} 2:1$ .

### 3. DISCUSSION OF TECHNIQUES

#### a) Estimation of Section Thickness by Interference Colours

The production of interference colours by thin films is treated fully in standard text-books on optics (for example, Jenkins and White, 1952). Briefly, the phenomenon is due to the reflection of light from the two surfaces of the film, interference taking place when the phases of the two reflected wave trains stand in a definite relationship to one another. The interference may be either destructive or cumulative, and, with white light, it follows that different parts of the visible spectrum will be destroyed and reinforced simultaneously. The resultant colour will depend on the combination of these two factors, which will, in turn, depend on the angles of incidence and reflection, the thickness of the film, and the index of refraction of the material of which the film is composed.

Because of the inter-play of these factors, the colours which are visible vary in an irregular manner with the film thickness. A theoretical treatment, in the case of plastic-embedded sections floating on a water surface, leads to the conclusion that simultaneous first order destruction and reinforcement of different parts of the spectrum, which provides the brightest

colours, takes place between about 900 Å. and 1,400 Å., while higher order interference persists up to a film thickness of about 6,000 Å., the brightness falling off gradually towards this value as the high-order wavelengths of destruction and reinforcement become closer together. Between about 600 and 900 Å., reinforcement alone is responsible for visible colour, which is correspondingly less bright for films of this thickness, while below about 600 Å., colours cease to be observed as the maximum wavelength of interference passes into the ultra-violet region.

In practice, the edge of a section thicker than about 1,500 Å. is clearly visible on the surface of the liquid, and such sections may, therefore, be rejected regardless of colour. Below this value, the section edge ceases to be definable, and, with decreasing thickness, very bright interference colours alone indicate the position of the ribbon, down to a thickness of about 1,000 Å. Pale shades such as pink or gold indicate a thickness of between 500 and 1,000 Å., while below this value, colours cease to be visible, and only the direct reflection of light indicates the presence of the sections, which consequently have a grey appearance.

While these figures for colour/thickness relations

are approximate, being based on the degree of electron opacity exhibited by sections which display them, they are, nevertheless, in reasonable agreement with theoretical predictions. Porter and Blum (1953) have observed a relationship of a similar nature between section thickness and interference colours. In the present work, only those sections which displayed very pale colours were used to obtain high-resolution micrographs.

b) Advance Mechanisms

While, in theory, mechanical methods of advance provide the most accurate section thickness, there are a number of factors which tend, in practice, to reduce this accuracy considerably. With the very small periods of advance which are required in thin sectioning, effects such as backlash, variable thicknesses of lubricating oil films, and thermal effects are sufficient to cause considerable deviation from the nominal thickness from section to section. At the minimum advance of 0.1 micron, using razor blades for cutting, the variation, as judged by interference colours, was as much as 30% to 50% of the nominal value, so that sections appreciably thinner than this were produced with a sufficiently sharp blade. Provided that sufficient time was allowed for thermal

equilibrium to be established before cutting began, it was ascertained that such variations were due to variation in the advance mechanism, since, on setting the advance to zero, no sections were cut.

In the case of glass knives, however, thermal drifting was found to persist for a much longer period, probably due to the lower thermal conductivity of glass. Far from being a disadvantage, however, thermal drift enabled ribbons of very thin sections to be obtained in many cases. The procedure was to set the advance to zero, and to cut a ribbon with the motor drive connected. Examination of this ribbon for interference colours with a binocular microscope or hand lens indicated its suitability for mounting. Should a series of such ribbons be required, it was frequently sufficient to move the illuminating lamp (normally positioned about two feet above the apparatus) gradually closer, when the thermal effects enabled as many as a dozen ribbons to be cut over a period of an hour.

Hartmann (1951) also used the zero-advance method to obtain sections thinner than those provided by the normal mechanical advance. He believed that the effect was due to compression of the plastic on the first cutting stroke, with subsequent slow expansion. However, in view of the observations mentioned, in

particular with regard to the different results obtained with steel and with glass knives, it seems more probable that thermal expansion effects are responsible.

c) Section Defects

The more obvious defects, such as knife marks, wrinkling, and tearing, are fairly easily recognised. It has occasionally been noticed, however, that ribbons of sections which are otherwise satisfactory have been spoilt by the occurrence of a regular banding effect, which takes the form of a series of characteristic thick and thin striations across the section, at right angles to the direction of cutting. The effect has been noted by Rhodin (1954) among others, but an analysis of its cause does not appear to have been made.

It is possible that the cross-banding is caused by a periodic vibration of the knife at its natural frequency during the time its edge is actually in contact with the block during cutting. It may be remedied by reducing the clearance angle between the front facet of the knife nearest the block and the direction of movement of the block. If razor blades are used for sectioning, a value of clearance angle between front facet and block of more than about  $20^{\circ}$  generally causes banding. The angle between the two blade facets is set, by the honing operation, to  $28^{\circ}$ , so that it may

be said that an angle between the back facet and the block face of less than  $50^{\circ}$  is necessary if freedom from this effect is to be expected.

That it is, in fact, the back facet which is the significant factor with regard to banding can be seen by considering a glass cutting edge. The clearance angle for a  $45^{\circ}$  glass knife of the type normally used must be maintained very small, not more than five or six degrees at most, and attempting to increase it causes pronounced banding. If, due to a slightly inaccurate measurement of the glass strip prior to breaking, a larger angle is given to the cutting facets, it is generally found that the knife will not cut in any position without banding occurring. On the other hand, with a smaller-angled knife, greater latitude in setting up becomes possible. Good knives with angles between the facets of less than about  $40^{\circ}$ , however, are hard to obtain, and are generally so irregular in shape as to present other alignment difficulties.

One further defect which occurs, more especially with the very thinnest sections, is compression. It is fairly easy to recognise compressed sections as they rest on the liquid surface after cutting, particularly if the block face is trimmed to a square. Compressed sections will then be rectangular, rather than square.

Compression is accompanied by slight tissue distortion, as evidenced in the electron microscope. Its occurrence depends to a slight extent on knife edge sharpness, but to a much greater degree on block hardness. The tendency for compression to occur is greatest with a soft block, although it appears to a slight extent on all extremely thin sections. Frequently, a block which yields badly compressed sections will, if allowed to remain at room temperature for a few days, harden sufficiently for subsequent cutting to be carried out with a negligible degree of compression.

CHAPTER 2. THE SPINAL CORD AND THE SPINAL NERVES. THE SPINAL CORD IS THE PART OF THE CENTRAL NERVOUS SYSTEM WHICH IS CONTAINED WITHIN THE SPINAL CANAL OF THE VERTEBRAL COLUMN. IT IS A LONG, TAPERING, CORD-LIKE STRUCTURE WHICH IS SURROUNDED BY THE SPINAL FLUID. THE SPINAL CORD IS DIVIDED INTO SEVERAL SEGMENTS, EACH OF WHICH IS ASSOCIATED WITH A PAIR OF SPINAL NERVES. THE SPINAL NERVES ARE COMPOSED OF AXONS OF NEURONS WHICH HAVE THEIR CELL BODIES IN THE SPINAL CORD. THE SPINAL CORD AND SPINAL NERVES ARE RESPONSIBLE FOR THE TRANSMISSION OF NERVE IMPULSES BETWEEN THE BRAIN AND THE REST OF THE BODY.

### CHAPTER 3.

### THE STRUCTURE OF THE SPINAL GANGLION CELL.

## 1. DESCRIPTION

A great deal is known about the structure of the nerve fibre and the nature of the nerve impulse, about the synapse and transmission, summation and facilitation. It is also known that without the cell body, its processes, axon and dendrites, cannot function, and recently some effort has been made to assess the significance of the geometrical arrangement of groups of nerve cells.

There remains the structure of the cell itself; its size and shape, the form of the nucleus, the nucleolus, and the cytoplasmic elements which together must express a cell metabolism integrated to the function of the central nervous system.

The considerable literature on the histology of the ganglia as a whole has been reviewed elsewhere (Bacsich and Wyburn, 1953). This work is concerned with the intra-cellular structure of the spinal ganglion cell as revealed at the higher resolution of the electron microscope.

There are only a few published electron microscopic studies devoted to the nerve cell - Palay and Wissig (1953), Hartmann (1953), De Robertis and Sotelo (1952) and Palay and Palade (1953). Beams, van Breemen, Newfanf and Evans (1952) include electron micrographs

in their report on the structure of spinal ganglion cells, but many of their preparations were treated with silver and are difficult to interpret. Up to the present time, electron microscopic studies of nerve cells have failed to produce any general agreement on the fine structure of the neuron. For example, there is as yet no clear conception of the physical background substance or the structure of the nuclear membrane of the spinal ganglion cell.

The characteristic features of the spinal ganglion cell are the cellular capsule, the structure of the cytoplasm, the nucleus and the nuclear membrane. Figure 11 is a low magnification electron micrograph of a complete cell, in which these features are clearly visible.

#### a) The Cellular Capsule

The ganglion cell is surrounded by a capsule of fine connective tissue fibres enclosing a ring of satellite cells in close contact with the nerve cell. According to Penfield (1932) each cell is surrounded by a sheath of reticular fibres, enclosing the capsule cells; and Cajal (1906), and Dogiel (1896) have described and illustrated the axon of the nerve cell, forming a pericellular nerve skein and complicated lamellar figures between the nerve cell and its cellular capsule.

In any field showing a group of ganglion cells, there may be pairs of cells within a common capsule, as, for example, in Figure 12. Figure 13 shows a capsular cell with a section of an axon in its cytoplasm. The axon is quite distinct from the nucleus of the cell, and the substance is similar to that of the nerve cell cytoplasm (Figure 14), with characteristic small mitochondria in both nerve cell and axon. The pericellular course of the axon is within the substance of the capsular cells, and, in this respect, resembles the small nerve fibres which Hess and Lansing (1953) have described running through the Schwann cell cytoplasm.

Between the ganglion cell and the capsule cell, there are a number of dense striae, which either run in bundles, or as separated strands forming an irregular pattern within the substance of the capsule cell. In appearance, density and size these striae resemble the myelin lamellae, and are regarded as lamellae of lipid material, probably in continuity with the myelin sheath of the nerve fibre.

Figure 15 shows a pair of cells sharing a common capsule and separated by an irregular line of dense material in continuity with, and obviously part of, the intracapsular lipid lamellar system. The spinal ganglion

cell, therefore, has the same general structural organisation as a nerve fibre; the neural substance within an envelope of lipid material is enclosed in a cellular sheath surrounded by a condensation of fine collagen fibrils. This is in accordance with the observations of Ghinn (1938), who finds a birefringence of the nerve cell membrane, indicating the presence of orientated lipid molecules and protein molecules 'suggesting a lipo-protein membrane similar to the nerve sheath in character'.

## b) Cytoplasm

### (i) Nissl's Substance

Sections of frozen-dried spinal ganglia, prepared as described on page 45, show in the light microscope some variation in cell size, but there is no outstanding difference between the cells on the basis of the quantity or quality of the Nissl's granules. The relative density or darkness of osmic-acid-fixed material observed in the electron microscope is an indication of electron scattering power which, in osmophilic structures, will be increased by the deposit of osmium. In contrast to the apparent uniformity of the intracellular structure of the ganglion cells observed with the light microscope, the electron microscopic examination of a large number

of sections of spinal ganglia shows two distinct cell types, correlated, not with size difference, but with the mode and distribution of Nissl's material. On the basis of this difference, it is possible to distinguish the two types - light and dark cell - which, in a fortunate section, may be present in the same field, as in Figure 17. Typically in the light cell, the Nissl's substance occurs as discrete aggregates of dense material of 1 to 2 microns in diameter. Figure 16 is an example of a light cell, while Figure 18 shows a light cell, contrasted with a dark one (Figure 19). The Nissl's aggregates are less dense and much larger than the mitochondria, from which they are quite distinct. They are distributed throughout the entire cytoplasm, including the perinuclear region. In the dark cell, the Nissl's substance is not arranged in aggregates, but is diffusely dispersed throughout the cell, giving a more homogeneous and denser appearance to the cytoplasm, so that the cell, as a whole, is darker, as in Figure 19.

In both cell types the basic structural component of Nissl's substance is an electron optically dense, finely granular material of particle size in the region of 50 to 200 Å. A single aggregate of Nissl's material is illustrated in Figure 20. The aggregates themselves are not of uniform density, but have darker areas where

there is a closer packing of the granules. Here and there, as in Figure 20, there is evidence of a lamellar orientation of the granules which may be due to the adsorption of the granules on to a reticulum. At times, in the dark cell, there is evidence of an orientation of the cytoplasm round the nucleus, as in Figure 21. Although in Figure 22 there are parallel running striae in the cell cytoplasm resembling the "endoplasmic reticulum" of Porter (1954), within the Nissl's aggregates themselves the granules are the conspicuous structural units. The close packing of the granules may, of course, mask an underlying structure, but the appearance of the aggregates is, in the most favourable sections, quite different from the basophilic component of, for example, acinar cells of the pancreas or parotid glands, where the prominent morphological characteristic is a series of parallel running filaments or striae representing profiles of a system of canniculi or thin-walled vesicles associated with granules of size range comparable to those of Nissl's material, which are the macromolecular units responsible for the basophilic reaction (Palay and Palade, 1953). Haguenu and Bernhard (1953) also found that the essential component of Nissl's material consists of granules from

70 Å. to 140 Å. in diameter, arranged in short parallel fibrils or in a very fine reticulum. The structural conformation of Nissl's substance, they concluded, was quite distinct from the filamentous "ergastoplasm" observed in other cells.

(ii) Neurofibrillae

The electron optical density of the nerve cell cytoplasm of both the dark and the light cells is largely, if not entirely, due to the Nissl's substance. In the clear patches of the cytoplasm between the Nissl's aggregates in the light cell, it is possible to show a background network of fine filaments (Figure 23). The filaments vary in width from 20 Å. to 50 Å. They have a discontinuous beaded appearance, random distribution and orientation, and form here and there loose bundles in which the individual unit filaments are still apparent. Figure 24 shows a section of axon of comparable thickness and magnification, with a similar filamentous network. These filaments are of the order of size of large organic molecules, and are probably protein. They may, in fact, correspond to the 'tangentially orientated protein molecules' which polarised optical studies indicate are present in the cytoplasm of nerve cells (Chinn, 1938).

This network of filaments is quite different from

the cytoplasmic fibrils described and shown by Hartmann (1953), which resemble rather the striae of 'endoplasmic reticulum'; and it is of quite a different size range from the coarse fibrillae of the silver preparations of Beams et al (1952). Its demonstration has been found to depend on very rapid fixation, followed by careful dehydration and embedding.

(iii) Mitochondria

The mitochondria are the densest structures in the cell cytoplasm, and in this respect, are comparable to the nucleoli. Figures 25 and 26 show the general organisation of the nerve cell mitochondria. They have an average size in cross section of 0.25 micron, and are much smaller than the mitochondria of the cells of the intestine (Palade, 1953), or those of the kidney tubule cells (Rhodin, 1954), which measure as much as 1 to 4 microns in length, and 0.3 to 0.7 micron in cross section. Figure 27 shows mitochondria from rabbit ovary, measuring about 1.5 micron by 0.4 micron. Comparison with nerve cell mitochondria shows that, while the internal structure of the latter is not so well-defined or regular as in the larger mitochondria, they have the same general organisation, with a double limiting membrane and internal structural arrangements resembling the

double lamellae of the typical mitochondrial cristae, as, for example, in the mitochondria of Figure 26. They are uniformly distributed throughout the cell cytoplasm. The limiting factor in the size of the mitochondria of the neuron is probably the width of its processes. While it is possible that the axon can deal locally with the routine maintenance of its own mitochondria, some migration of mitochondria from cell to axon seems likely to be a normal procedure in development and repair.

### c) Nucleus

#### (i) Nucleoplasm

The details of nuclear structure observed in electron microscopic studies up to the present have been disappointingly few. The nerve cell provides no exception. In well-fixed specimens, the nucleoplasm is either uniformly granular in appearance (Figure 29), or else 'matted', with small clumps of material distributed evenly throughout the nucleus (Figure 29). This difference is not related to the occurrence of 'light' or 'dark' cells, and nuclei have been found with all gradations from the almost homogeneous granular aspect to the heterogeneous 'clumpy' appearance. Sometimes, but by no means always, the

granular appearance is accompanied by a crenated nucleus (Figure 31). In both cases, the fundamental substance appears to be the same, namely a fine solid granular material of indeterminate structure. There is no suggestion of any ordered background, nor does the nuclear material itself seem orientated in any preferred direction.

Here and there throughout the nucleus are scattered flakes of chromatin, which are recognised by their greater electron density. In sections cut near the centre of the nucleus there are also visible one or more prominent nucleoli. Frequently, flakes of chromatin are found in close contact with the nucleolus (figure 32), or in close apposition to it.

The nuclei themselves are oval or round in shape, and have a regular limiting membrane. Occasionally, however, deep indentations accompanied by breaks are visible (figure 30), or the membrane may have the crenated appearance already mentioned (figure 31). The structure of the nuclear membrane is described in detail on page 66.

(ii) Nucleolus

The dark, strawberry-like nucleolus with irregular contour is characteristic of the spinal ganglion cell (figure 32). Occasionally, there are two nucleoli in

a nucleus (figure 33). The nucleoli are amongst the densest objects in the cell, and, while they generally have a characteristic vacuolated or fenestrated appearance, they occasionally appear as a completely solid, black mass. This great density of the nucleolus has made it a rather unfavourable structure for electron microscopic study. Even in the thinnest sections, there is no discernible ultra-structural background in the dark-staining material of which it is composed, nor was any evidence obtained of a limiting membrane. This is in agreement with the observations of Borysko and Bang (1951) on the nucleoli of normal and pathological cells, and also with those of Danon (1952), Dempsey (1953) and Hartmann (1953). The intensity of staining indicates structural density, probably increased by osmium deposition.

In shadowed sections, this structural density is emphasised by the manner in which the nucleolus is raised above the surrounding nucleoplasm (figure 34), while the vacuolated appearance is shown to be in fact due to the presence of vacuoles, and not to the inclusion of solid material of low electron density which might equally be inferred from the unshadowed micrographs.

Even with the aid of shadowed preparations, it is difficult to interpret the sectioned nucleolus in terms

of structure. The vacuolisation could be due to thick strands forming a skein, or to twisted tubules cut in section. The nucleolus is said to represent reserve protein, and, according to Caspersson (1950) and Hyden (1943), consists of nuclear protein with a high proportion of histone, and is the main source of nuclear ribonucleic acid. In what way the typical appearance of these nucleoli is related to their structural chemistry is not known. If the views of Caspersson on protein synthesis are accepted, then the prominent nucleolus is related to the production of Nissl's substance associated with the activity of the nerve cell.

### (iii) Nuclear Membrane

It is now accepted that the nucleus has a theca or envelope, generally referred to as the nuclear membrane, forming a structural entity distinct from nucleoplasm and cytoplasm. The appearance of the membrane depends on the plane of section through the nucleus. Tangential or peripheral sections through the circumference give a direct view looking down on the surface of the membrane, while a perpendicular or radial section through the centre of the nucleus generally cuts through the nucleolus and shows the nuclear membrane in a plane at right angles to the tangential section. Thus the picture of the membrane

differs in the two types of section and can be combined to construct a three-dimensional perspective.

Figure 35 represents a tangential section and shows a broad zone of membrane, approximately two microns by one micron in a section estimated to be 0.1 micron in thickness. After 'optimum' fixation, the most prominent features in tangential sections of the membrane are disc-like nodes with an average diameter of 850 Å., irregularly spaced in the substance of the membrane at a separation distance of from 250 Å. to 1,800 Å. Figure 36 shows a section of a nuclear membrane rather nearer the centre of the nucleus. Approximate estimates give a value of 10,000 for the number of nodes present on the entire nuclear membrane. At a higher magnification, the nodes are seen in more detail (figure 37). There is a dark cortex, a central dark spot, and an intervening lighter area.

Figure 38 is a shadowcast micrograph of a peripheral section where the methacrylate was extracted before shadowcasting. The nodes show in sharp relief above the rest of the structures, and have a raised cortical and central part separated by a depressed area. The nodes appear to be solid structures embedded in the nuclear membrane, and, compared with the rest of the material in the section, have suffered relatively little distortion in the extraction process.

In radial section, the total thickness of the membrane varies from cell to cell, and, in fact, is not uniform round any single nucleus. In general, the measured thickness lies between 600 Å. and 1,000 Å. The membrane itself is made up of two principal components, the nodes and the continuous supporting membrane. The nodes are less transparent to the electron beam than the continuous membrane and even in low magnification micrographs of radial sections they show up as dark bands on the membrane (figure 39). The precise structural details visible vary from membrane to membrane and indeed show differences within the same membrane. Not all of these are due to variations in the angle of cutting. Small areas from individual membranes all cut at approximately the same level are shown in Figures 40, 41, and 42. Figure 40 shows an area of nuclear membrane where both the nodes and supporting membrane are well resolved. The dark areas A, B, C, D, and E correspond in size and spacing to the nodes seen in tangential sections, and are about 800 Å. to 1,000 Å. in both dimensions. The osmophilic material of the nodes is located within a double wall which traverses the membrane thickness. The pore marked A shows this double wall. The osmium-absorbing characteristics of this wall suggest that it is composed

of two lipid layers with an intervening protein layer. Some of the general density of the nodes could represent material streaming through the nuclear membrane between the lipoprotein layers, which would, therefore, form the cylindrical bounding wall of a central canal or pore.

The supporting membrane shows stratification into layers parallel to the nuclear circumference - in favourable sections as many as 7 or 8 layers may be visible. The layers are spaced 100 Å. to 150 Å. apart, and are of low electron absorbing power, and, therefore, low density. This may be due to their failure to retain osmium, and suggests that they are predominantly protein in nature.

Figure 41 shows another type of radial section. The supporting membrane is more clearly defined than the pores, which suggests that here the lipid is partially dispersed along the plane of the continuous membrane. In this particular cell, the nucleoplasm and cytoplasm are of less than normal density, but, since the membrane itself is of more than average density, this transparency is not due to a decrease in section thickness. This variation in the density, thickness and distribution of structural components is normal in sections of nuclear membranes cut from blocks of tissues where 'optimum' fixation had been obtained.

Figure 42 is a radial section showing the non-uniformity of the membrane structures round a single nucleus. The two types of structural features, the nodes and the supporting membrane, are visible in different parts of the membrane.

d) Nerve fibre

In longitudinal sections of nerve fibres, the myelin sheath is broken up into lamellae of 500 to 600 Å. thick. These are aggregates of smaller lamellae. Hess and Lansing (1953) describe an alternation of narrow bands of 80 Å. with thicker bands of 160 Å. Examination of the myelin sheath at high resolution enables it to be resolved into individual dark parallel lines, representing the lamellae of which it is built up (figures 24 and 43). The thickness of the dark lines is about 85 Å., while the intervening lighter spaces are about 110 Å., although there is some variation in these dimensions along the fibre. This may be attributed to variations of the plane in which the myelin has been sectioned, since the true spacing will only be evident where the myelin lies at right angles to the direction of cutting.

Figure 45 is a micrograph of a section of nerve fibre which has been extracted and shadowed. The thicker lamellae, of 500 Å. or more in width, are visible,

but the individual unit lamellae are not seen in shadowed sections. This may be taken as an indication that they are separated from each other, not by spaces, but by material of low electron density, probably protein, as suggested by Finean (1954). The neurilemma is not visible, but the endoneurium, represented by strands of connective tissue, can be seen at the outer edge of the myelin.

A typical small myelinated nerve fibre with Schwann cell is shown in Figure 44. This is an extracapsular fibre, and therefore, although the cell and particularly its nucleus resembles a capsular cell, in virtue of its position relative to the nerve fibre it is now a Schwann cell. The nucleus occupies most of the cell body, and there is a well-defined nuclear membrane with a cell membrane 300 Å. thick. This corresponds to the Schwann membrane described by Hess et al (1953) and considered by them to be the same as the neurilemma.

#### e) The Effect of Delayed Fixation on Nervous Tissues

The neuron is adapted for rapid metabolic response, and is therefore susceptible to any delay in fixation. Fixation for the electron microscope, since it involves the diffusion of slowly penetrating osmic acid, presents particular difficulties in this respect. It has been

found that, even with the utmost precautions, fixation of a series of blocks does not give 'optimum' results in every case, although the electron microscope offers the advantage of facilitating the recognition of poorly-fixed blocks once the appearance of the normal tissue has been established.

Figure 46 is a section of tissue where there was a delay in fixation amounting to between one and two minutes. The cytoplasm is fairly normal, but the nucleus and nuclear membrane have begun to show slight distortion which is almost certainly due to post-mortem change. This change is still more apparent in Figure 47, showing tissue where fixation was delayed by up to five minutes. There appears to be an increase in electron density in the cell substance, which has shrunk leaving irregular clear spaces. There is evidence of a new structural arrangement in the form of globules of approximately spherical or hollow spherical character, probably representing a lowest common denominator of the various tissue components in the cell. A still more advanced stage in the process of degeneration is represented by Figure 48. Here, the time between death and the commencement of fixation was about twelve or fifteen minutes.

The delay also causes structural changes in the nuclear membrane, shown by figure 49, which is a radial section cut through a nuclear membrane of the same tissue as that of Figure 46. Some shrinkage of the nucleus is evident from the clear area between the nuclear membrane and the cytoplasm. The osmophilic material is apparently organised into spheres of the type described above, and seems detached from the membrane. It is evident that, even with this very short delay in fixation, time the membrane constituents begin to dissociate and regroup into a new pattern. Where there was appreciably delayed fixation the sectioned blocks had no nuclear membranes of the type illustrated.

## 2. DISCUSSION

The cytoplasmic structure of the spinal ganglion cell is complex. According to Penfield (1932), the cytoplasm contains Nissl's granules, Golgi substance, mitochondria, neurofibrillae, and black and yellow granules. The aim of this work was to re-investigate intra-cellular structure at the high resolution now available with the electron microscope.

### a) Nissl's Substance

After fixation and staining with toluidine blue, Nissl's material appears in the light microscope as rod-shaped granules varying in density and distribution in different nerve cell groups, and in the same cell from time to time. The particular physical form the substance assumes probably varies with the chemical treatment of the tissue. According to Pease and Baker (1951), after a coarse fixation, Nissl's substance is represented as a flocculent precipitate.

It is now accepted that Nissl's substance is the basophilic component of the nerve cell cytoplasm. Ultra-violet spectrophotometry, together with histochemical tests based on ribonuclease digestion, indicate that the chemical nature of the basophilic substance is ribonucleoprotein. The granules which, within the limits of available resolution, represent the unit

structure of Nissl's substance, thus contain ribonucleoprotein. whether Nissl's material exists in the living cells as the discrete aggregates found in the fixed preparations is still uncertain. Bensley and Girsh (1933) maintain that Nissl's substance occurs as clumps of material in the living cell, and, in ultracentrifuge experiments with spinal ganglion cells (Beams and King, 1935), the Nissl's substance acts like definite masses of greater density embedded in a lighter medium and moves to the centrifugal pole. On the other hand, ultra-violet photomicrographs of living spinal ganglion cells (Koenig and Feldman, 1954) show absorption curves characteristic of RNA with a homogeneous distribution of the absorbing material throughout the cell cytoplasm and its processes, while in the fixed preparation, the distribution of the absorbing material is heterogeneous.

It is, of course, well known that there are variations in the physical form and quantity of Nissl's substance in different nerve cells, and the electron microscope has revealed differences in the texture of the cytoplasm of the cells of the same spinal ganglia, as in the 'light' and 'dark' cells. This difference is unlikely to be due to any fixation artifacts since the two types of cell are randomly distributed in the

sections examined, without reference to any particular position in the blocks which could affect the time of fixation. The pattern of cytoplasmic basophilia, whether a discrete or diffuse arrangement of RNA granules, is characteristic of the nerve cell, and presumably is determined by the particular functional requirements of the neuron. There is a size spectrum of peripheral nerve fibres connected to the cells of the spinal ganglion which is related to the different cutaneous sense modalities. There is also a size range of cells in the spinal ganglia which it is reasonable to assume has a similar functional significance, and, if this is so, each functional group of neurons would be concerned with its characteristic frequency and conduction rate of stimuli. This qualitative difference at functional level might well impose some variation on the pattern of distribution of basophilic material throughout the cytoplasm in the different cell groups.

Figure 17, however, shows a pair of cells, one dark and one light, which from their juxtaposition it is assumed belong to the same functional group. Hyden (1943) has shown that the protein content of a nerve cell varies conspicuously during its normal range of activity, and if the views of Caspersson (1950)

on the protein-forming systems of cells are accepted, then the well-known differences in the Nissl's content of the resting, as compared to the active nerve cell, are simply phases in the cycle of cell activity. On this basis, the light and dark cells are stages in the cycle of depletion and restoration of Nissl's substance.

b) Neurofibrillae

The neurofibrillae of the fixed preparations of nerve cells which are just visible with the light microscope are of quite a different order of size (from 1 micron to 0.1 micron in diameter) from the fine filaments shown in the present preparations. There is no evidence, in the electron micrographs, of such neurofibrillae in the cytoplasm of the spinal ganglion cells, and in agreement with the observations of Fernandez-Moran (1952) it seems probable that the microscopic neurofibrillae of the fixed cell, like those of the fixed axon, are lateral aggregations of the finer filaments which occur during fixation. The neurofibrillae which are massed at the end of ultracentrifuged spinal ganglion cells (Beams and Kirshanblit, 1940) could also be produced by an aggregation of the small filaments during the experiment.

There is, however, evidence of a common fibrillar organisation in the cytoplasm of the nerve cell and the axon, based on the fine filaments of 20 Å. to 50 Å., and these form, singly or in groups, the structural units in both cytoplasm and axoplasm. In an electron microscopic study of cultured embryonic nerve tissue, De Robertis and Sotelo (1952) found that fine strands appear in the homogeneous matrix of the cytoplasm of the developing and differentiating nerve cells. Sections of axons within the cellular capsule of the cell have axoplasm with mitochondria and filaments indistinguishable from the cytoplasm of the adjacent cell, as in figures 13 and 14. The axon filaments show orientation in longitudinal sections, but there is no evidence of aggregation into neurofibrillae. Meyer (1954), in an electron microscopic study of nerve fibres grown in vitro, describes a fine longitudinal striation of fibrils of 250 Å. to 400 Å. in diameter - considerably thicker than the filaments of 20 Å. to 50 Å. It is unlikely that there exist two size ranges of structural conducting unit in different types of axon, and a more probable explanation is an aggregation of the finer filaments during fixation. It is not surprising to find that the axon, as an extension of the cell cytoplasm, has the same

morphology, filaments, mitochondria, and, according to De.Robertis and Franchi (1953), small granules (Nissl's substance?). As a corollary, it could be expected that the axon should participate in the metabolic activity characteristic of the parent neuron.

c) Nuclear Membrane

The special interest in the structure of the nucleocytoplasmic boundary is related to its function both as a cellular interface, at which chemical reaction takes place, and as a structural barrier between the nucleus and the cytoplasm.

The phasic activity of the nerve cell requires an adaptive intracellular organisation capable of the necessary metabolic responses. While the nature of the influence of the interphase nucleus is, as yet, not at all clear, the evidence from experimental work indicates that it has some effect on cytoplasmic protein synthesis, and recent observations on the behaviour of nucleoli in chromatolytic neurons (Lindsay and Barr, 1955) suggests that the nucleus is concerned in the synthesis of Nissl's substance. This implies a free interchange of material between the cytoplasm and the nucleus, and special structural arrangements at the nucleocytoplasmic boundary to permit this two-way molecular movement.

Holtfreter (1954) has pointed out that although both nuclear membranes and cell membranes are predominantly proteins and lipids, the nuclear membrane does not act as a semipermeable membrane, but, as he has demonstrated, the thick nuclear envelope of amphibian oocytes offers no obstacle to the free passage of medium-sized protein molecules, such as haemoglobin. This functional difference must have a structural basis. Callan and Tomlin (1950) examined isolated specimens of the nuclear membrane of amphibian oocytes with the electron microscope. They described an outer layer studded with a regular pattern of 'pores'. Similar units were later reported by Gall (1954), who repeated this work, and recently by Pollister, Gettner and Ward (1954) who examined thin sections of the same material. Holes or pores in the nuclear membrane of 'Amoeba Proteus' have been reported by Harris and James (1952), Bairati and Lehman (1952), and more recently by Bahr and Beerman (1954). Afzelius (1955) has recently examined the nuclear membrane of various sea urchin and starfish oocytes with the electron microscope, and describes a double membrane studded with pores which in this case appear to be solid structures. Apart, however, from casual references to the occurrence

of 'ring-like' structures in an odd section of the nuclear membrane (De Robertis, 1954 and Rhodin, 1954), nothing resembling the pores of the nuclear membrane of the amphibian oocyte has been recorded in the electron microscopic reports on the structure of the nuclear membrane of cells of vertebrate tissues.

Semipermeable membranes consist mostly of proteins and lipids, but, functionally, the nuclear membrane is different from a cell plasma membrane. It is known that quite large constituents can pass through the nuclear membrane. For example, in the ovary of certain Crustacea and Hemiptera, large droplets of nucleoprotein (possibly molecular fractions of the gene complex) are extruded through the nuclear membrane, and entire nucleoli may pass through as well. (Lison and Fautrez-Firlefyn, 1950, and Schrader and Leuchtenberger, 1952).

Moreover, apart from the characteristic behaviour of nucleoli in nerve cells, there are reports of more spectacular changes such as multiplication, swelling, and subsequent extrusion of nucleoli during the secretory phases of certain insect gland cells. Another unique feature of the nuclear membrane is, of course, its quite sudden dissolution at the end of prophase, and its reappearance at telophase,

when it is formed in the first place from the bounding material of the chromosomes.

The current conception of the structure of the nuclear membrane is based on optical tests which indicate that there are orientated arrangements of molecules at the nuclear boundary. Chinn (1938), from polarised optical studies of the nuclear membrane, found evidence of a lamellar arrangement of orientated protein molecules. Monné (1942) believes that the nuclear envelope is a double membrane consisting of a firm nucleo-protein layer free of lipids and a thin cytoplasmic protein-lipid layer. It is reported, however, that the optical properties of the nuclear envelope change after fixation, and that in living nuclei there is no optical anisotropy, a birefringent nuclear membrane only appearing after fixation (Baud, 1949). Nevertheless, phase contrast microscopy of living cells confirms the presence of a physical membrane between the nucleus and the cytoplasm. (Frey-Wyssling, 1953).

The nuclear membrane is commonly shown in electron micrographs of thin sections as double, occasionally triple, parallel lines of increased density which are interpreted as lamellae cut in section (Porter, 1954; Sjostrand and Rhodin, 1953). In his electron micro-

scopic study of nerve cells, Hartmann (1953) comments on the variations in thickness and structure of the nuclear membrane within the same cell group. He gives a range of thickness for the membrane of from 200 Å. to 600 Å., compared with the figure of 1,000 Å. estimated by Pease and Baker (1951), also for the nuclear membrane of nerve cells. The difference is probably due to variations in the angle of the section cutting through the nucleus. Watson (1954) has described pores in the nuclear membrane of pancreatic cells, and gives an approximate estimation of 10,000 pores for the entire nuclear membrane. His pores, however, are shown as simple interruptions in the continuity of a lamellar membrane, and are quite different from the nodes of the nuclear membrane of spinal ganglion cells.

The term 'pore', 'hole', or 'canal' as applied to the structure of the nuclear boundary is misleading - there can never exist in the living cell any pore or hole empty of material; and, as Holtfreter (1954) states, any gaps will be covered by a film of some substance, possibly phospholipids.

Figure 50 is a three-dimensional diagram of the nuclear membrane, which is based on an interpretation of the tangential and radial sections seen in the micrographs, figures 35 to 42. The nodes are solid cylind-

rical units with thick walls and a centre filled with material diffusing through the membrane; not merely circular gaps or holes in a flat layer of material. Such an interpretation would, to some extent, reconcile the findings of Callan and Tomlin (1950) with those of Gall (1954), who regarded the pores as solid granules made up of a number of smaller spherical units. Holtfreter (1954) has stated that dehydration of the lipid layer of the nuclear membrane may cause disintegration and consequently a granular appearance. The nodes seen in tangential sections of the nucleus are much too regular to be artifacts, and although, of course, they may have undergone some changes as compared to the living structure, their presence in the fixed specimens indicates that the membrane is not a homogeneous structure, but has a pattern of regions with a characteristic morphology.

The nodes of the nuclear membrane of the spinal ganglion cell and the pores of the nuclear membrane of amphibian oocytes are broadly comparable in structural pattern and size order - remarkably so considering the different preparatory techniques. The annuli described by Afzelius (1955) as occurring in the nuclear membrane of sea-urchin oocytes also bear a very close resemblance to the nodes described in the present work.

The nuclear membrane, therefore, unlike the permeable plasma membrane, is not a uniform arrangement of structure, but has differentiated regions, probably basically of a similar nature, but variously identified, in a range of cell types, as pore, nodes, granules or ring-like formations.

The variation in the structure of different regions of any one nuclear membrane is common to adjacent cells in sections of carefully fixed material, and is, therefore, unlikely to be due to fixation artifacts. If the membrane is to act as phase boundary in the living cells, controlling both the flow of small-sized ionic molecules and large-sized proteins and nucleoproteins, then it clearly cannot be a simple osmotic barrier excluding only in terms of molecular size. It must have some mechanism whereby it can act selectively, in certain circumstances, even allowing the diffusion of large molecules and rejecting small molecules. The normal range of structural difference which can occur in nuclear membranes suggests that the selective mechanism is a phasic structural rearrangement affecting part or the whole of the membrane. The nuclear membrane is, in fact, a labile structure. It is suggested that the nodes are the units regulating the selective permeability of the membrane, since they have

been observed most frequently in active nuclei, for example oocytes and nerve cells. According to the present interpretation, the nodes are lipo-protein-lined pores some 1,000 Å. in diameter and 1,000 Å. thick, and should allow the passage of large molecules - the type of diffusion reported by Holtfreter. The more closely-knit type of structure with the apparently continuous lipid layer, or the double membrane type of structure reported by Sjostrand and Rhodin (1953) and by Palade (1953) represents a functionally inactive phase impermeable to large-sized components.

There is not enough known about the detailed structure and disposition of molecular components in the membrane to allow more than speculation on the movements within the membrane which determine the regional change in structural pattern. It may be that the lipids in the membrane have surface-active substituted groups, and that these groups are adsorbed by a diffusing component when presented at the interface. This adsorption could initiate the migration of the lipids and hence the membrane reorganisation. Other examples of the surface reorganisation of lipid are known in biological studies of surface structure, and the results reported here are not inconsistent with a mechanism of this type.

d) Golgi Apparatus

In electron micrographs, the Golgi apparatus of the nerve cells has been shown as clumps of dense filaments (Beams et al., 1952), as 'vesicles with an osmophilic lamellar membrane', (Hartmann, 1953), while Pease and Baker (1951) regard all such structures as artifacts.

In a number of sections examined in the present work, round osmophilic structures very similar to Hartmann's Golgi vesicles were observed, but they were not a regular feature of the properly fixed spinal ganglion cell.

Until the structural chemistry of the Golgi apparatus is understood, and it is possible to correlate its protean manifestations as an intracellular entity with known variables, it is likely to remain a polemical subject.

**CHAPTER 4.**

**FREEZE-DRYING FOR THE ELECTRON MICROSCOPE.**

## 1. INTRODUCTION

Freeze-drying as a method of fixing tissues for electron microscopy has so far been unsatisfactory. Fullam and Gessler (1946) published electron micrographs of frozen-dried liver which showed serious distortion of cellular structure. Sjostrand (1949) examined sections of mouse pancreas fixed by freeze-drying, and obtained micrographs which appeared to preserve the structure at low magnification. Later, Wyckoff (1951) in an electron microscopic investigation into the fixation and dehydration of tissue proteins, examined the effect of freeze-drying gelatin. He found that freeze-drying resulted in the formation of an open-meshwork, containing spaces which were much larger than those in non-frozen-dried material, and which could be attributed to ice-crystal formation. Apart from a micrograph of frozen-dried guinea-pig retinal rod, presented by Sjostrand (1953a) without comment on its preparation, there is no published evidence of a satisfactory result from the preparation of frozen-dried tissues for electron microscopy.

In the present work, rabbit kidney was used to test the efficiency of freeze-drying of tissues for the

electron microscope, and controls were obtained by at the same time fixing kidney tissue in buffered osmic acid. The chemically-fixed material was prepared for sectioning in the usual way, but the frozen-dried tissues were embedded directly in the monomer of polybutyl methacrylate and subsequently sectioned, using the techniques already described on pages 41 to 44.

## 2. DESCRIPTION

### a) Kidney fixed in Osmic Acid

Thin sections of kidney tissue fixed in osmic acid showed the following structural features characteristic of kidney tubule cells:

#### Brush Border

This consists (figure 51) of a series of tubular prolongations at the free margin of the tubule cells, enclosing material of density similar to that of the cell cytoplasm (Sjostrand and Rhodin, 1953). The prolongations are surrounded by an electron-dense membrane, which appears to be single (figure 52), with a width ranging from 30 Å. to 50 Å. There is no evidence of any continuous membrane uniting the prolongations adjacent to the lumen.

#### Mitochondria

Figures 53 to 55 are high resolution micrographs of mitochondria, and show the characteristic limiting double membranes, and internal cristae which also consist of double membranes. In addition, circular or elliptical rings and granules are visible, probably representing the cristae cut in cross-section.

**b) Frozen-Dried Tissue**

In the case of frozen-dried kidney, typical structures could not be observed. There was no evidence of brush border or mitochondria, or even of cell or nuclear membranes. Figure 56 shows a typical result of freeze-drying. The intra-cellular structure is completely disrupted and broken up. Such a result is consistent with the fenestration effect of ice-crystal formation.

### 3. CONCLUSION

The vacuum-embedding technique used in this investigation has enabled thin sections of frozen-dried material to be obtained, and examined with the electron microscope. This examination has shown that such tissues are unsuitable for demonstrating ultra-structure because of artifacts probably caused by ice-crystal formation. It is uncertain whether these artifacts occur during rapid cooling, or whether some, at least, is a result of recrystallisation of tissue moisture at the drying temperature of around  $-40^{\circ}\text{C}$ . This drying process has been discussed, from a theoretical viewpoint, by Harris (1951; 1954) for the tissue blocks used in light microscopy.

It is clear that the problem of freeze-drying of tissues for electron microscopic examination requires further investigation involving, in particular, the theories concerning vitrification and ice-crystal formation.

**TABLE OF**

**REFERENCES**

REFERENCES.

- AFZELIUS, B.A. (1955), *Exp. Cell Res.*, 8, 147.
- VON ARDENNE, M. (1939), *Z. wiss. Mikroskop.*, 56, 8.
- BACSICH, P. and WYBURN, G.M. (1953), *Quart. J. Microsc. Sci.*, 94, 89
- BAHR, G.F. and BEERMAN, W. (1954), *Exp. Cell Res.*, 6, 519.
- BAIRITI, A. and LEHMAN, F.E. (1952), *Experientia*, 8, 60.
- BAKER, R.F. and MODERNE, F.W.S. (1952), *J. appl. Phys.*, 23, 159.
- BAUD, C.A. (1949), *Bull. Histol. Tech. Micr.*, 5, 99.
- BEAMS, H.W. and KING, R.L. (1935), *J. comp. Neurol.*, 61, 175.
- BEAMS, H.W. and KIRSHANBLIT, H.W. (1940), *Anat. Rec.*, 76, 95.
- BEAMS, H.W., van BREEMEN, F.G., NEUFANF, D.M. and EVANS, T.C. (1952), *J. Comp. Neurol.*, 96, 249.
- BENSLEY, R.R. and GIRSH, I. (1933), *Anat. Rec.*, 57, 205.
- BORYSKO, E. and BANG, F.B. (1951), *Bull. John Hopkin's Hosp.*, 89, 468.
- BRADFIELD, J.R.G. (1954), *Nature, Lond.*, 173, 184.
- CAJAL, S.R.Y. (1906), *Ergebn. Anat. EntwGesch.*, 16, 177.
- CALIAN, H.G. and TOMLIN, S.G. (1950), *Proc. Roy. Soc.*, B 137, 367.
- CASPERSSON, T.O. (1950), "Cell Growth and Cell Function," W.W. Norton & Co., Inc. (New York).
- CHINN, P. (1938), *J. Cell. Comp. Physiol.*, 12, 1.
- CLAUDE, A. and FULLAM, E.F. (1946), *J. Exp. Med.*, 83, 499.
- COCKS, G.G. and SCHWARZ, C.M. (1952), *Rev. Sci. Instr.*, 23, 8.
- DANON, D. (1952), Thesis, M.D., 2145, University of Geneva.

- DEMPSEY, E.W. (1953), Amer. J. Anat., 93, 331.
- De ROBERTIS, E. (1954), J. Histo- and Cytochem., 2, 341.
- De ROBERTIS, E. and FRANCHI, C.M. (1953), J. appl. Phys., 24, 1421.
- De ROBERTIS, E. and SOTELO, J.R. (1952), Exp. Cell Res., 3, 433.
- DOGIEL, A.S. (1896), Anat. Anz., 12, 140.
- Van DORSTEN, A.C. (1948), Philips Tech. Rev., 10, 135.
- EAVES, G., and FLEWETT, T.H. (1954), Exp. Cell Res., 6, 155.
- EDEN, M., PRATT, A.W. and KAHLER, H. (1950), Rev. Sci. Instr., 21, 802.
- FERNANDEZ-MORAN, H. (1952), Exp. Cell Res., 3, 282.
- FINEAN, J.B. (1954), Exp. Cell Res., 6, 283
- FREY-WYSSLING, A. (1953), "Sub-microscopic Morphology of Protoplasm", Elsevier Pub. Co. (London).
- FULLAM, E.F. and GESSLER, A.E. (1946), Rev. Sci. Instr., 17, 23.
- GALL, J.F. (1954), Exp. Cell Res., 7, 197.
- GEREN, B.B. and McCULLOCH, D. (1951), Exp. Cell Res., 2, 97.
- GESSLER, A.E. and FULLAM, E.F. (1946), Amer. J. Anat., 78, 245.
- GREY, C.E. and KELSCH, J.J. (1948), Exp. Med. Surg., 6, 368.
- GREY, C.E., KELSCH, J.J. and SCHUSTER, M.C. (1948), J. appl. Phys., 19, 123.
- HAGUENAU, F. and BERNHARD, W. (1953), Exp. Cell Res., 4, 496.
- HALL, C.E. (1953), "Introduction to Electron Microscopy," 226. McGraw Hill Bk. Co. (London).
- HALL, C.E., JAKUS, M.A. and SCHMIDT, F.O. (1945), J. appl. Phys., 16, 459.

- HARRIS, R.J.C. (1951), Sympos. "Freezing and Drying," Inst. of Biol., London.
- HARRIS, R.J.C. (1954), "Biological Applications of Freezing and Drying," Academic Press, Inc. (New York).
- HARRIS, P. and JAMES, T. (1952), *Experientia*, 8, 384.
- HARTMANN, J.F. (1951), *Exp. Cell Res.*, 2, 126.
- HARTMANN, J.F. (1953), *J. comp. Neurol.*, 99, 201.
- HESS, A. and LANSING, A. (1953), *Anat. Rec.*, 117, 175.
- HILLIER, J. (1951), *Rev. Sci. Instr.*, 22, 185.
- HILLIER, J. and CANAAN, K. (1951), *J. appl. Phys.*, 22, 114.
- HILLIER, J. and GETTNER, M.E. (1950a), *J. appl. Phys.*, 21, 889.
- HILLIER, J. and GETTNER, M.E. (1950b), *Science*, 112, 520.
- HOLTFRETER, J. (1954), *Exp. Cell Res.*, 7, 95.
- HYDEN, H. (1943), *Acta physiol. scand.*, 6, Supp. 17, 1.
- JENKINS, J. and WHITE, R. (1952), "Fundamentals of Optics," McGraw Hill Bk. Co. (New York).
- KOENIG, H. and FELDMAN, D. (1954), *J. Histo- and Cytochem.* 2, 334.
- IATTA, H. and HARTMANN, J.F. (1950), *Proc. Soc. Exp. Biol. N.Y.*, 74, 436.
- LEYON, H. (1954), *Exp. Cell Res.*, 6, 497.
- LINDSAY, H.A. and BARR, M.L. (1955), *J. Anat.*, 89, 47.
- LISON, L. and FAUTREZ-FIRLEFYN, N. (1950), *Nature, Lond.*, 166, 610.
- McCULLOCH, D. (1951), Thesis, Mass. Inst. Tech.
- MARTON, L. (1934a), *Nature, Lond.*, 137, 911.
- MARTON, L. (1934b), *Phys. Rev.*, 46, 527.

- MASSEY, B. (1953), Stain Tech., 28, 19.
- MEYER, H. (1954), Exp. Cell Res., 7, 22.
- MONNE, L. (1942), Ark. Zool., 34b, 205.
- MUDD, S. and ANDERSON, T.F. (1942), J. Exp. Med., 76, 103.
- NEWMAN, S.B., BORYSKO, E., and SWERDLOW, M. (1949a), J. Nat. Bureau Stand., 43, 183.
- NEWMAN, S.B., BORYSKO, E., and SWERDLOW, M. (1949b), Science, 110, 66.
- O'BRIEN, H.C. Jr. and MCKINLEY, C.A. (1943), Science, 98, 455.
- PALADE, G.E. (1952), J. Exp. Med., 95, 285.
- PALADE, G.E. (1953), J. Histo- and Cytochem., 1, 188.
- PALAY, S.L. and PALADE, G.E. (1953), J. appl. Phys., 24, 1419.
- PALAY, S.L. and WISSIG, S.L. (1953), Anat. Rec., 116, 301.
- PEASE, D.C. and BAKER, R.F. (1948), Proc. Soc. Exp. Biol. N.Y., 67, 470.
- PEASE, D.C. and BAKER, R.F. (1951), Anat. Rec., 110, 505.
- PENFIELD, W. (1932), "Cytology and Cellular Pathology of the Nervous System," vol. 1; Paul & Hocker, (New York).
- Le POOLE, J.B. (1947), Philips Tech. Rev., 9, 33.
- POLLISTER, A.W., GETTNER, M. and WARD, R., (1954), Science, 120, 571.
- PORTER, K.R. (1954), J. Histo- and Cytochem., 2, 346.
- PORTER, K.R. and BLUM, J. (1953), Anat. Rec., 117, 685.
- PORTER, K.R., CLAUDE, A. and FULLAM, E. (1945), J. Exp. Med., 81, 233.
- RHODIN, J. (1954), "Correlation of Ultra-structural Organisation and Function in Normal and Experimentally changed Proximal Convolute Kidney Cells of the Mouse", Karolinska Institutet. (Stockholm).

- RICHARDS, A.G., ANDERSON, T.F. and HANCE, R.T. (1942),  
Proc. Soc. Exp. Biol. N.Y., 51, 148.
- ROSZA, G. and WYCKOFF, R.W.G. (1950), Biochim. biophys. Acta,  
6, 334.
- SCHRADER, F. and LEUCHTENBERGER, C. (1952), Exp. Cell Res.,  
3, 136.
- SJOSTRAND, F.S. (1949), Sympos. "Freezing and Drying", Inst.  
of Biol., London.
- SJOSTRAND, F.S. (1952), Private communication.
- SJOSTRAND, F.S. (1953a), Nature, Lond., 171, 30.
- SJOSTRAND, F.S. (1953b), J. Cell. Comp. Physiol., 42, 15.
- SJOSTRAND, F.S. (1953c), Experientia, 9, 68.
- SJOSTRAND, F.S. and RHODIN, J. (1953), Exp. Cell Res., 4, 426.
- STEDMAN, H.F. (1945), Nature, Lond., 156, 121.
- STRANGEWAYS, T.S. and CANTI, R.G. (1927), Quartl. J. Micros.  
Sci., 71, 1.
- WATSON, M.L. (1953a), Biochim. biophys. Acta, 10, 349.
- WATSON, M.L. (1953b), Biochim. biophys. Acta, 8, 369.
- WATSON, M.L. (1954), Biochim. biophys. Acta, 15, 475.
- WILLIAMS, R.C. and WYCKOFF, R.W.G. (1946), J. appl. Phys.,  
17, 23.
- WYCKOFF, R.W.G. (1951), Disc. Farad. Soc., 11, 230.
- ZWORYKIN, V.K., MORTON, G.A., RAMBERG, E.G., HILLIER, J. and  
VANCE, A.W. (1945), "Electron Optics and the  
Electron Microscope" (Chap. 4), Chapman and  
Hall (London).

THE ELECTRON MICROSCOPY OF TISSUE SECTIONS

WITH SPECIAL REFERENCE TO THE STRUCTURE

OF SPINAL GANGLIA

(Diagrams and Illustrations)

Thesis submitted to the University of Glasgow

for the Degree of Ph.D.

by

James Hossack, B.Sc.

May, 1955.

T A B L E    O F    C O N T E N T S

FIGURE 1	Relationship between Resolution Limit and Specimen Thickness	PAGE 1
2	Advance Mechanism of Microtome	2
3	Modifications to Advance Mechanism	2
4	Photograph of Modified Microtome	3
5	Holder for Razor Blades	4
6	Holder for Glass Knives	4
7	Hone used for sharpening Razor Blades	5
8	Photograph of Microtome with Razor Blade Holder	6
9	Photograph of Microtome with Glass Knife Holder	7
10	Modified Freeze-drying Apparatus	8
-----		
11	Complete Spinal Ganglion Cell	9
12	Two Cells sharing a Common Capsule	10
13	Section through Capsular Cell and Nerve Fibre	11
14	Cross-section of Capsular Nerve Fibre	11
15	Inter-cellular Membrane	12
16	Typical 'Light' Cell	12
17	'Light' and 'Dark' Cell in same field	13
18	Typical 'Light' Cell	14
19	Typical 'Dark' Cell	14
20	Nissl's Substance	15
21	Perinuclear Orientation in 'Dark' Cell	16

FIGURE 22	Reticular Orientation of Nissl's Substance in 'Light' Cell	page 16
23	Cytoplasmic Filaments	17
24	Filaments in Axon of Nerve Fibre	17
25	Mitochondria of Nerve Cell	18
26	Nerve Cell Mitochondria at Higher Magnification	18
27	mitochondria from Rabbit Ovarian Tissue	19
28	Nerve Cell Nucleus with heterogenous appearance	20
29	Nucleus with more homogeneous appearance	20
30	Nucleus with irregular membrane	21
31	Nucleus with crenated Membrane	21
32	nucleolus	22
33	Nucleus with two Nucleoli	22
34	Shadowcast Nucleolus	23
35	Tangential Section of Nucleus, showing Nodes in the Nuclear Membrane	23
36	Section of Nuclear Membrane, cut nearer centre of Nucleus	24
37	Enlarged portion of Tangential Section of figure 35	24
38	Shadowcast Tangential Section of Membrane	25
39	Radial Section of Nucleus, showing appearance of Membrane	26
40	Radial Section showing Nodes in Membrane	27
41	Radial Section showing supporting Membrane	27
42	Radial Section showing both Nodes and supporting Membrane	27
43	Myelin Sheath from Nerve Fibre, showing the lamellar structure	28

FIGURE 44	Nerve Fibre with Schwann Cell	page 28
45	Shadowcast Section of Nerve Fibre	29
46	Nerve Cell with Delay in Fixation amounting to one to two minutes	30
47	Nerve Cell with Delay in Fixation amounting to five minutes	30
48	Nerve Cell with Delay in Fixation amounting to twelve to fifteen minutes	31
49	Nuclear Membrane from Tissue where Delay in Fixation amounted to one to two minutes	31
50	Diagrammatic Representation of Nuclear Membrane of Nerve Cell	32
-----		
51	Brush Border from Rabbit Kidney Tubule Cell	33
52	Prolongations of Brush Border (Enlarged)	34
53	Mitochondria from Kidney Tubule Cell	34
54	" " " " "	35
55	" " " " "	35
56	Section from Frozen-dried Kidney	36

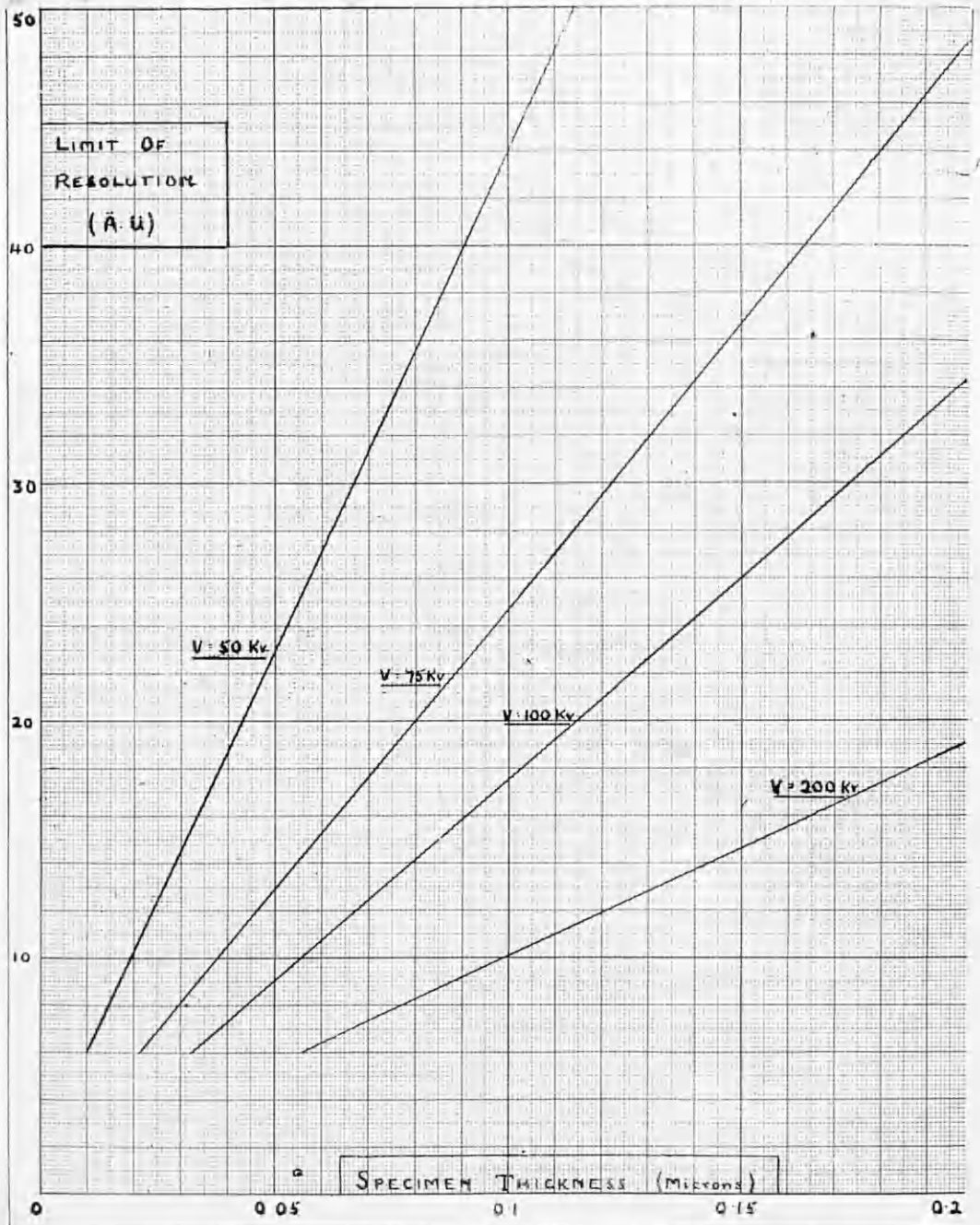


Figure 1. Graph showing the relationship between limit of resolution and specimen thickness for various values of beam potential.

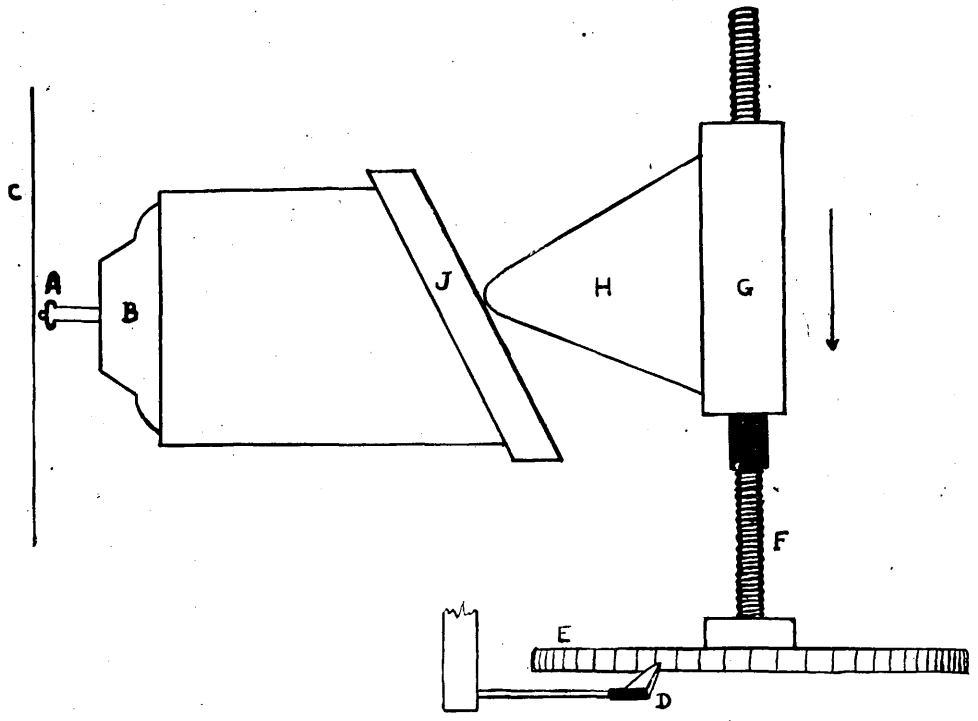


Figure 2. Diagram showing the advance mechanism of the Spencer Rotary Microtome.

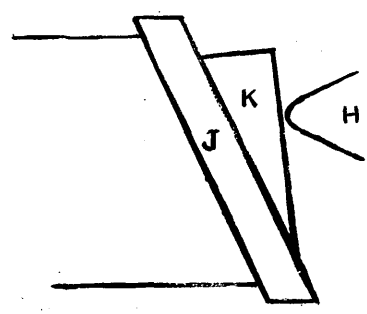


Figure 3. Method of modifying the advance mechanism to reduce the unit advance. An additional wedge, K, is inserted which has a smaller angle than the original.

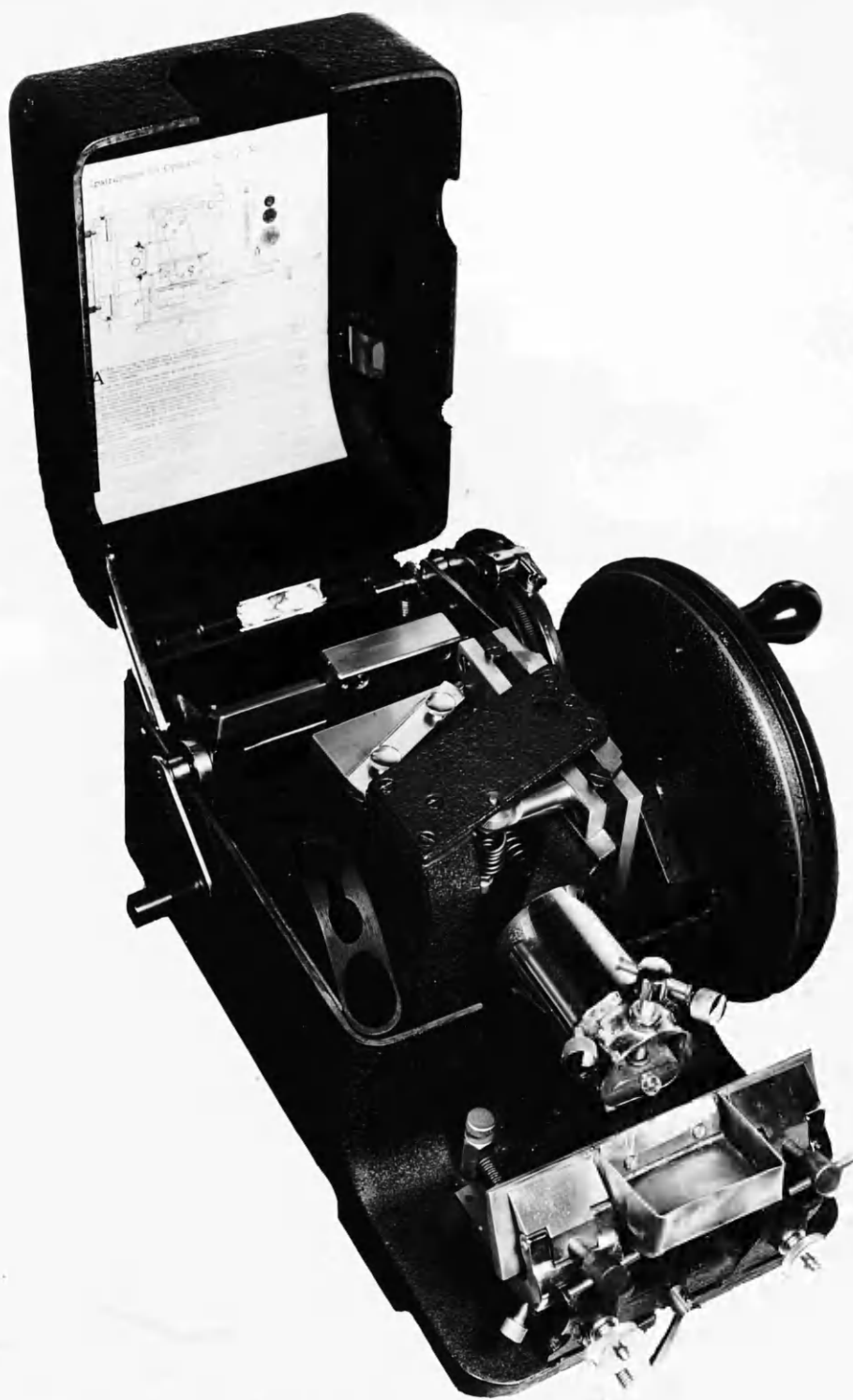


Figure 4. Photograph of the modified Spencer Rotary Microtome.

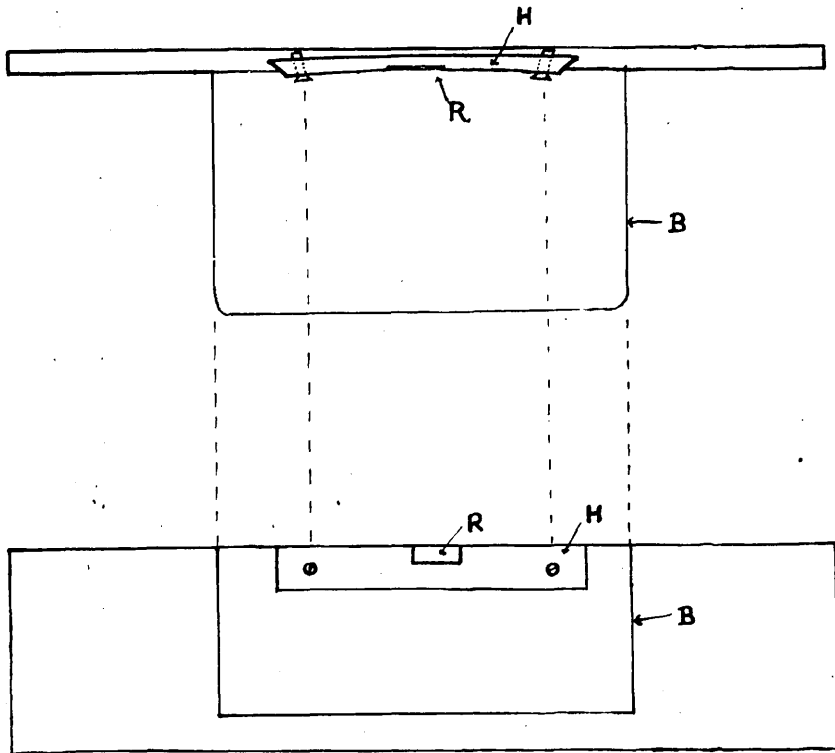


Figure 5. Diagram of the razor blade holder for thin sectioning.

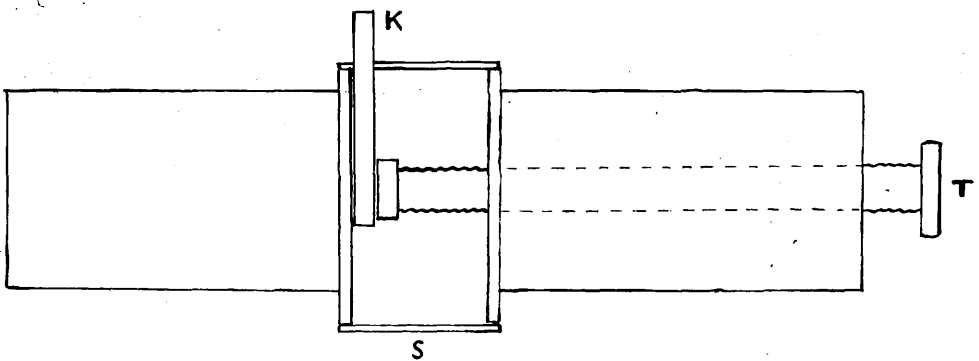


Figure 6. Diagram of the glass knife holder.

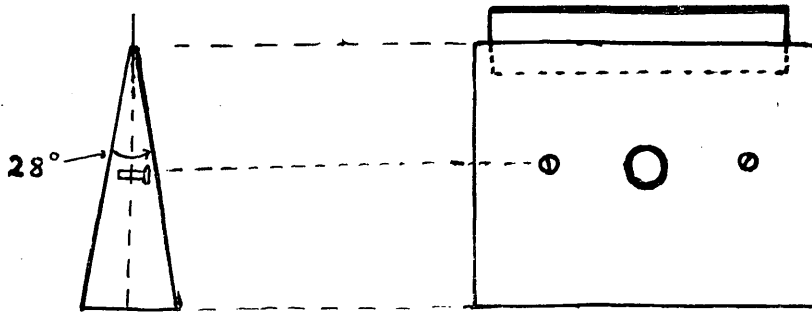


Figure 7. Diagram showing the hone used for razor blade sharpening.

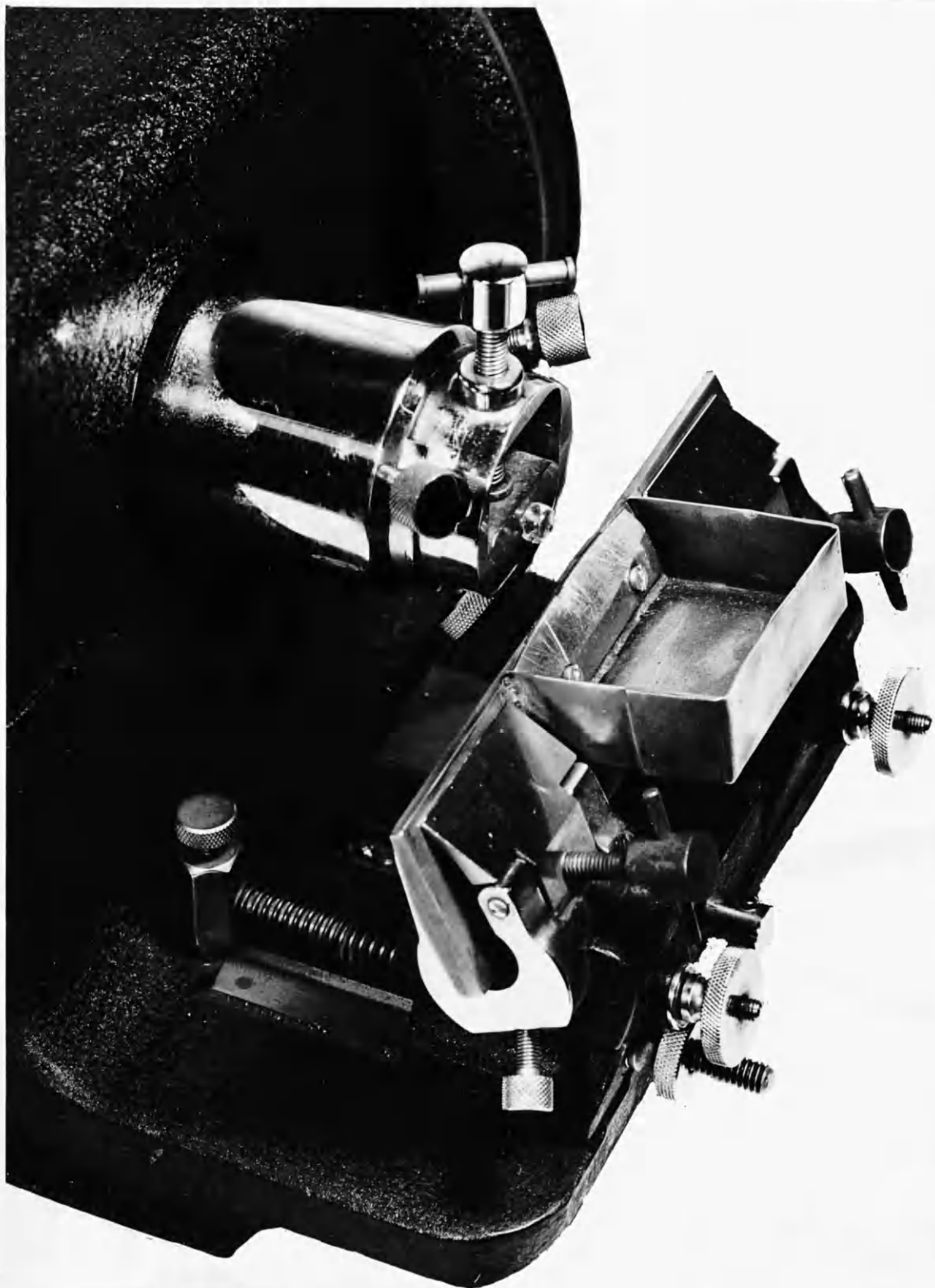


Figure 8. Photograph of the microtome, showing the razor blade holder in position for sectioning.

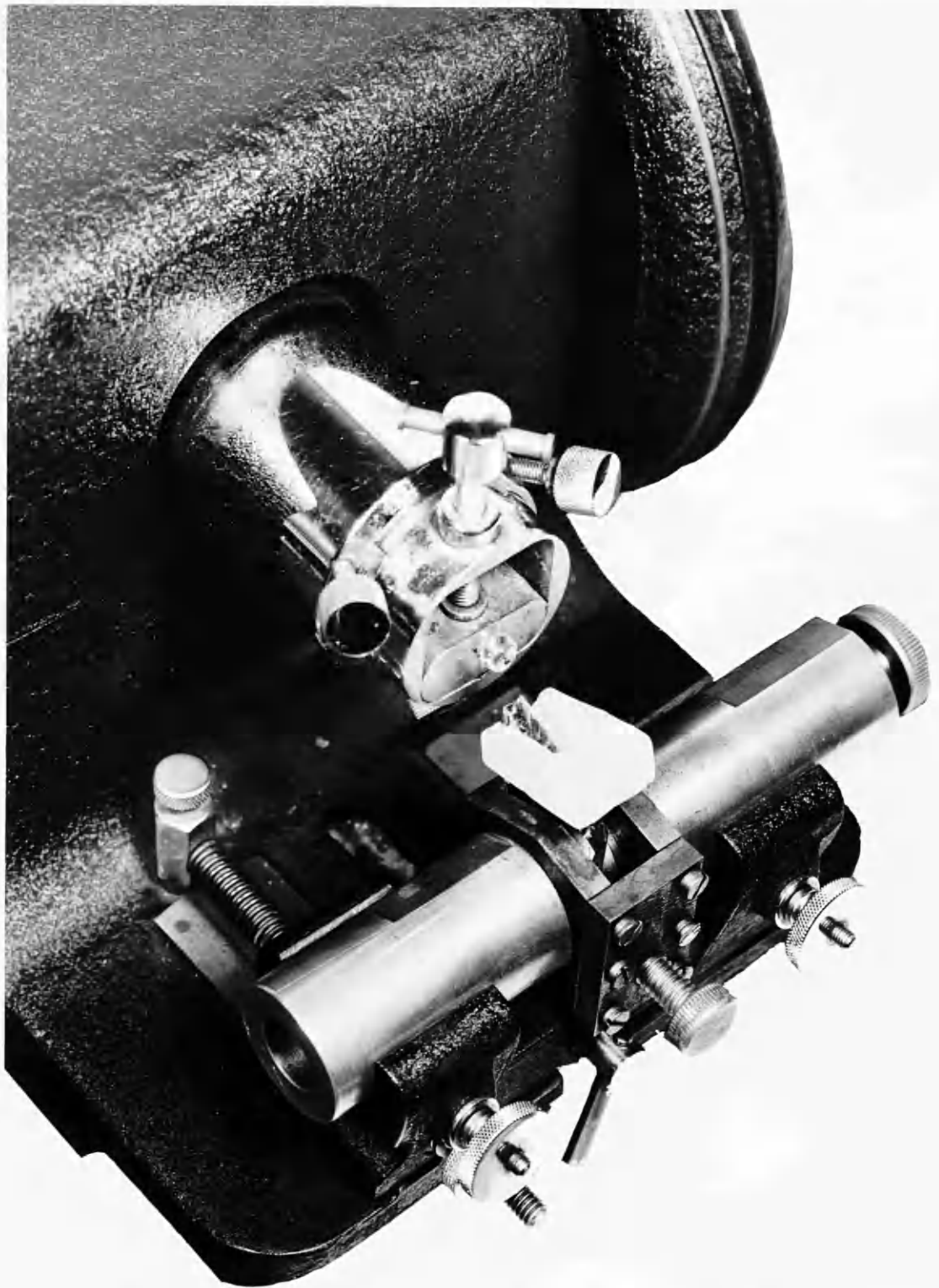


Figure 9. Photograph of the microtome with a glass knife set up in its holder for sectioning.

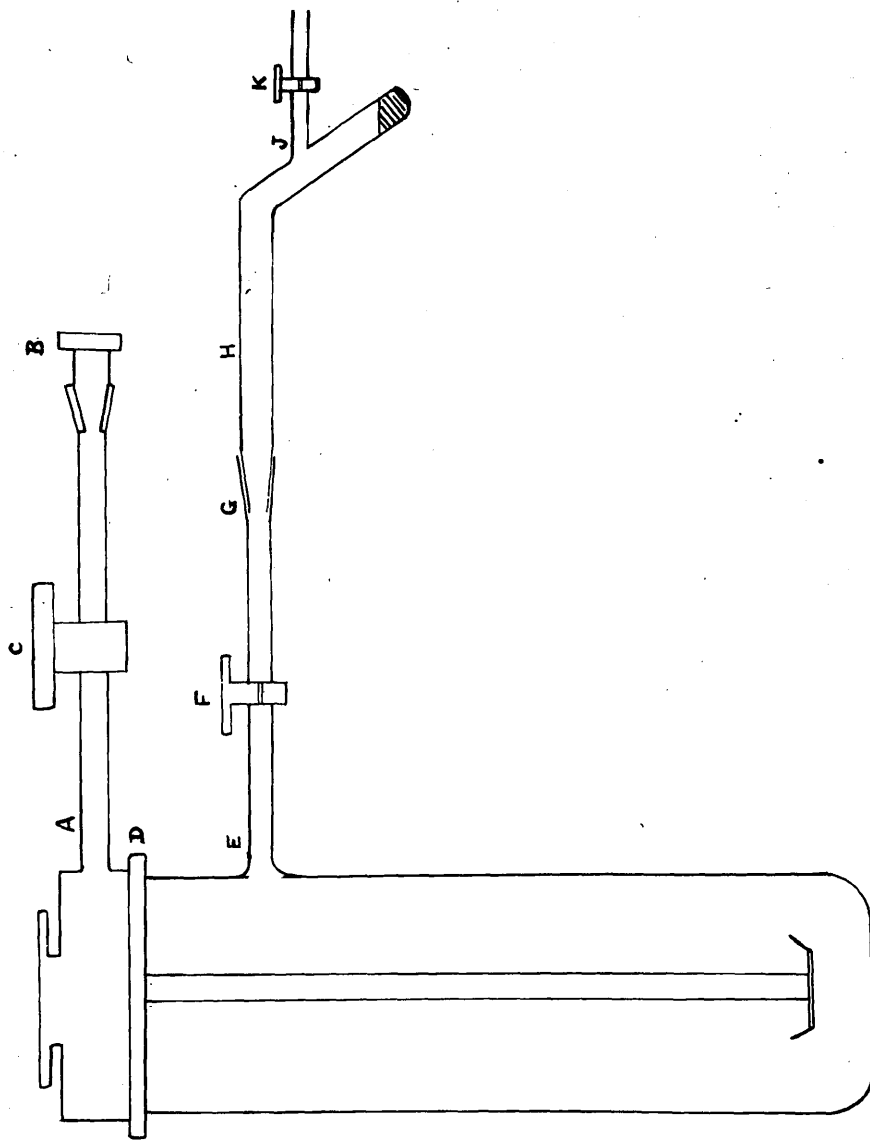


Figure 10. Diagram showing the modifications made to the "Edwards" freeze-drying tube to enable direct vacuum-embedding in methacrylate monomer to be carried out.

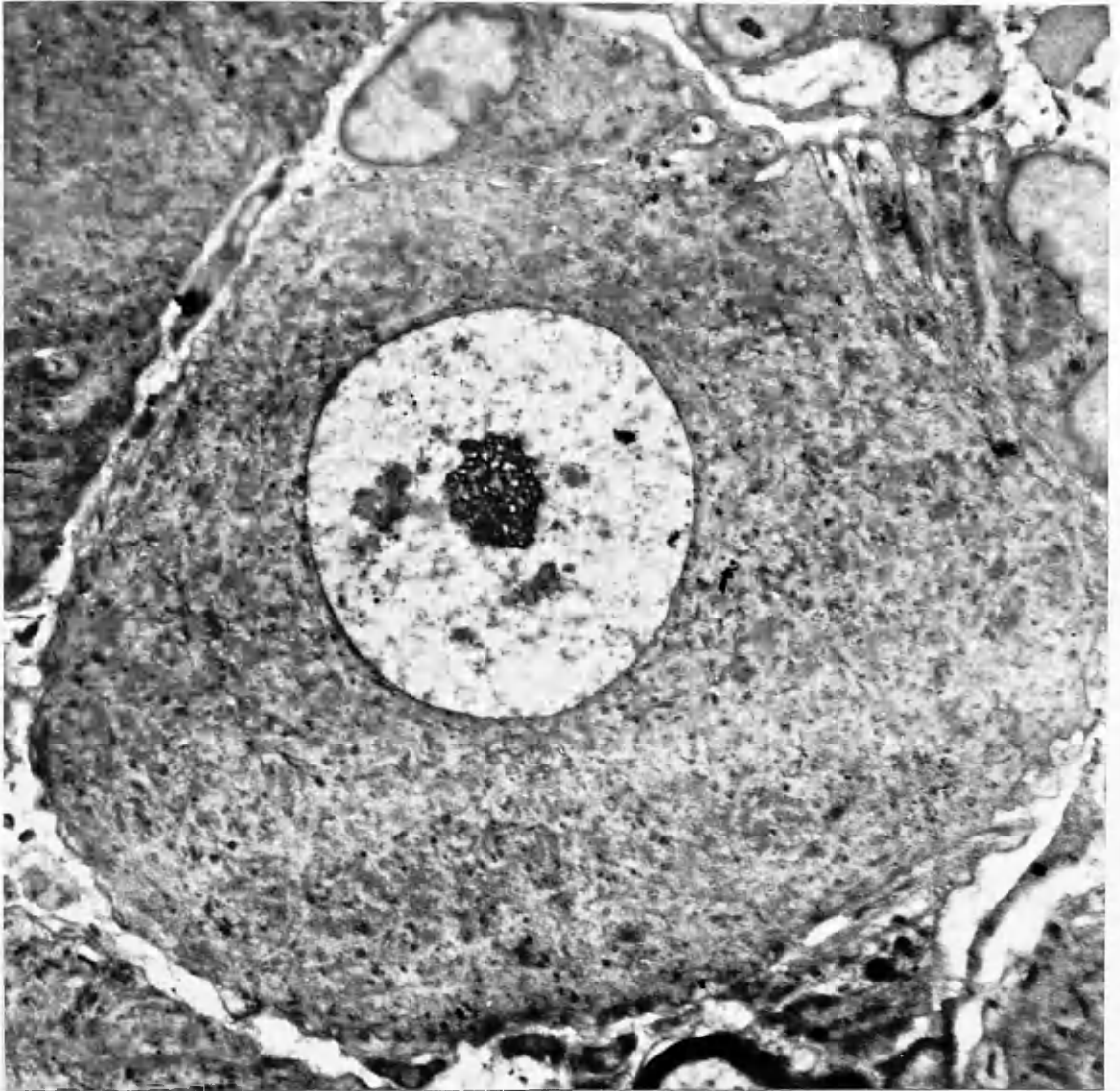


Figure 11. Complete spinal ganglion cell, showing the nucleus and nucleolus, the cytoplasmic structure, and the capsular cells, which are separated from the main ganglion cell by a series of reticular fibrils. 6,000 x.

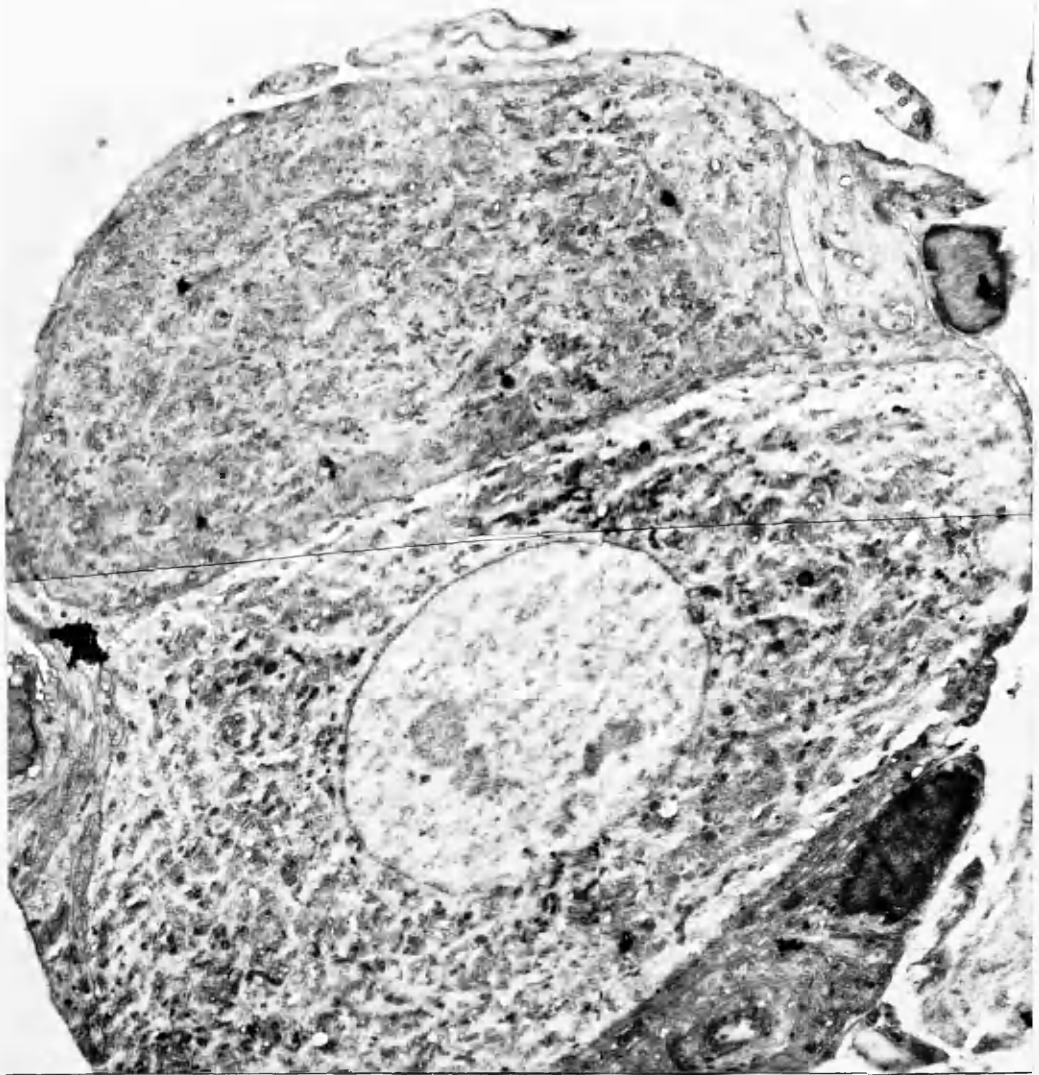


Figure 12. Two spinal ganglion cells sharing a common capsule. 5,000 x.

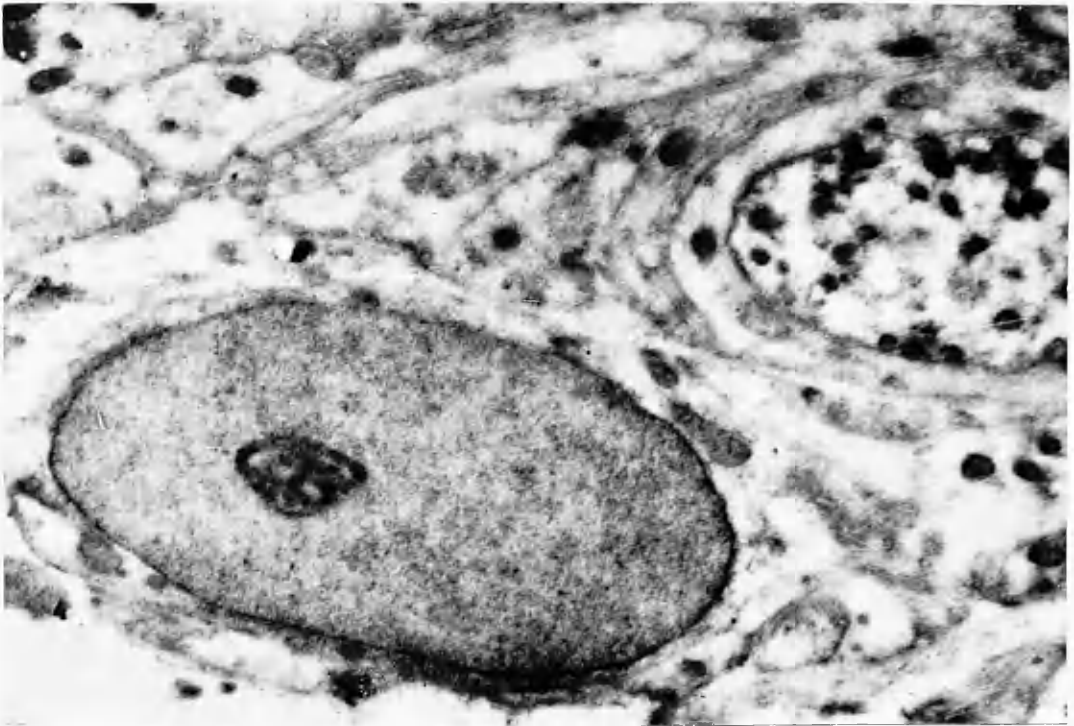


Figure 13. A section through a capsular cell (left of field) and a nerve fibre, showing the nucleus of the cell, and the small mitochondria of the axon. (22,500 x.)

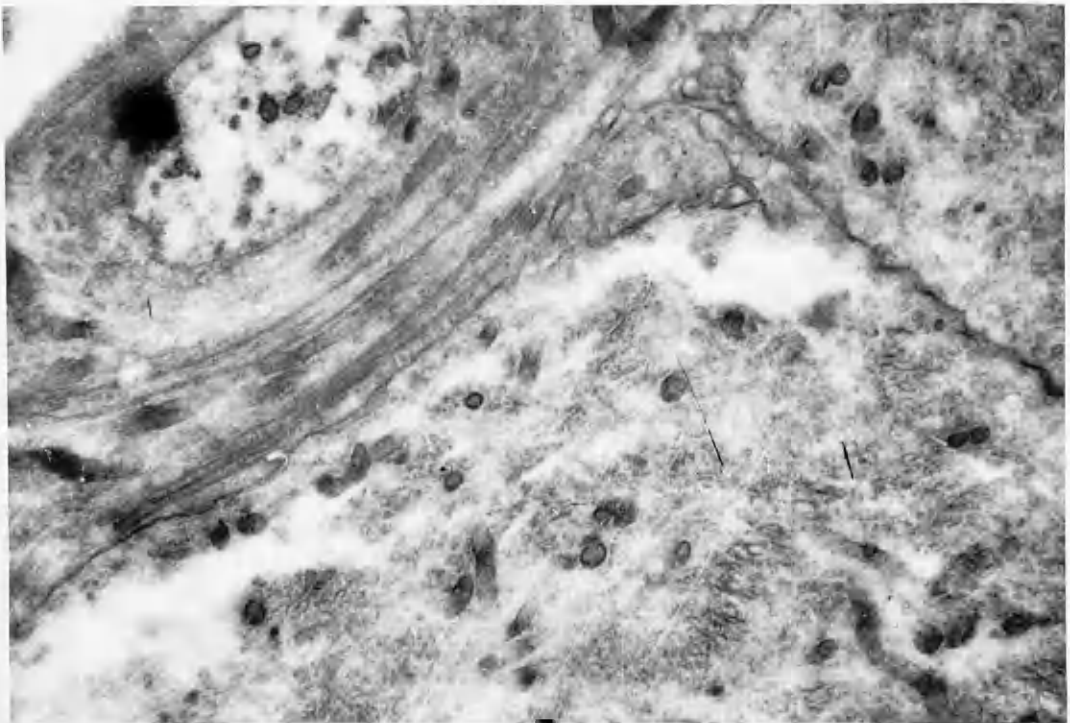


Figure 14. Cross-section of a capsular nerve-fibre, the axon of which is similar in appearance to the cytoplasm of the ganglion cell. The myelin sheath appears to be continuous with the inter-cellular membrane. (20,000 x.)

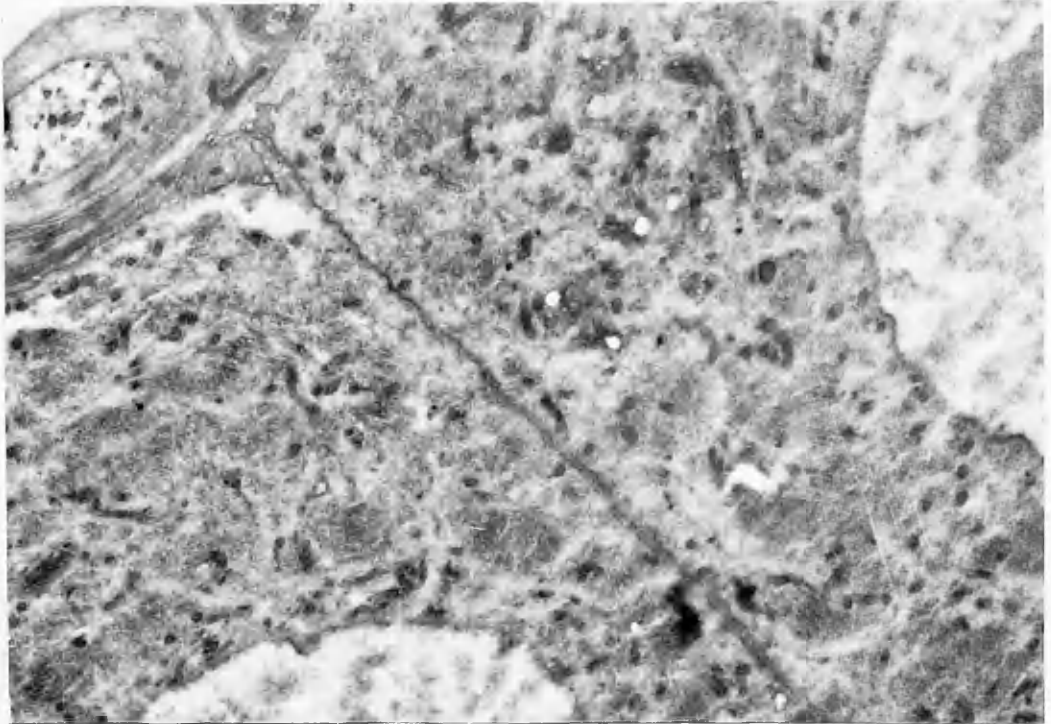


Figure 15. Extension of the field of figure 14, showing the continuity of the capsular myelin sheath and the inter-cellular membrane, which in places has a lamellar appearance. 10,000 x.

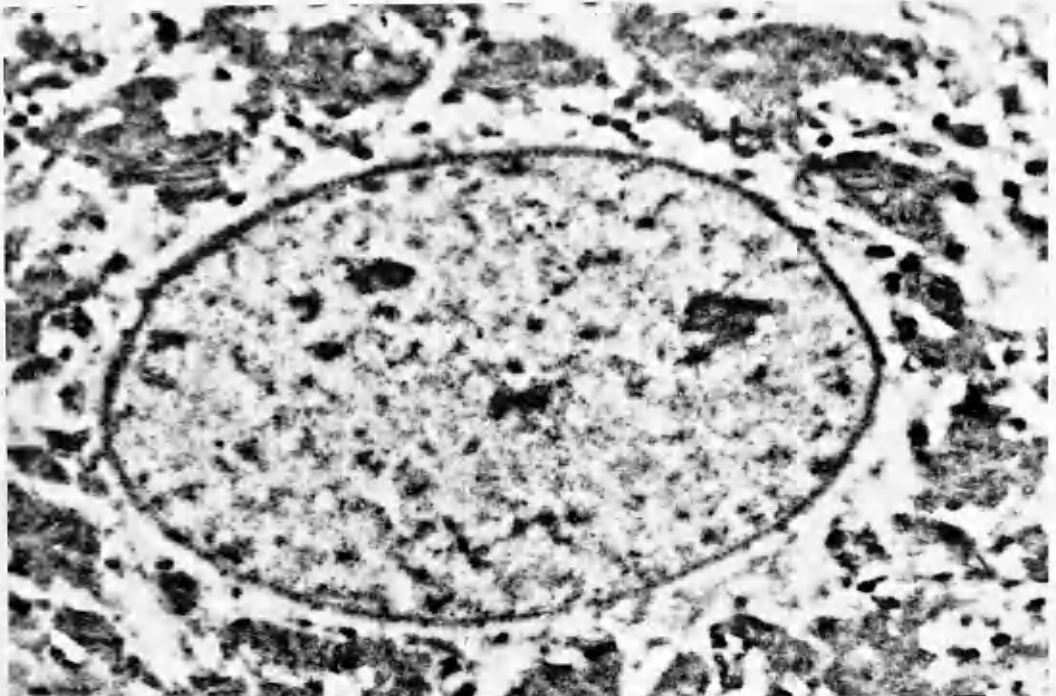


Figure 16. Nucleus and surrounding cytoplasm of a typical 'light' cell, with dense irregularly shaped Nissl's aggregates measuring about one to two microns. (9,000 x.)

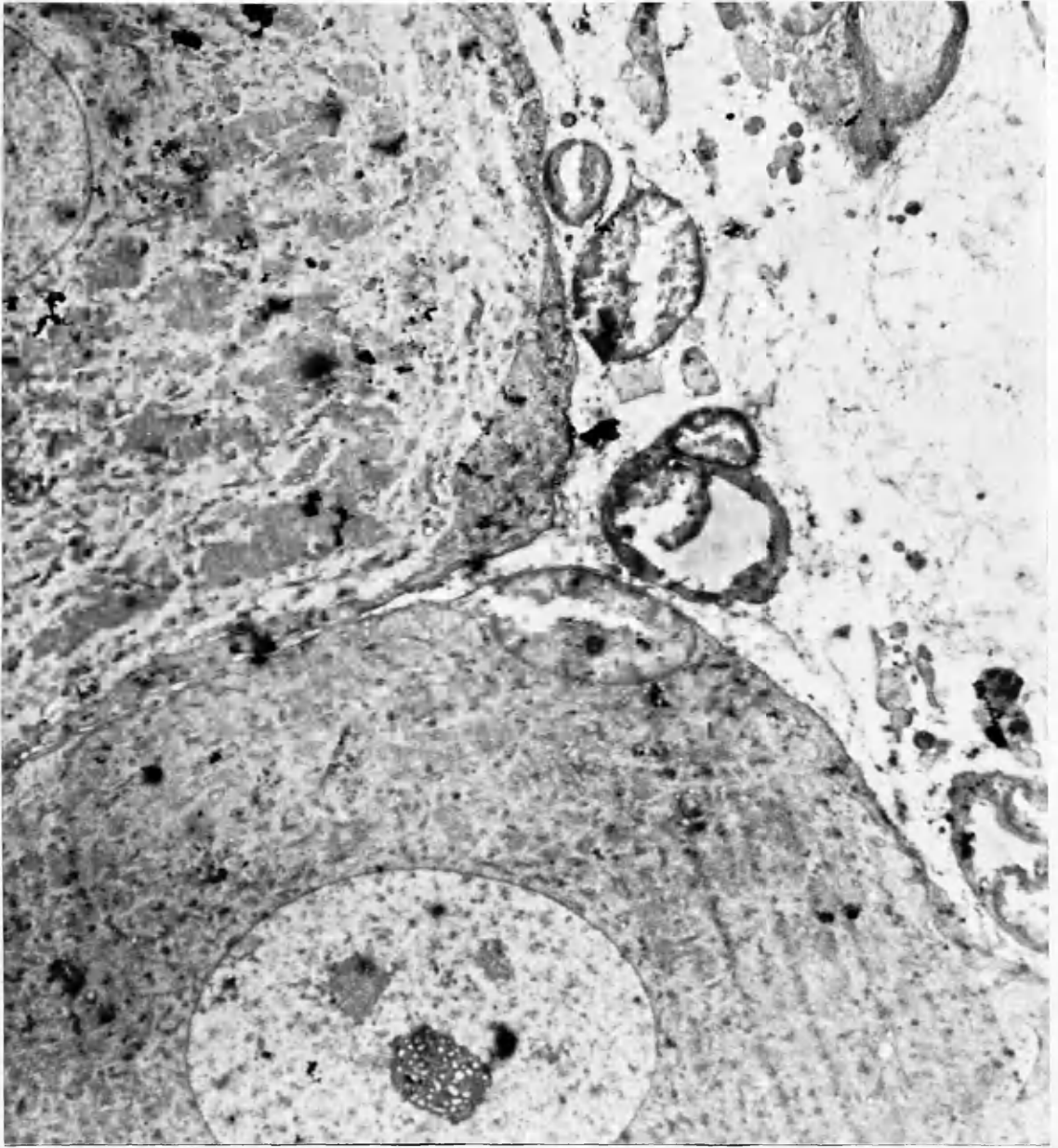


Figure 17. Two spinal ganglion cells, one 'light' and one 'dark', showing the discrete arrangement of Nissl's aggregates in the upper (light) cell and the diffuse distribution in the lower (dark) cell. 6,000 x.

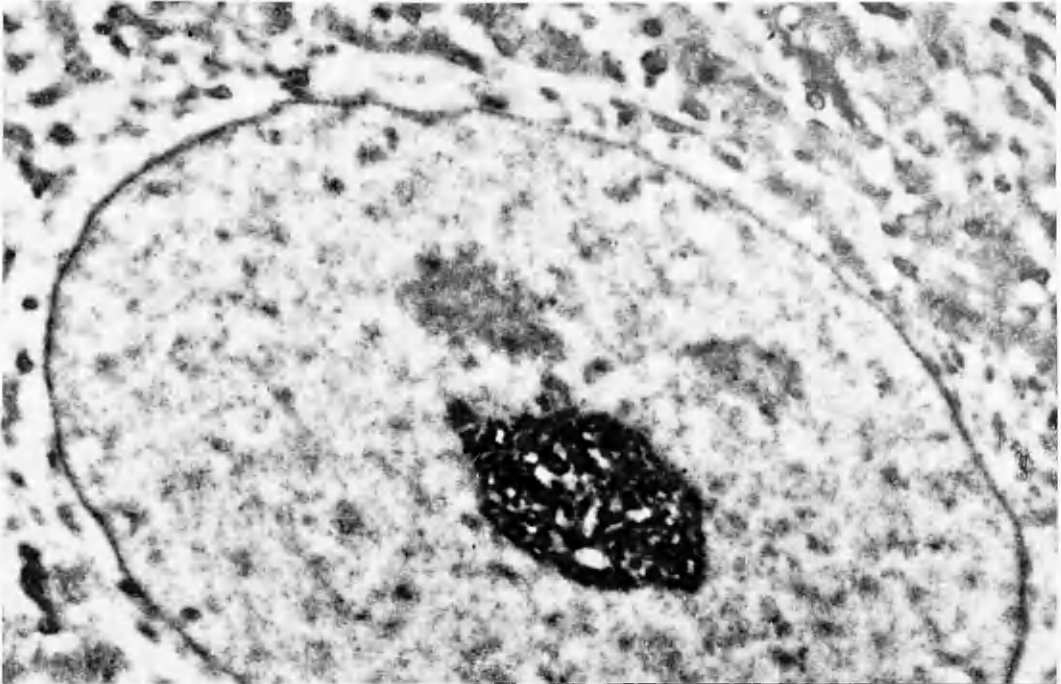


Figure 18. Typical 'light' cell, showing the Nissl's aggregates, and the similarity in density between the nucleus and cytoplasm. 11,000 x.

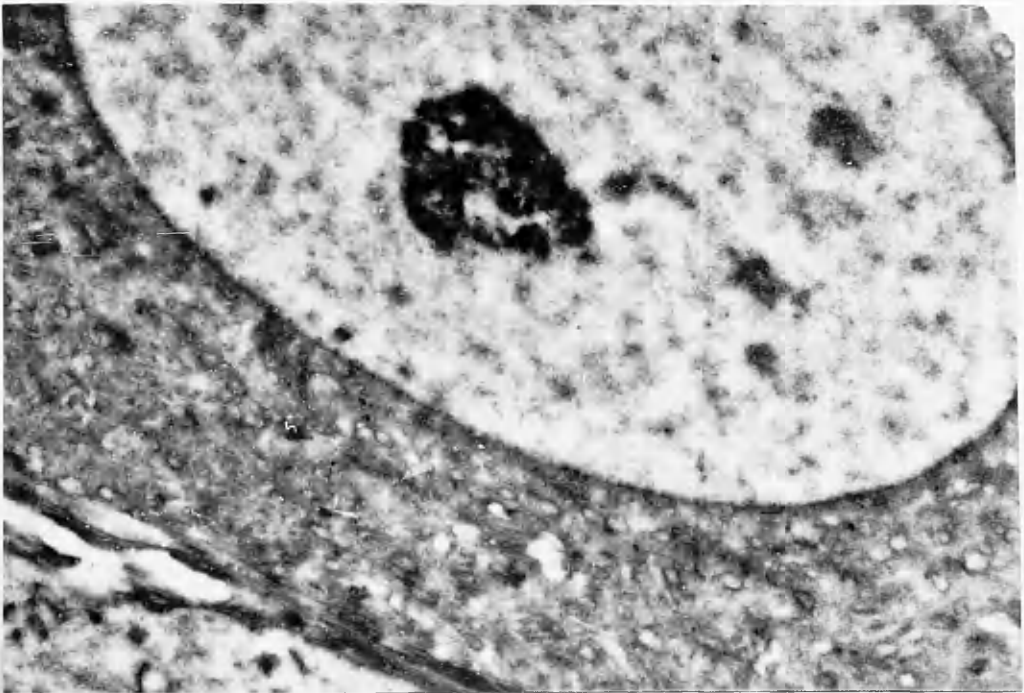


Figure 19. Typical 'dark' cell, showing the denser cytoplasm, with its more homogeneous distribution of the Nissl's material. 12,000 x.

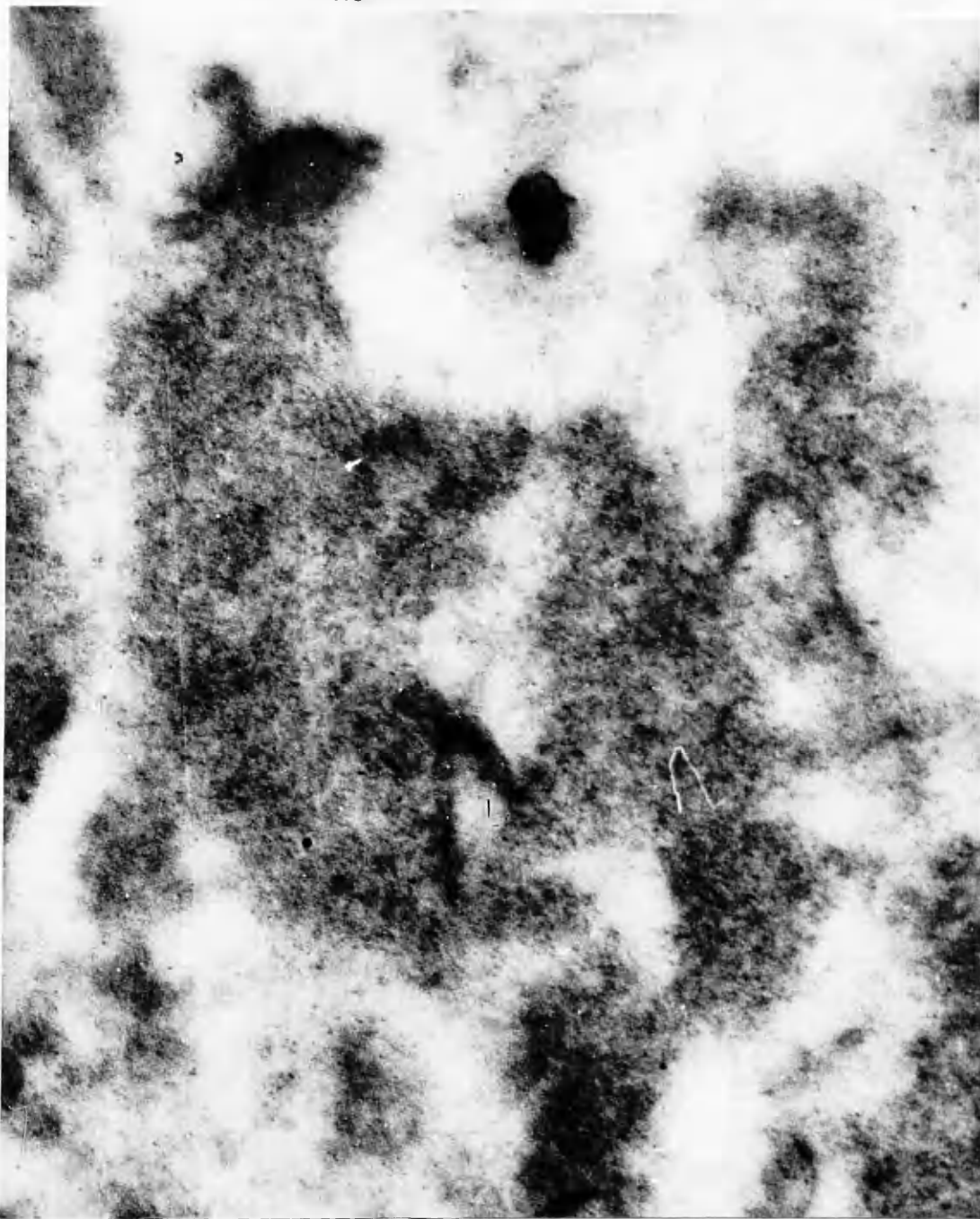


Figure 20. Nissl's substance, showing the particulate nature of the component granules, which have a size range of from 50 to 200 Å. There is evidence of orientation of the granules in places, in particular near the mitochondrion towards the top left of the picture. (75,000x.)

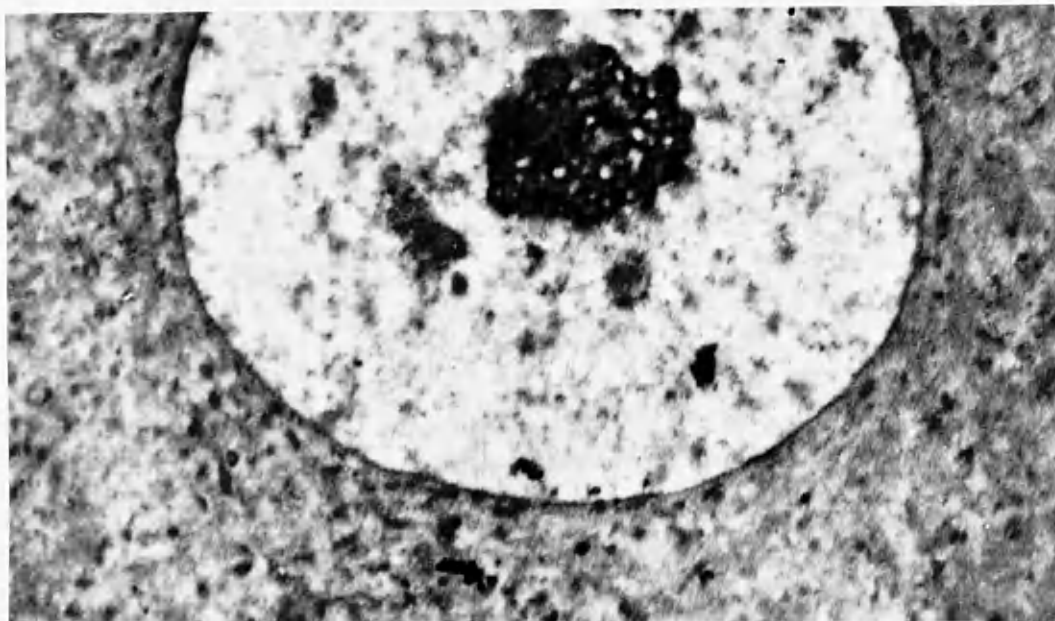


Figure 21. Higher magnification micrograph of the dark cell of figure 11, showing the perinuclear orientation of the cytoplasm. 12,500 x.

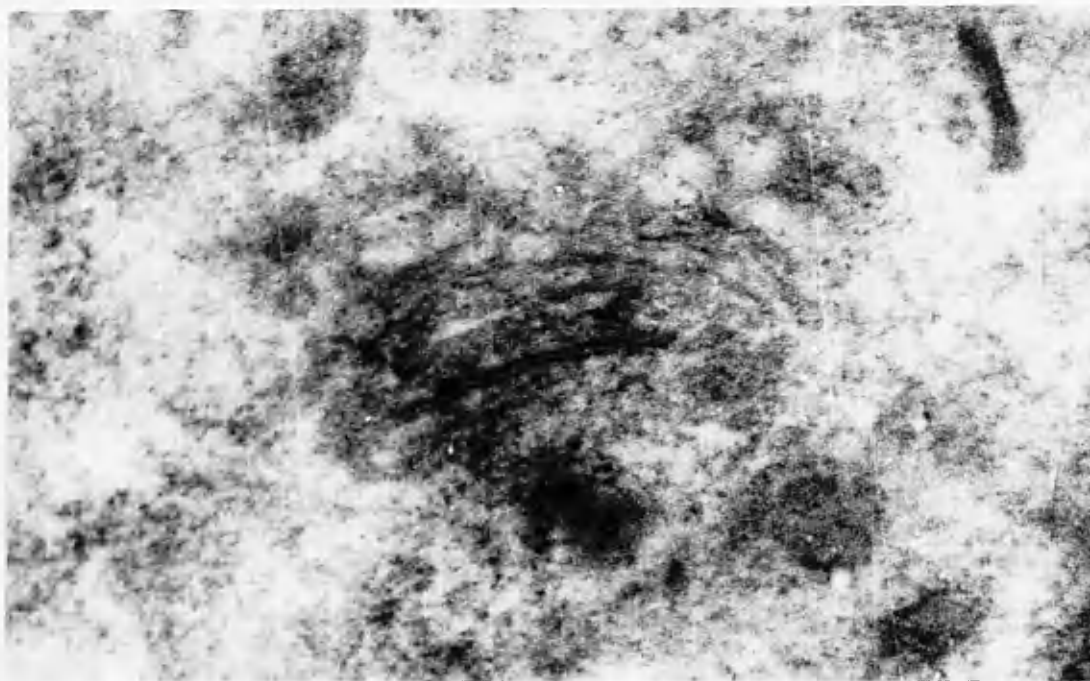


Figure 22. Micrograph showing the reticular organization of Nissl's substance in the cytoplasm of a light cell. 90,000 x.

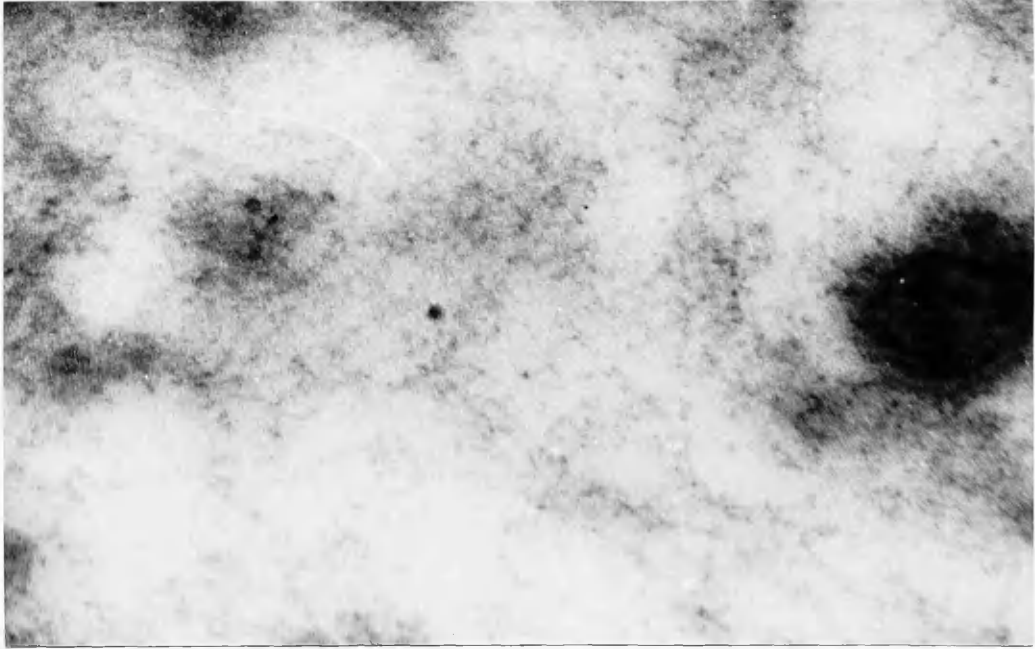


Figure 23. An area of cytoplasm free from Nissl's substance, showing cytoplasmic filaments. A dense mitochondrion is visible on the right of the field. (75,000 x.)

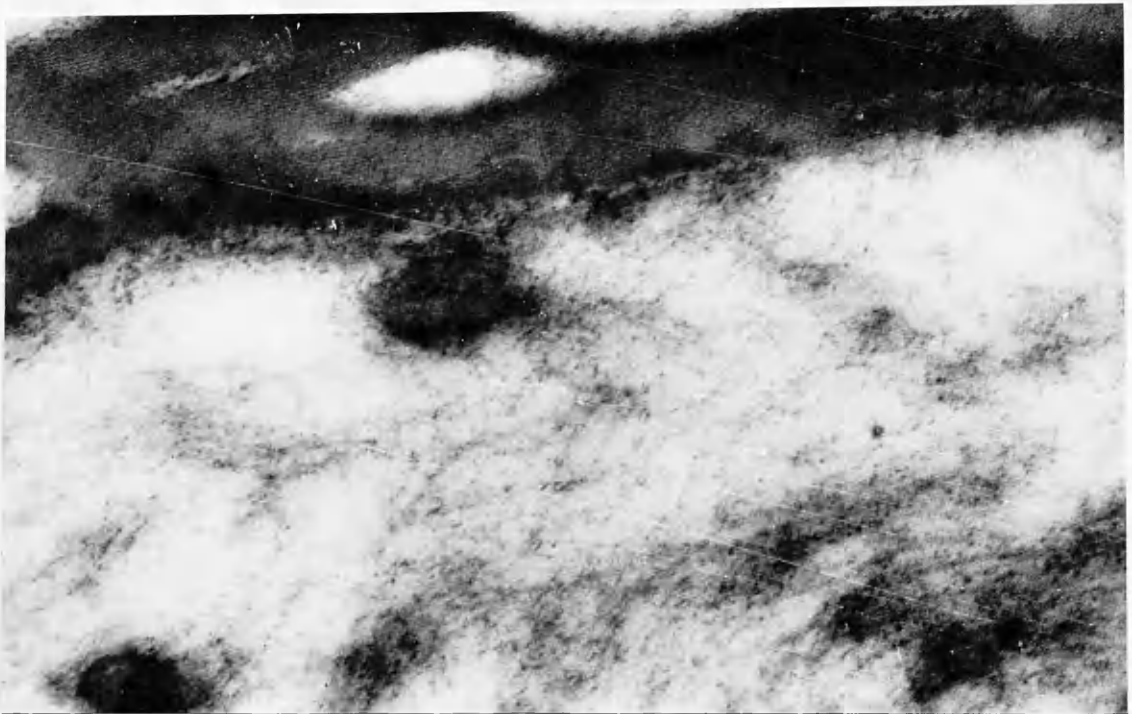


Figure 24. A longitudinal section of nerve fibre, the axon of which contains filaments similar in appearance to those of the cell cytoplasm of figure 23. The myelin sheath is composed of dark lamellar bands with a regular spacing of about 110 A. 75,000 x.

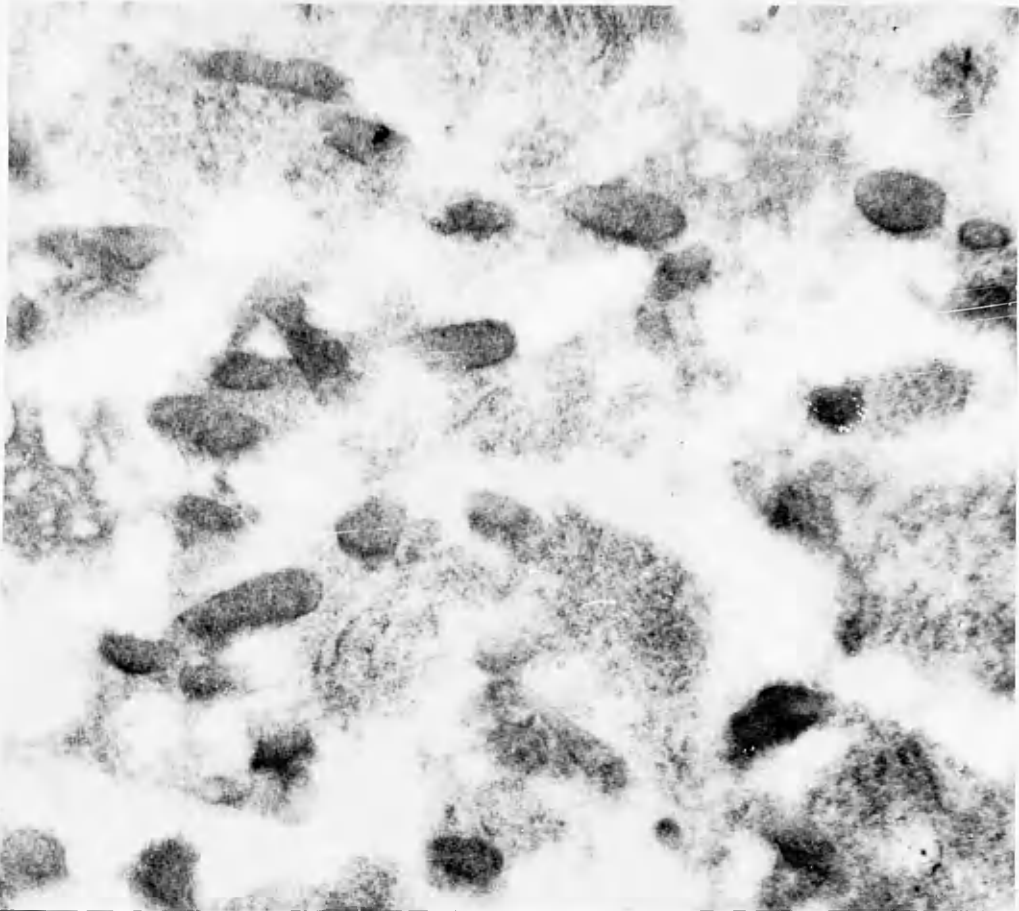


Figure 25. An area of cytoplasm showing mitochondria, which are denser than the Nissl's substance and have limiting membranes and internal cristae. 35,000 x.

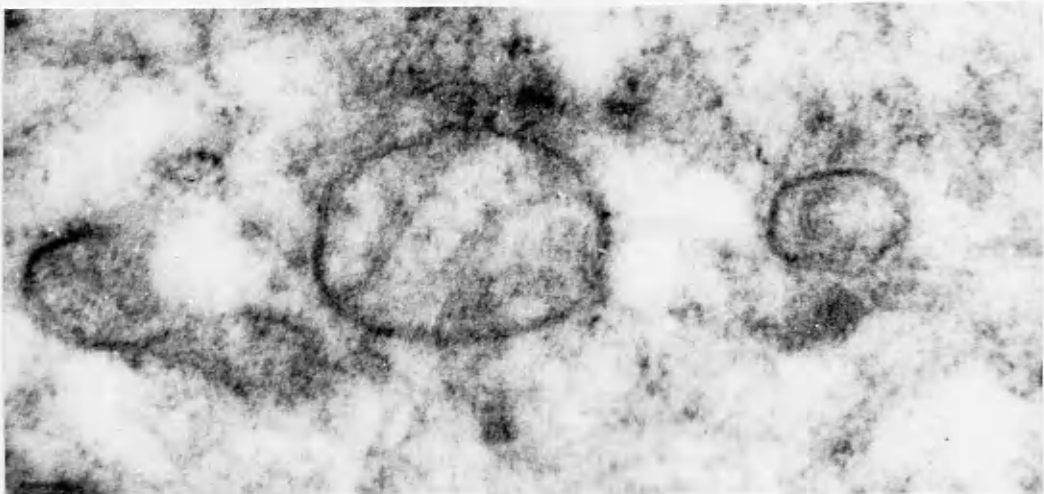


Figure 26. High magnification micrograph of nerve cell mitochondria, showing the double nature of their outer membranes and internal cristae. The mitochondrion in the centre of the field is larger than the average nerve cell mitochondria, and measures about 0.35 micron in cross-section. 95,000 x.



Figure 27. Mitochondria from rabbit ovarian tissue, showing their larger size by comparison with the mitochondria of nerve cells. The mitochondrion in the upper part of the micrograph measures 1.6 micron by 0.35 micron. 63,000 x.

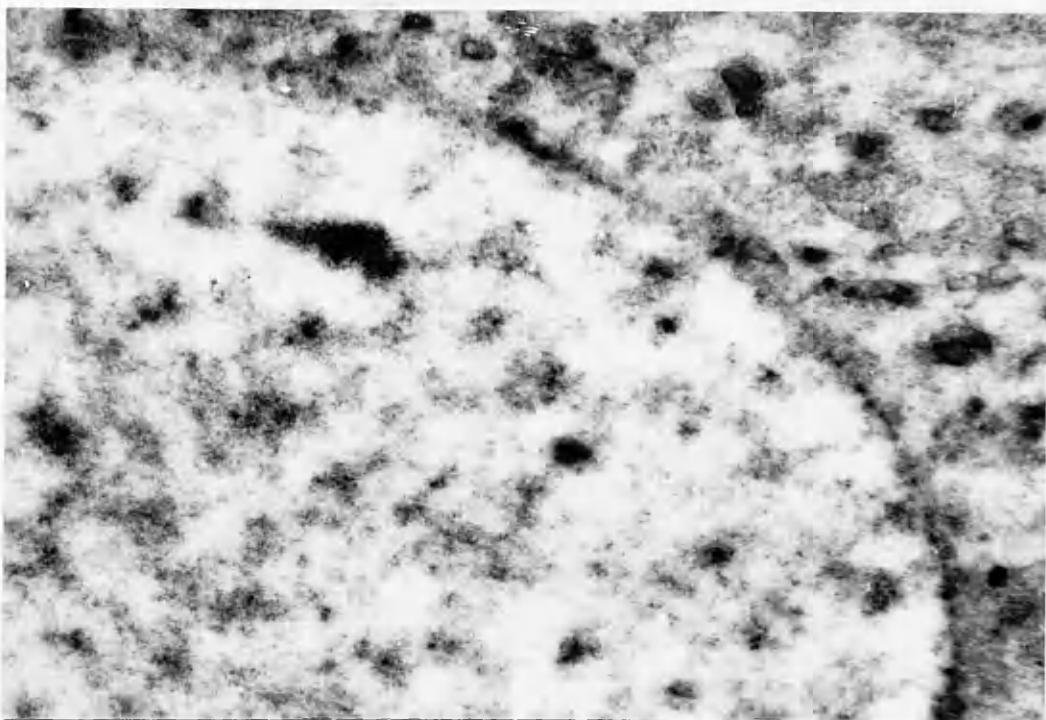


Figure 28. Nucleus of spinal ganglion cell, showing the heterogenous appearance of the nucleoplasm.

20,000 x.

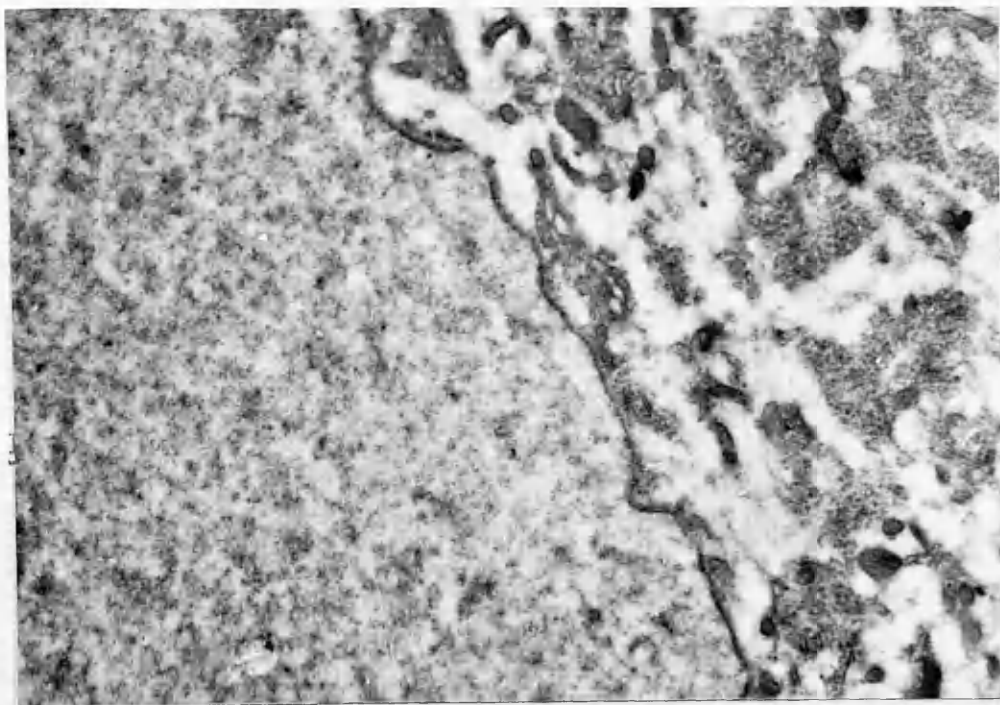


Figure 29. An example of a nucleus with a more homogeneous nuclear substance, which is sometimes, but not always, accompanied by a crenated nuclear membrane as in the above example.

22,000 x.

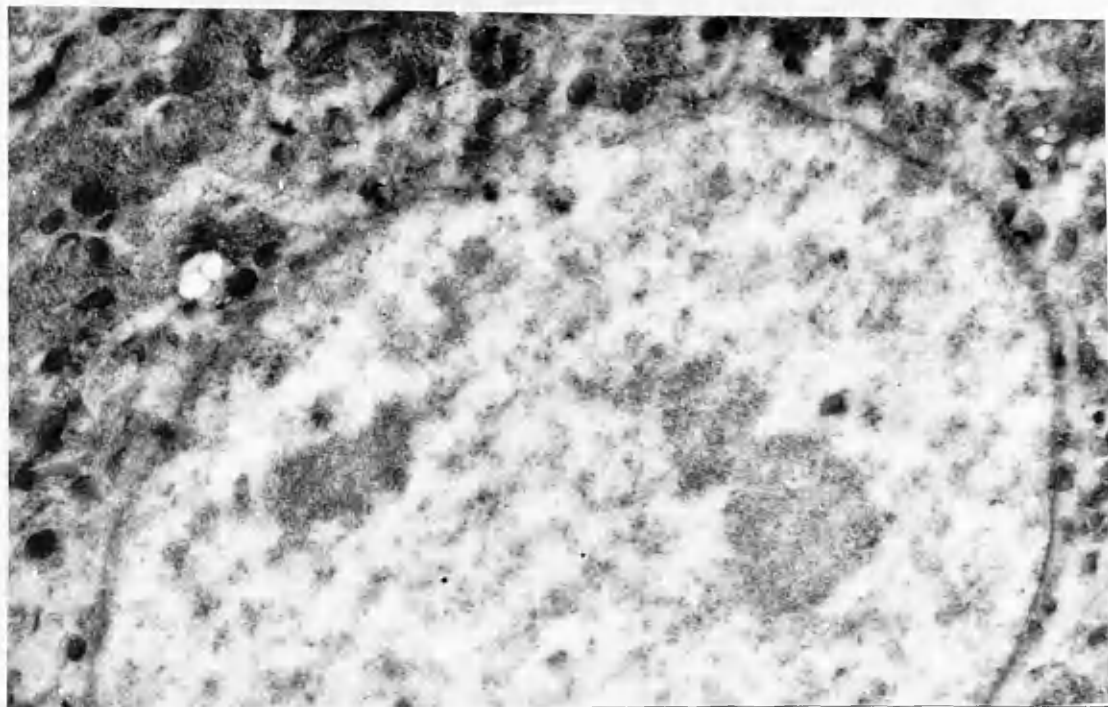


Figure 30. A nucleus with an irregularly-shaped membrane which in places has deep indentations accompanied by breaks. 15,000 x.

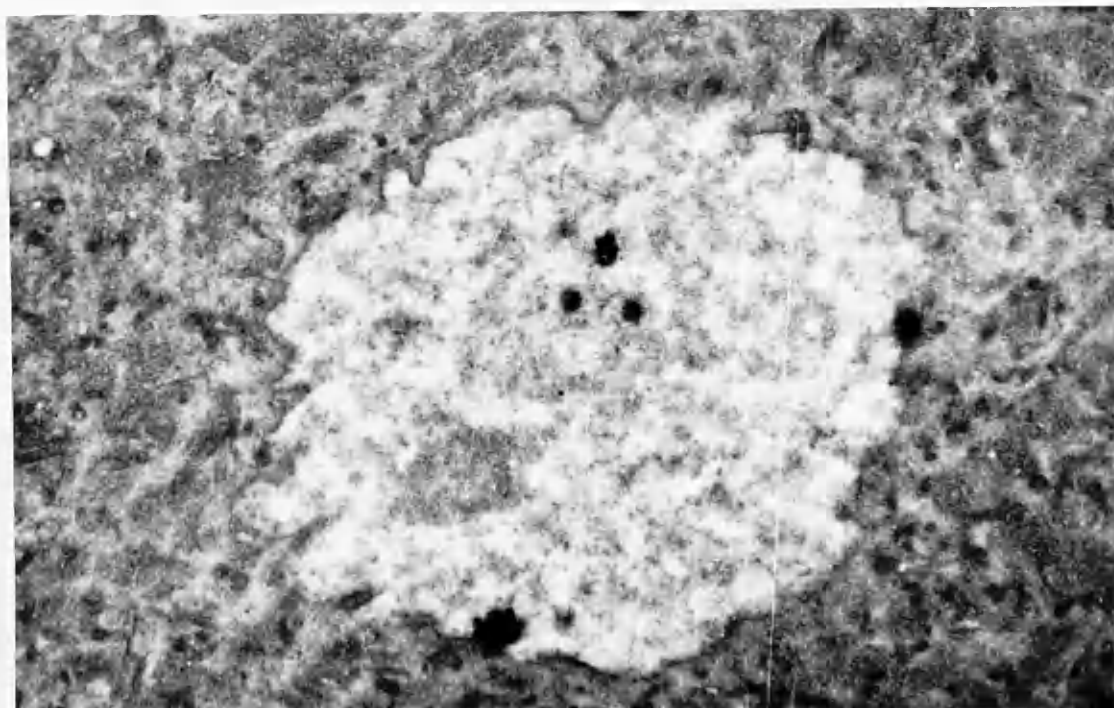


Figure 31. Nucleus with a typical 'crenated' membrane. 11,000 x.

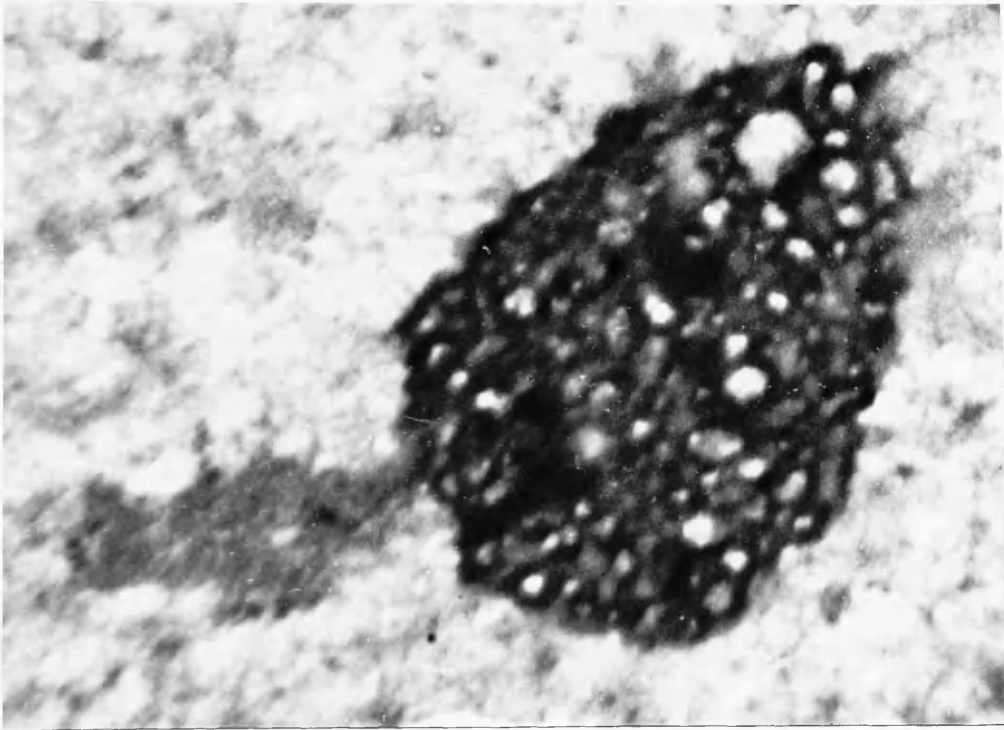


Figure 32. A nucleolus, with a flake of chromatin adhering to it, showing the irregular contour, vacuolated appearance, and absence of a limiting membrane. (29,500 x)

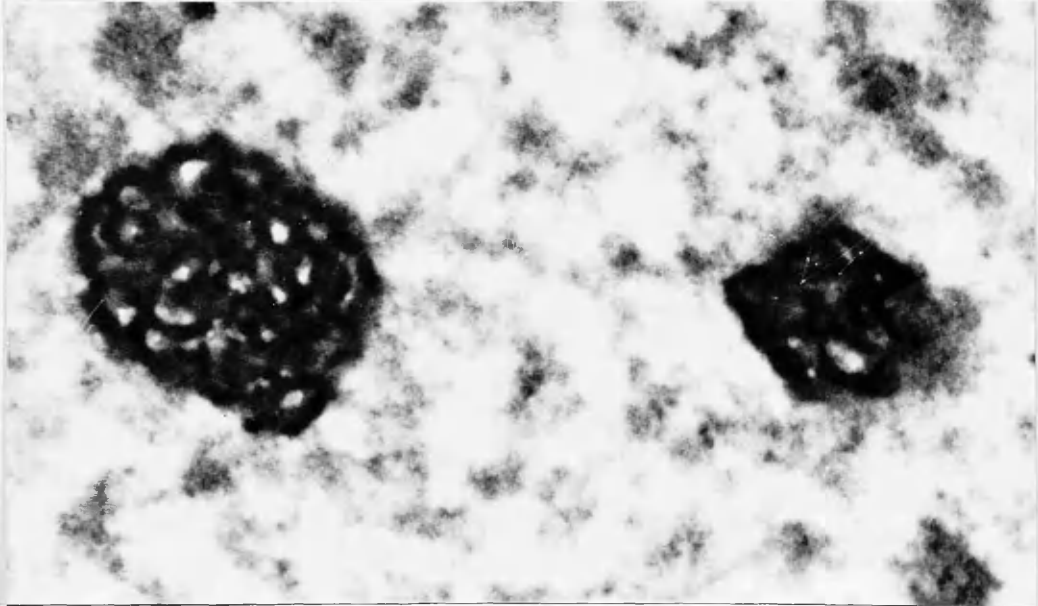


Figure 33. An example of a nucleus with two nucleoli. The difference in size is probably a result of the plane of section through the nucleus. 20,000 x.

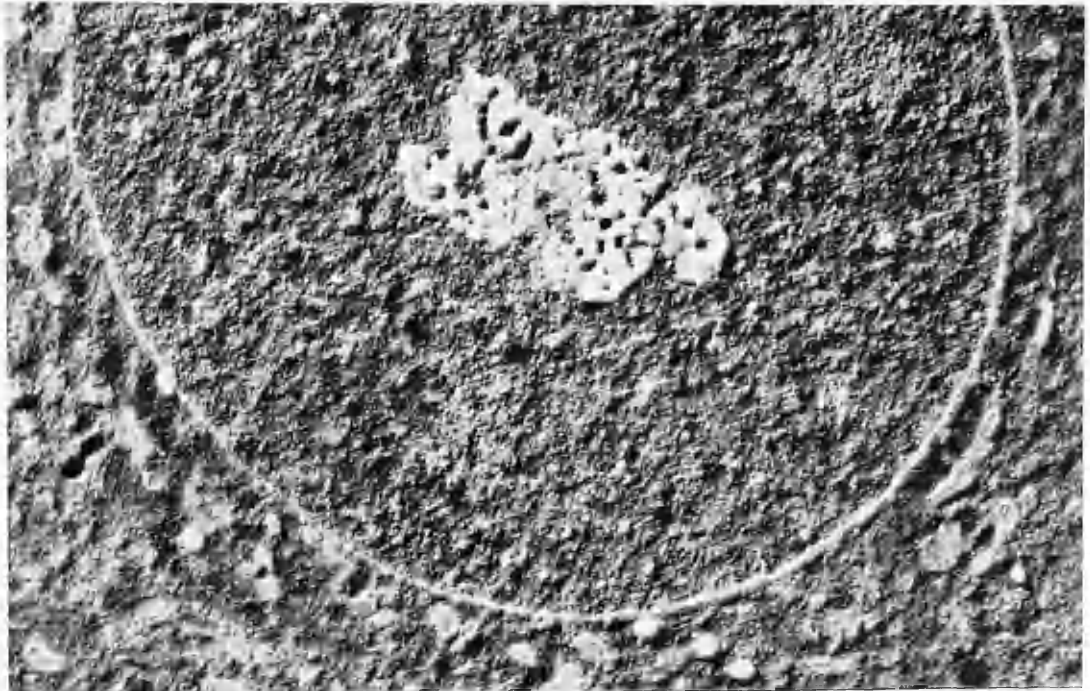


Figure 34. Shadowcast micrograph of a nucleus, showing the solid nucleolus, the vacuolated appearance of which is clearly due to the occurrence of actual vacuoles or holes. 14,000 x.

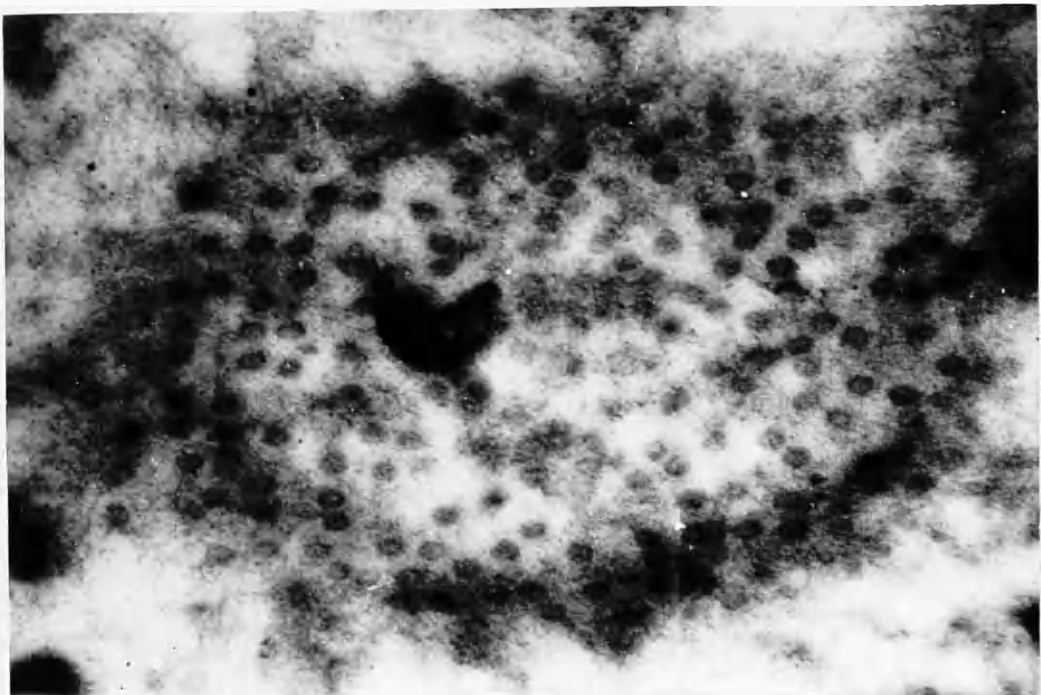


Figure 35. A section of nuclear membrane cut tangentially. The irregular distribution of nodes over the surface of the membrane is clearly visible. 42,000 x.

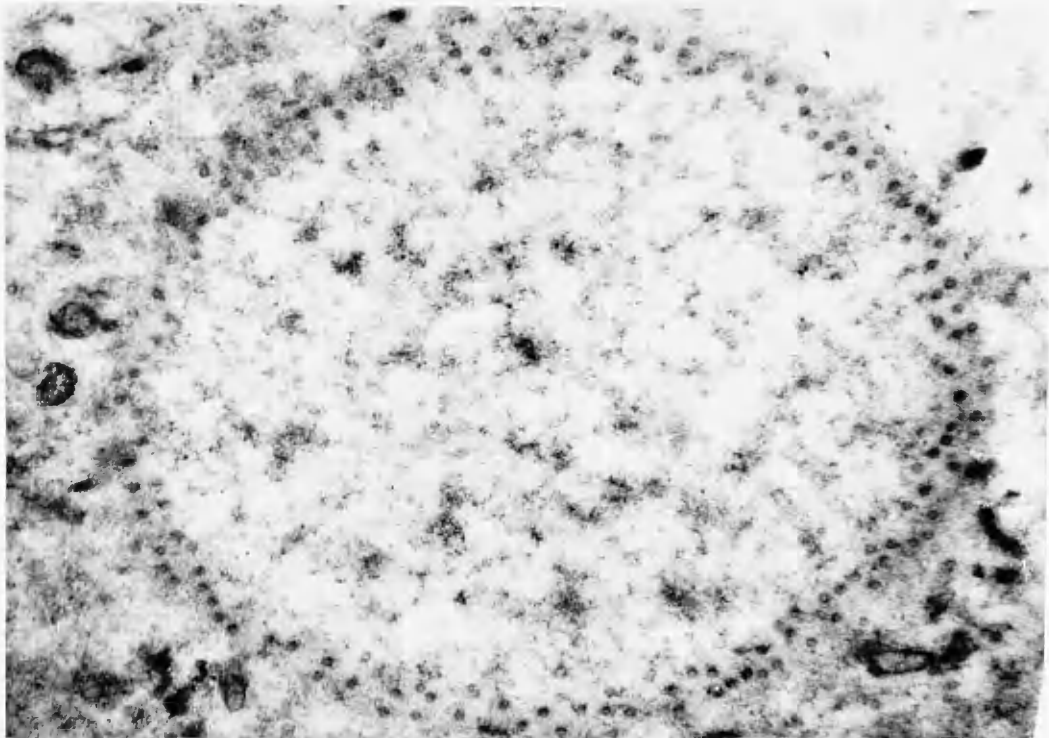


Figure 36. Section cut nearer the centre of the nucleus than Figure 35. The nodes are still clearly visible, however. 22,500 x.

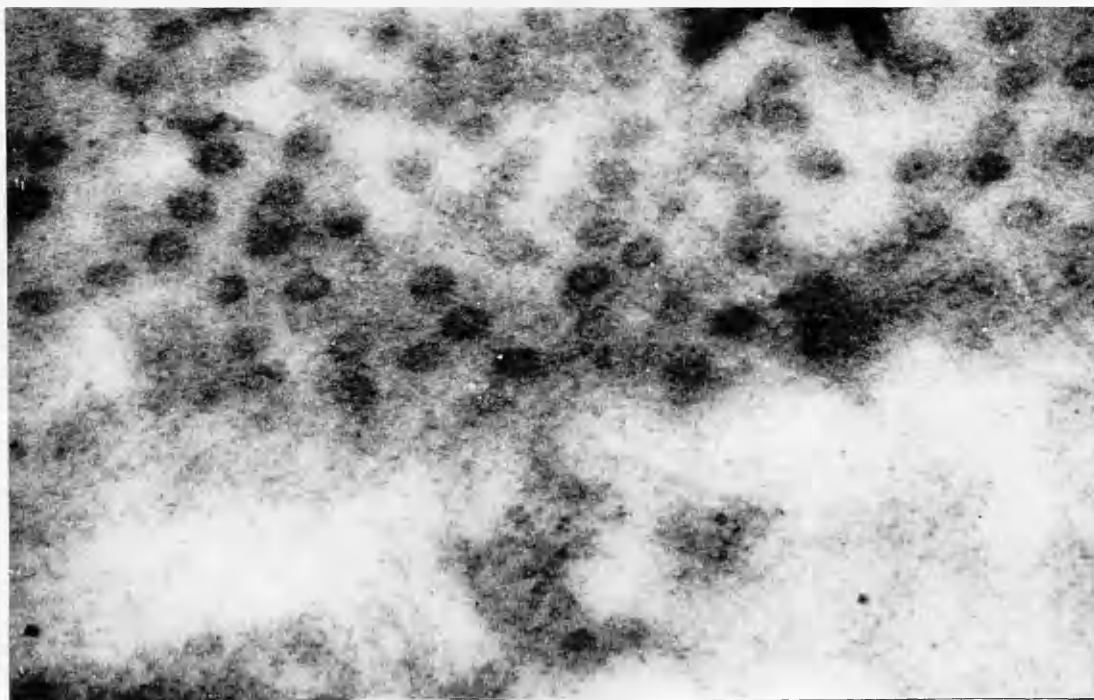


Figure 37. Enlarged portion of figure 35, showing the nodes in more detail. Some of them show a dark periphery and a dark central area. 75,000 x.

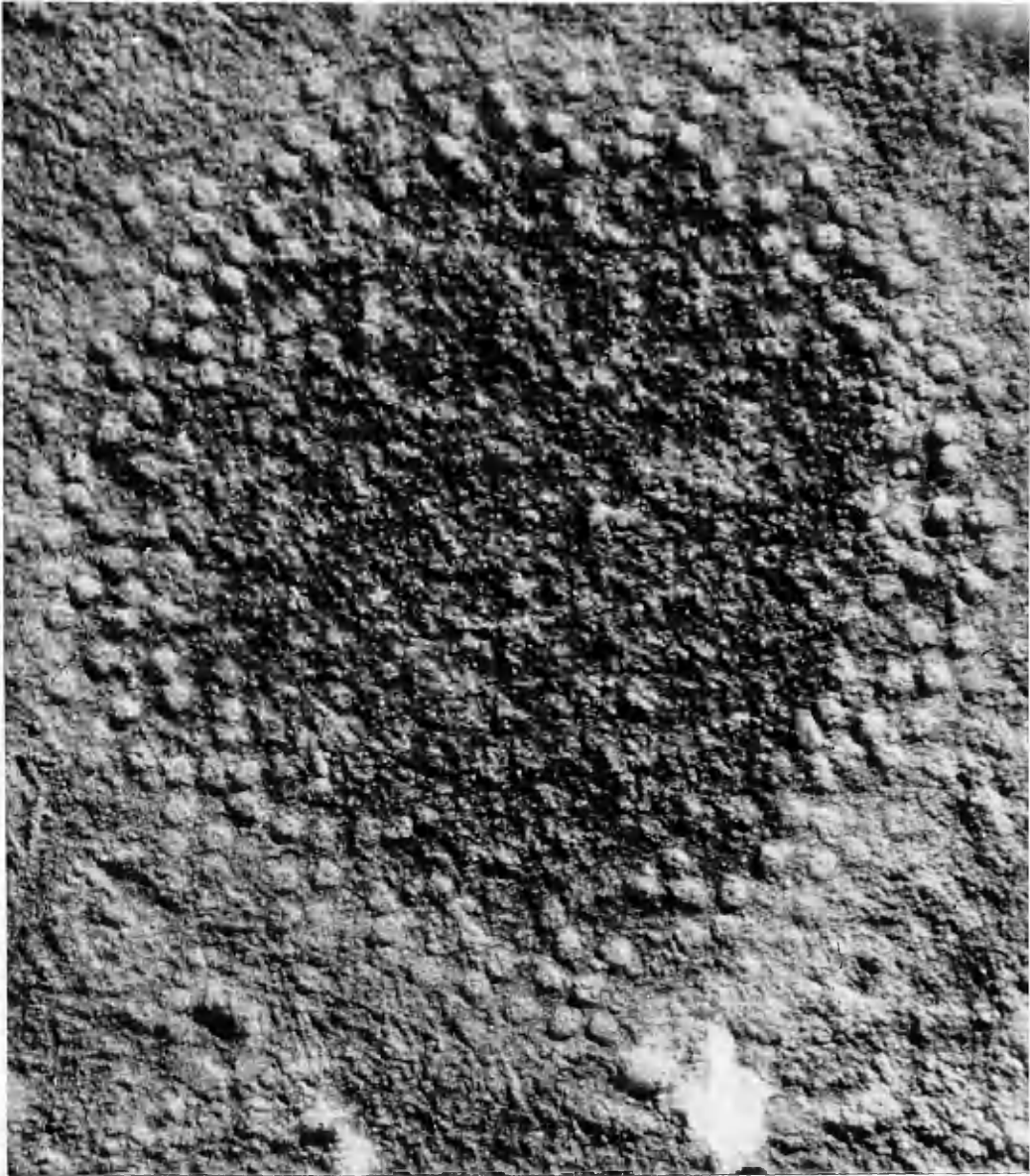


Figure 38. Micrograph of a peripheral section extracted and shadowcast. The nodes are solid cylindrical structures, and show a raised cortical and central part, separated by a depressed area. 42,000 x.

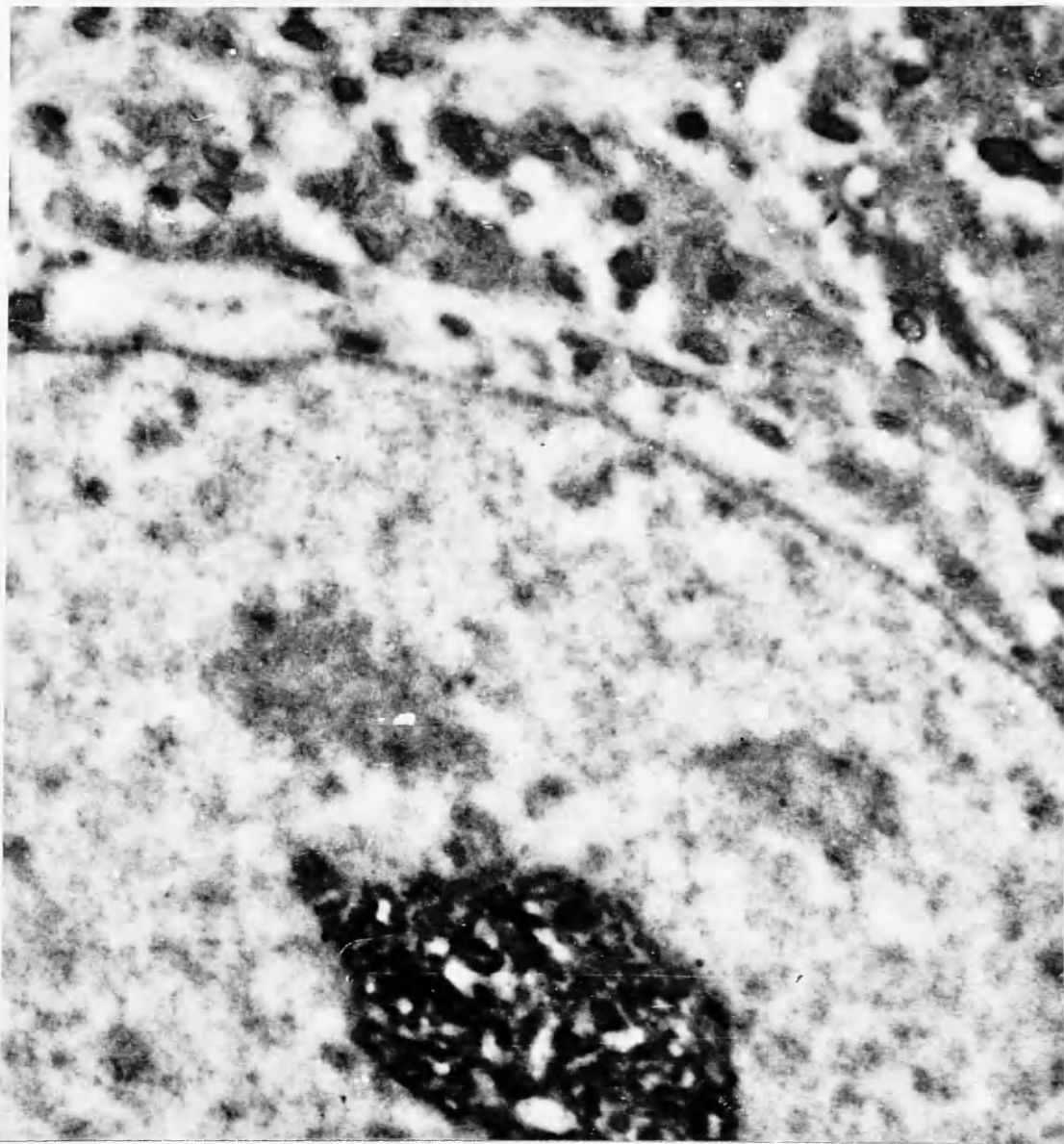


Figure 39. Radial section through nucleus, showing the nucleolus. The banded appearance of the membrane is evident, the size of the dark bands corresponding to the node dimensions. 18,000 x.



Figure 40. Radial section of nuclear membrane, showing the appearance of the nodes. The dark areas A, B, C, D and E correspond in size and spacing to the nodes seen in tangential sections. The nodes are bounded by a double wall which traverses the membrane thickness.

60,000 x.

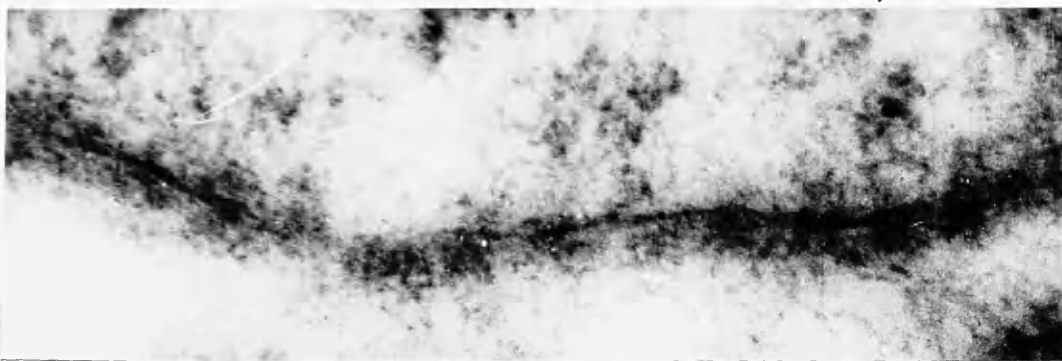


Figure 41. Radial section of nuclear membrane in which the supporting membrane is more clearly defined than the nodes, and in places is made up of several individual dark-staining layers.

60,000 x.

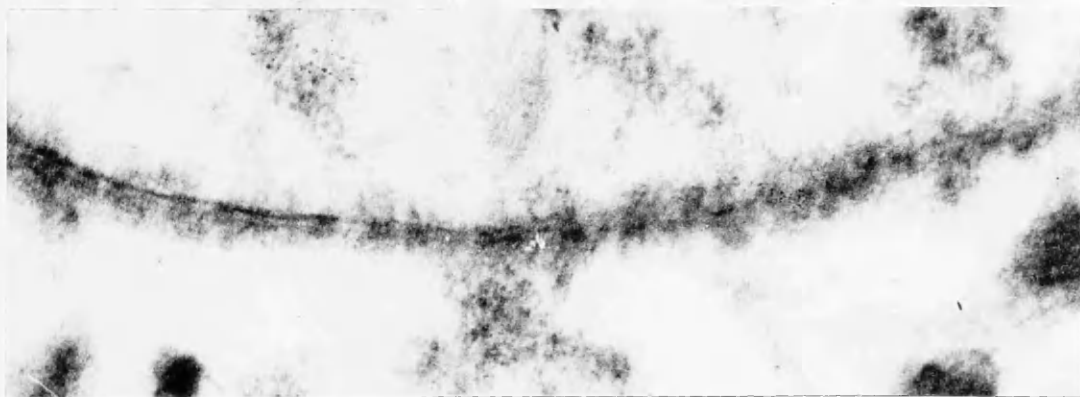


Figure 42. In this micrograph, the supporting membrane is more clearly defined to the left of the field, while the nodes are more evident on the right.

30,000 x.



Figure 43. Longitudinal section of nerve fibre myelin sheath, showing the individual lamellae of which it is composed. 110,000 x.



Figure 44. Transverse section of nerve fibre, showing Schwann cell with nucleus, and Schwann membrane. 14,000 x.

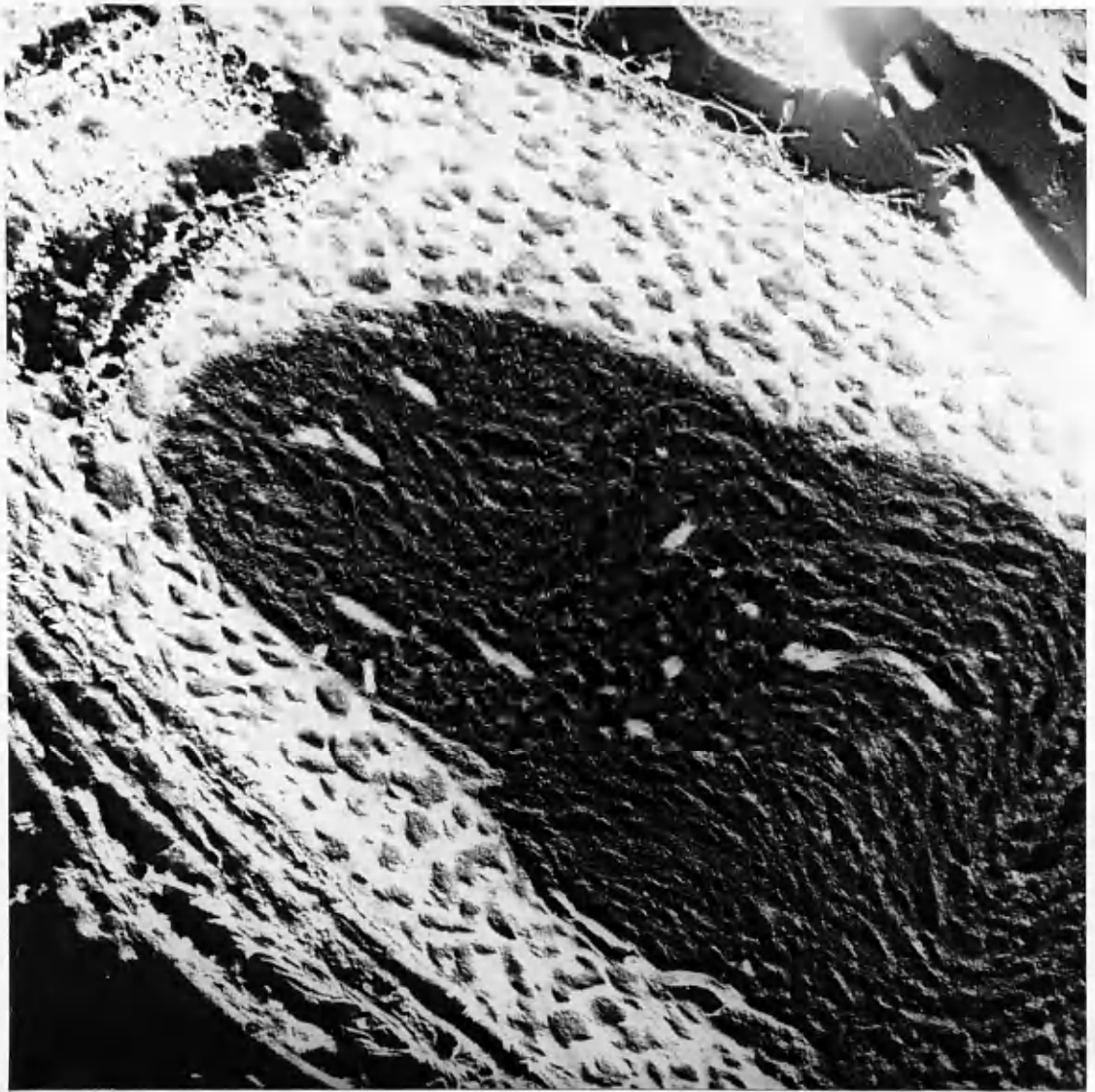


Figure 45. Oblique section of nerve fibre, shadowcast. The individual myelin lamellae are not visible. On the outer edges of the myelin sheath, strands of tissue are visible, representing the endoneurium. 35,000 x.

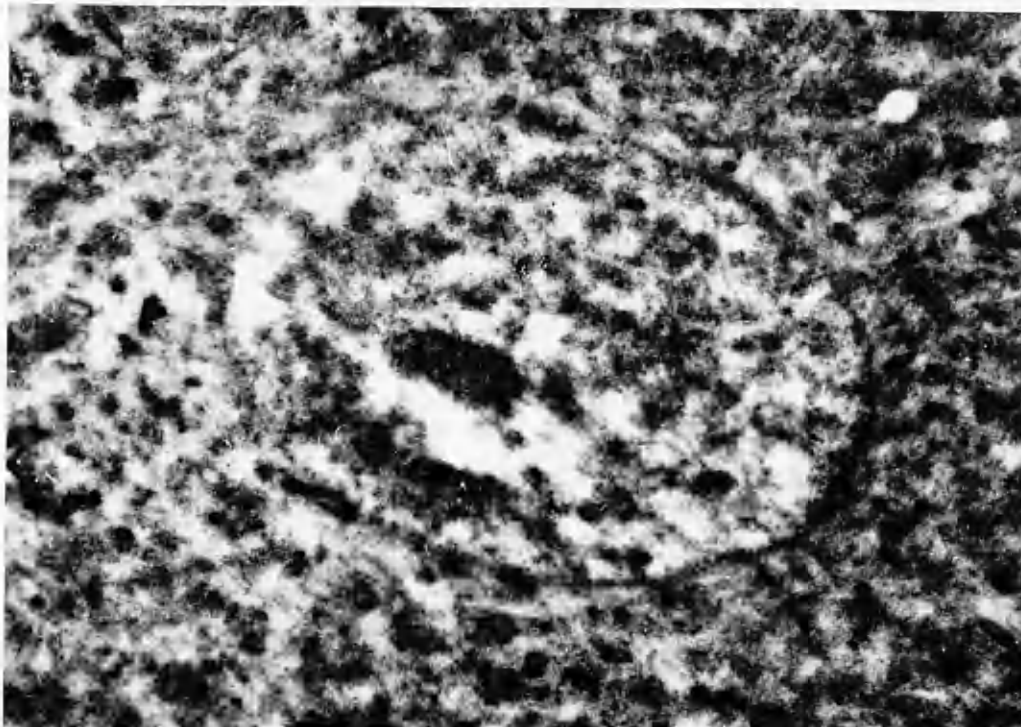


Figure 46. Section of nerve cell from ganglion where fixation was delayed for one to two minutes. 9,000 x.

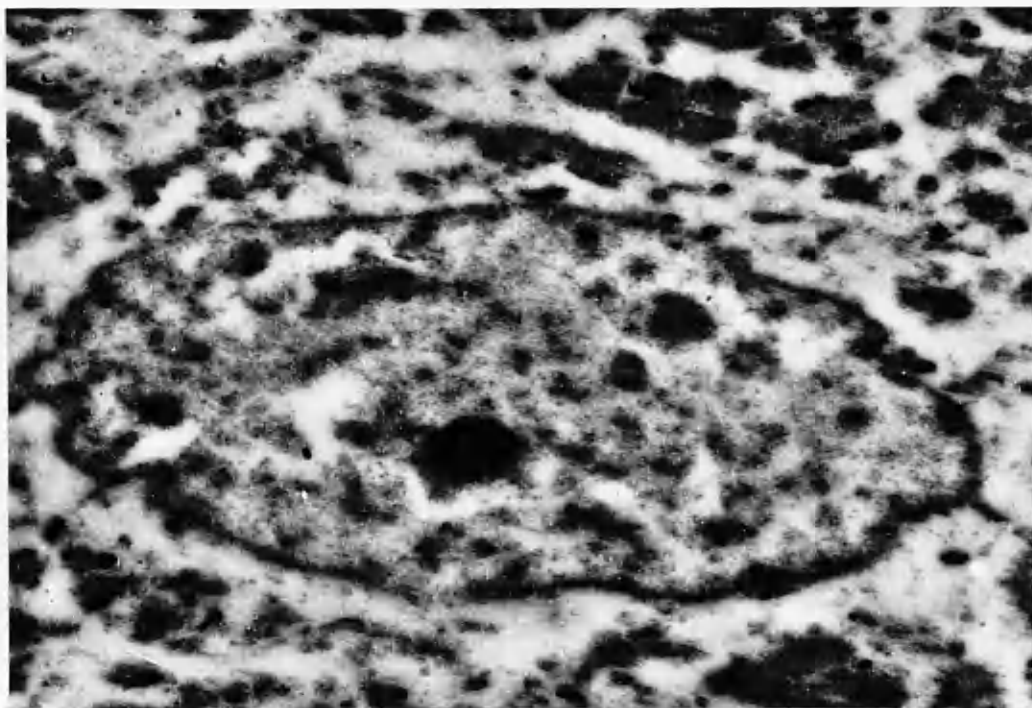


Figure 47. Section from ganglion which had about five minutes' delay in fixation. The slight distortion visible in figure 46 is accentuated. 8,500 x.

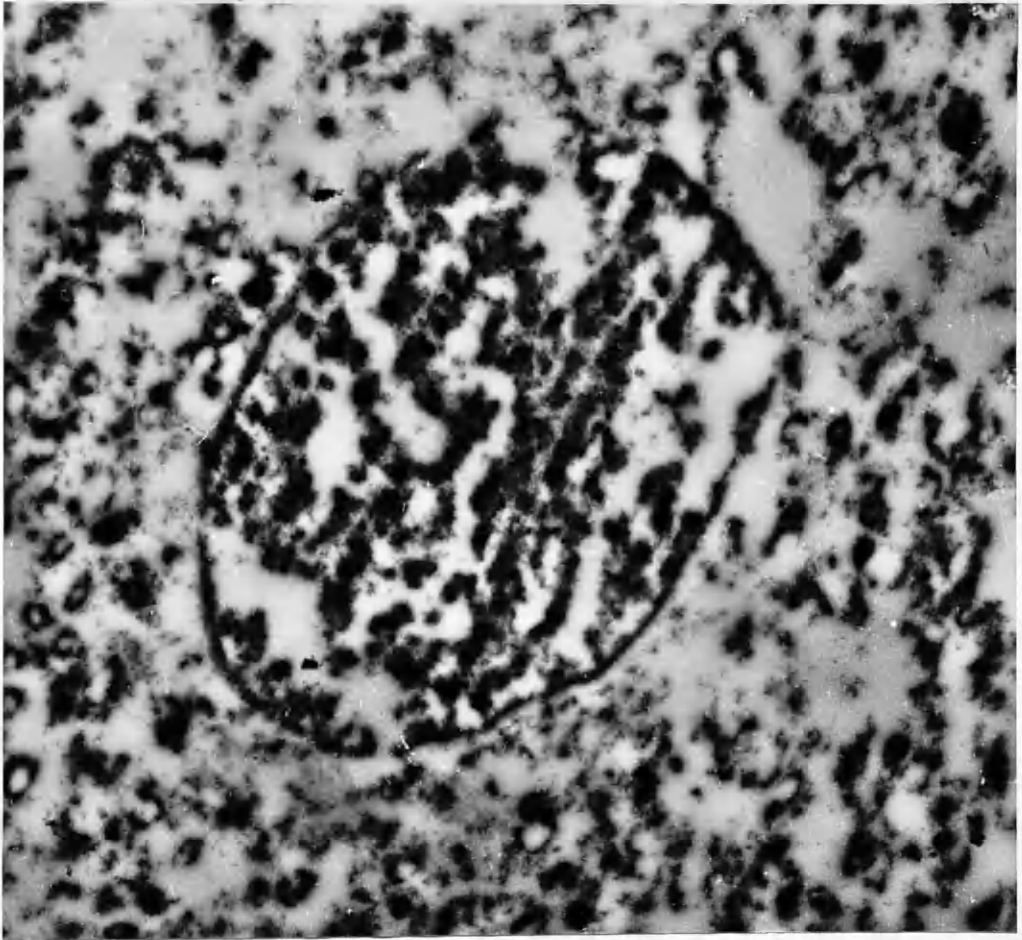


Figure 48. Section from ganglion where there was between twelve and fifteen minutes' delay in fixation. The cellular material seems shrunken, and is organised into lipid-like spheres. 9,000 x.

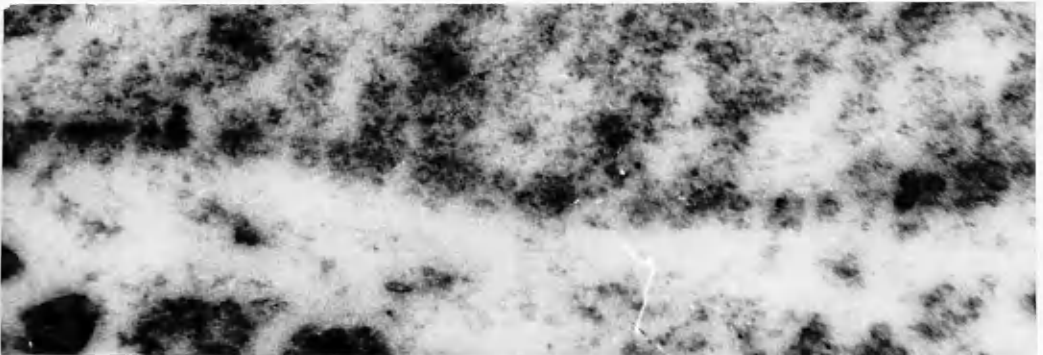


Figure 49. Section of nuclear membrane from same block as figure 46. Slight shrinkage of the cytoplasm, and distortion of the nodes, is evident. 36,000 x.

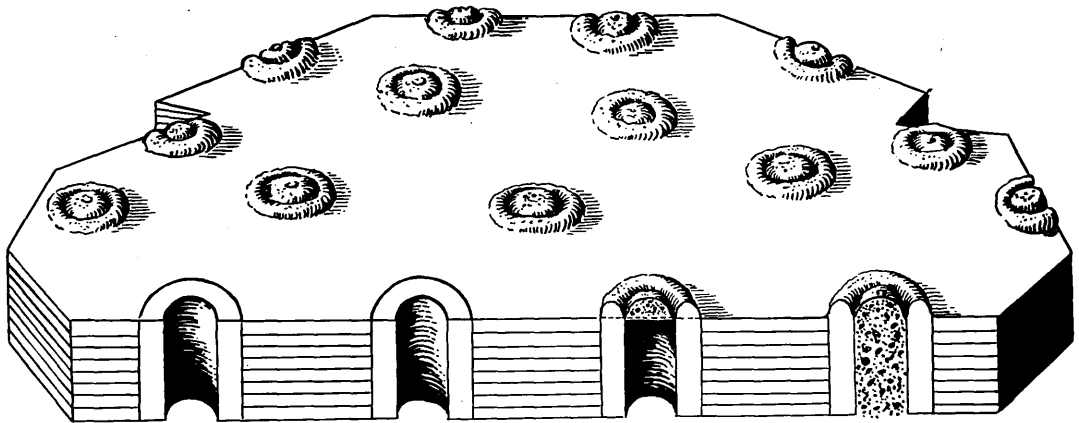


Figure 50. Diagrammatic representation of the main components of the nuclear membrane.



Figure 51. Brush border from convoluted kidney tubule cell, showing the tubular prolongations. 42,000 x.



Figure 52. Enlarged view of the tubular prolongations shown in figure 51. Each one in the left of the field appears to be enclosed by a membrane approximately 30 to 50 Å. in width. 78,000 x.

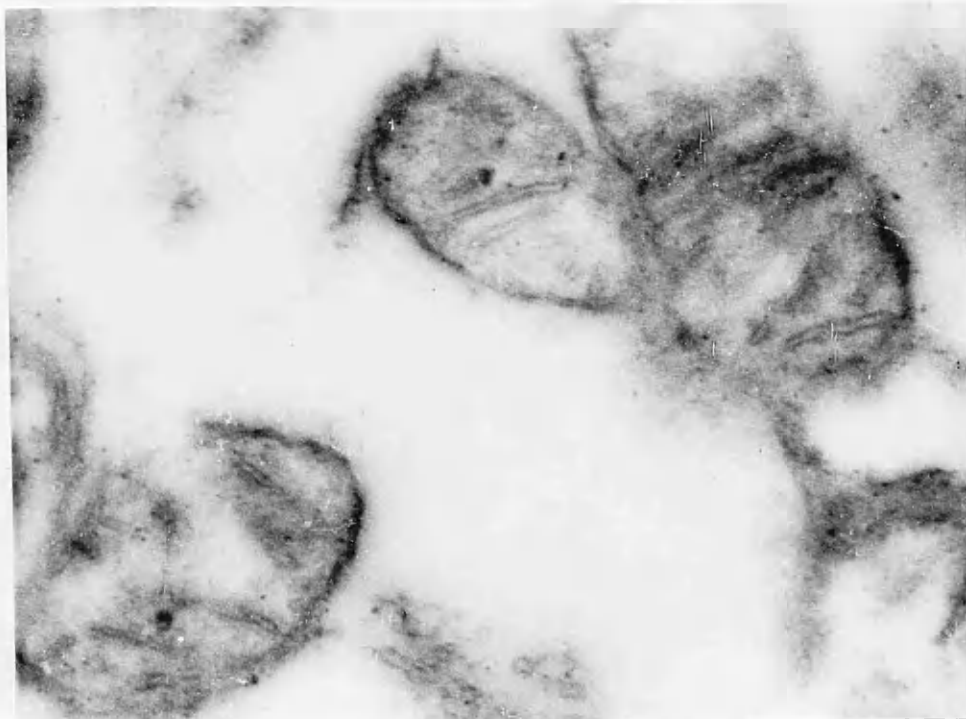


Figure 53. Mitochondria from kidney tubule cell, showing the double limiting membranes and internal double cristae. 120,000 x.



Figure 54.

75,000 x.



Figure 55.

125,000 x.

Figure 54 and 55 are of mitochondria, showing the outer membranes and internal cristae, and in addition elliptical rings and granules in the mitochondria which may represent the cristae cut in cross-section.

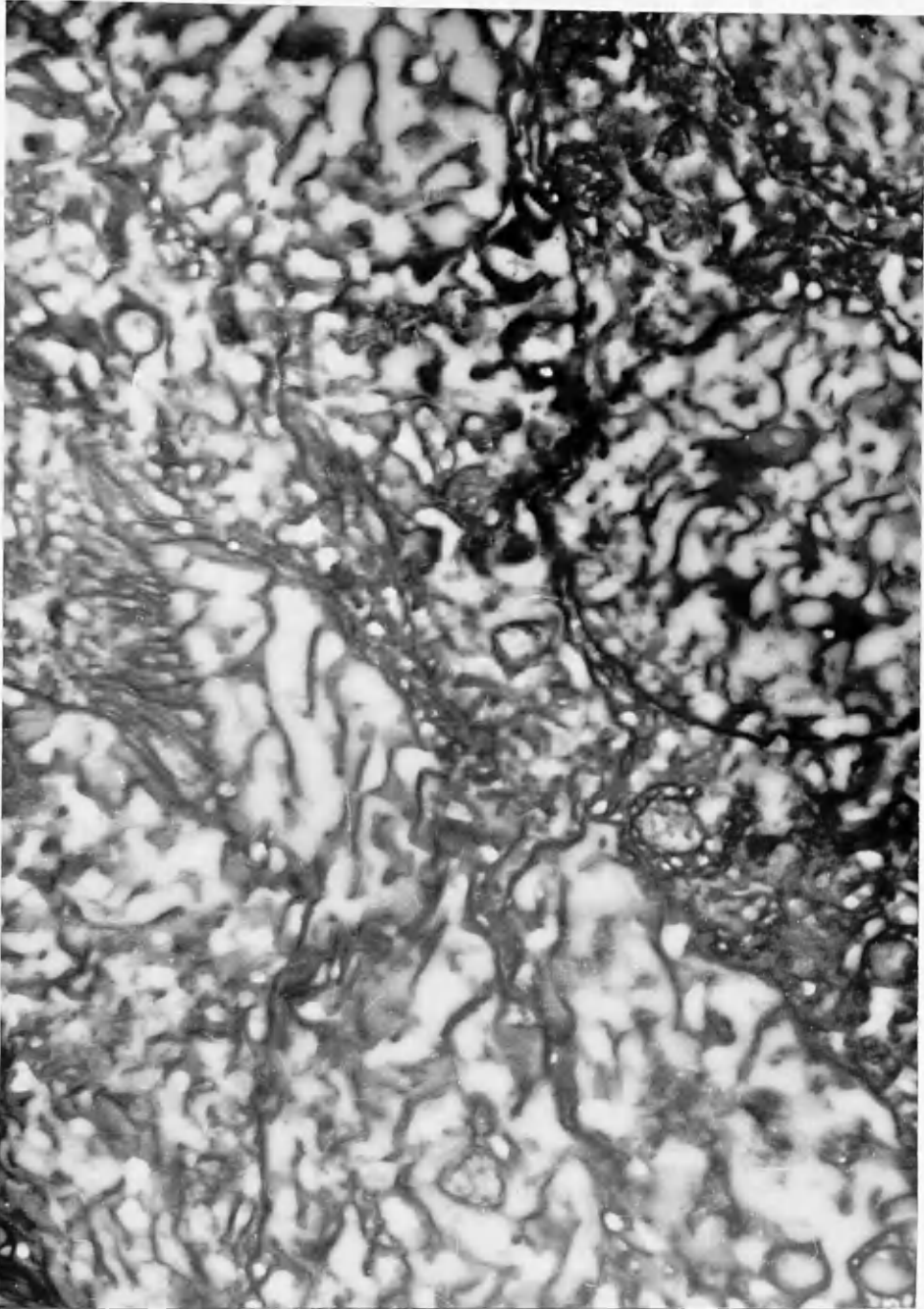


Figure 56. Section of frozen-dried kidney convoluted tubule, showing the typical fenestration effect in tissue fixed by this method. There is no evidence of brush border or mitochondria, and little evidence of cell or nuclear membranes. 8,000 x.